The Regulation of Alternative Pre-mRNA Splicing, Activity-Induced Splicing and Adaptive Splicing by DNA Methylation

By

Ling Liu

A Thesis Submitted to the Faculty of Graduate Studies of

The University of Manitoba

in partial fulfillment of the requirements for the degree of

DOCTOR OF PHILOSOPHY

Department of Physiology & Pathophysiology

University of Manitoba

Winnipeg

ABSTRACT

Many molecular bases for the long-term adaptive changes in cells remain unknown. Alternative splicing contributes dramatically to protein diversity and allows for the fine-tuning of gene functions in response to changing extracellular stimulation. It's a flexible process that could be spatiotemporally and dynamically regulated in response to various extracellular stimuli by the combined effects of specific RNA elements, cis- and trans-acting factors, epigenetic modifications as well as other regulatory factors. The effect of repeated stimulations on gene expression can often be distinct from that of a single stimulation, like in sustained regular exercises or long-term drug abuse. However, it remains unclear how splice variants are controlled in this process, and whether DNA methylation or MeCP2 (Methyl-CpG Binding Protein 2) regulate this potential process.

Here, by a depolarization-splicing system, it shows that while the majority of exons kept their homeostatic levels after repeated stimulations, a small group of synaptic exons are indeed adaptively spliced in a significantly different way from or even opposite to that by a single treatment upon membrane depolarization. For further exploration, I established an exon DNA methylation-splicing reporter assay system to conveniently examine the methylation effect on splicing by mutagenesis. In combination with a pair-wise genome/transcriptome-wide analysis, it shows that the adaptively spliced exons are controlled by DNA methylation. More interestingly, a group of adaptive synaptic exons is aberrantly spliced upon DNA methylation change in rat GH3 pituitary cells or due to mutation of the mC- or splicing factor-binding domains of the MeCP2 in patients with Rett syndrome, an autism spectrum disorder. In this thesis, the data established the role of DNA methylation in the adaptive splicing of synaptic exons in response to repeated stimulations by cellular activities and demonstrated similar changes in MeCP2-mutated Rett syndrome patients, many of whom suffer from progressive epileptic attacks after birth. It showed clearly that repeated rather than a single or short-term abnormal neuronal activity plus epigenetic dysregulation of either DNA methylation or MeCP2 aggravate aberrant splicing of synaptic genes, specifically in the hippocampus of Rett syndrome patients and likely other neurological diseases as well.

ACKNOWLEDGEMENT

I would like to express my deepest sincere gratitude to my advisor Dr. Jiuyong Xie, for continuously encouraging and guiding me through my graduate education. He has provided me a professional Ph.D. training just as I expected. He has been a great supervisor in directing my research program, being patient with my progress, giving help with interdisciplinary collaboration, and always giving prompt responses to my emails and questions. The critical and logical thinking that he has passed on to me benefits my research and everyday life. His impressive dedication and passion for science that he has shown on every workday inspire me to be excellent in my career in science and medicine. I also really appreciate the tremendous effort he has made to improve our fitness and the relationships between lab members. He frequently organized all lab members to hike, rafting, or BBQ together, sometimes with Dr. Robert Shiu, which is a beautiful time that I will never forget.

I wish to express my gratitude to my advisory committee members Drs. Janice Dodd, Etienne Leygue, and Suresh Mishra, for their helpful, valuable and encouraging advice, suggestions, comments throughout my Ph.D. program. I would like to appreciate the generosity they have displayed by spending their time to carefully listen to me, to discuss my research project, and to clarify my confusion. Their doors have always been open for me, and they are always there to provide their help. They are all knowledgeable and brilliant scientists as well as responsible and professional committee members. I would immensely appreciate it that they have set up a role model for me and encourage me to be a respectable and excellent researcher just like them.

Sincere thanks to all lab members for creating a supportive and delighted working environment. I want to especially thank Dairong Feng for her patience and guidance at the beginning of my Ph.D. training, Urmi Das, Hai Nguyen and Lei Lei for their great help and contribution to my work. Especially, I would like to thank Urmi Das, who always responds to me promptly when I ask for help, and the time she spends helping me with my project. I also want to thank the former lab members Wenguang Cao, Jinghua Feng, Niaz Mahmood, Jason Wu, Nan Liang and Muhammad Sohail for their help and support.

I want to thank my parents, sisters, friends and teachers for their support and encouragement. I owe my deep gratitude to my husband, Zhengtang Liu. He’s the person who has always provided me unreserved love, patience, understanding and suggestion. I also want to

express my appreciation to my landlady Simone Fourcade who has watched over me during my Ph.D. period, and two cats of hers, Mignon and Mini, which have brought me a lot of fun.

DEDICATION

This work is dedicated to my husband, Zhengtang Liu, our parents, Kuixuan Liu and Yuhua Liu, Bingyuan Liu and Surong Han.

LIST OF FIGURES

LIST OF TABLES

ABBREVIATIONS

Abbreviation	Full name
-CH3	methyl group
5-aza-C or 5-azaC	5-azacytidine
5-aza-dC	5-aza-2’-deoxycytidine
5hmC	5-hydroxymethylation
5mC	5-methylcytosine
AD	Alzheimer's disease
AHP	afterhyperpolarization
ALS	amyotrophic lateral sclerosis
AMPK	AMP-activated protein kinase
APD	action potential duration
Arg	arginine
AS	alternative splicing
ASER	antisense estrogen receptor
BK	big potassium
BSA	bovine serum albumin
BSMAP	whole genome bisulfite sequence MAPping program
Ca^{2+}	Calcium ion
CaMK	calcium/calmodulin-dependent protein kinase
CaRRE1	CaMK IV-responsive RNA element
CaV	voltage-gated calcium channel
CGI	CpG island
Cl^-	Chloride ion
CNS	central nervous system
CO_2	carbon dioxide
CREB	cAMP responsive element binding protein
CREM	cAMP-responsive element modulator
CRISPR	clustered regularly interspaced short palindromic repeats

CTCF	CCCTC-binding factor
DAG	diacyl glycerol
DAVID	Database for Annotation, Visualization and Integrated Discovery
dCas9	dead Cas9
DEXSeq	Detecting differential usage of exons from RNA-seq data
Dlg1	Discs large homolog 1
DMEM	Dulbecco's Modified Eagle's Medium
DMS	differentially methylated CpG site
DMSO	dimethyl sulfoxide
DNA-PK	DNA-dependent protein kinase
DNMT	DNA methyltransferase
DRB	5,6-Dichloro-1-beta-Ribo-furanosyl Benzimidazole
ds	double strand
DTT	dithioreitol
EDTA	ethylenediamine tetraacetic acid
EGFR	epidermal growth factor receptor
Ehmt2	Euchromatic histone-lysine N-methyltransferase 2
eNOS	endothelial nitric oxide synthase
Epb41l3	erythrocyte membrane protein band 4.1 like 3
ERK	extracellular signal-regulated kinase
ESE	exonic splicing enhancer
EtBr	ethidium bromide
FBS	fetal bovine serum
GFP	green fluorescent protein
GH	growth hormone
HAT	histone acetyltransferase
HDAC	histone deacetylase
HMD	highly methylated domain
hnRNP	heterogeneous nuclear ribonucleoprotein
hnRNP LL	hnRNP L-like

HP1	heterochromatin protein 1
HS	horse serum
iCLIP	individual-nucleotide resolution UV crosslinking and immunoprecipitation
IGV	Integrative Genomics Viewer
JNK	Jun amino-terminal kinase
K^+	potassium ion
KA	kainic acid
KCl	potassium chloride
Kidins220	kinase D interacting substrate 220
KO	knockout
LINE-1	long interspersed element-1
Lys	lysine
MAPK	mitogen-activated protein kinase
Mapt	Microtubule Associated Protein Tau
MATS	Multivariate Analysis of Transcript Splicing
mCG or mCpG	CG methylation
mCH or mCpH	CH methylation
MeCP2	methyl-CpG binding protein 2
MedIP	methylated DNA immunoprecipitation
$MgCl_2$	magnesium chloride
mM	millimolar
MNK	mitogen-activated protein kinase-interacting kinase
mRNA	messenger RNA
MSRE	methylation-sensitive restriction enzyme
Na_3VO_4	Sodium Orthovanadate
NaCl	sodium chloride
NES	nuclear export signal
NLS	nuclear localization signal
NMD	nonsense-mediated decay
NMDA	N-methyl-d-aspartate

Nrg-1	Neuregulin-1
PBS	phosphate buffered saline
PD	Parkinson's disease
piRNA	piwi-interacting RNA
PKA	cAMP-dependent protein kinase A
PKC	protein kinase C
PMD	partially methylated domain
PMSF	phenylmethylsulfonyl fluoride
Pol II	RNA polymerase II
pre-mRNA	messenger RNA precursor
PRL	prolactin
PSF	polypyrimidine tract-binding protein (PTB)-associated splicing factor
PTB	polypyrimidine tract-binding
PTK	protein tyrosine kinase
PTM	post-translational modification
Py	polypyrimidine
Pyk2	Ca2+/CaM-dependent proline-rich tyrosine kinase 2
RE	repetitive element
RRM	RNA-recognition motif
RT-PCR	reverse transcription-polymerase chain reaction
RTT	Rett syndrome
SAM	S-adenosylmethionine
Sam68	Src-associated in mitosis, 68 kDa protein
SAPK	stress-activated protein kinase
SC35	splicing component, 35 kDa
SDS	sodium dodecyl sulfate
SELEX	Systematic Evolution of Ligands by EXponential Enrichment
sgRNA	single guide RNA
siRNA	small interfering RNA

snRNP	small nuclear ribonucleoprotein
SR	serine/arginine-rich
SRE	splicing regulatory element
SS	splice sites
STREX	Stress Axis-Regulated Exon
SWI/SNF	SWItch/Sucrose Non-Fermentable
SZ	schizophrenia
TDP-43	TAR DNA-binding Protein 43
TET	ten-eleven translocation methylcytosine dioxygenases
TKI	tyrosine kinase inhibitor
TSS	transcriptional start site
TTX	tetrodotoxin
Tween 20	polyoxyethylene-20-sorbitan monolaurate
U	unit
U2AF	U2 auxiliary factor
UTR	untranslated region
UV	ultraviolet
WGBS	whole-genome bisulfite sequencing
μg	microgram
μl	microliter
μM	micromolar

Table of Contents

CHAPTER I Literature Review

1. Adaptive change at the cellular level

The term *cellular adaptation* refers to the changed response that cells make to adapt to varying types of external stimuli [1]. Since the beginning of the last century, researchers have been attracted to the exploration of cellular adaptation in some physiological organ systems, including auditory adaptation [2], visual adaptation [3], and adaption of respiratory and circulatory cells to hypoxia stress [4]. In the 1970s, the study of pathological forms of adaptation, opioids dependence and tolerance, firstly proposed the concept of *adaptive change* in cells. It describes an altered quantitative relationship between extracellular stimulus and cellular response upon two or more stimulations in terms of *adaptive hypersensitivity* and *adaptive desensitization* [5, 6]. Adaptive hypersensitivity refers to the phenomenon in which a given stimulus will induce an array of stronger and stronger biological responses over the repeated stimulations that eventually amplify the original response within cells. In contrast, adaptive desensitization describes an opposite phenomenon that eventually represses the original response.

Besides the drug addiction, such cellular adaptive change has been identified to play a role in both physiological and pathophysiological activities, e.g., chronic exercise-induced hormone secretion in response to resistance exercise [7], memory formation [8] or forgetting process [9], adaptive immune memory [10], acoustic adaptation in the human auditory cortex [11], visual adaptation [12], stress adaptation [13]. For example, repeated, but not a single, bouts of resistance exercise will elevate growth hormone concentration in the human body [7].

2. Alternative splicing

Pre-mRNA splicing was first discovered in 1977 in the studies of adenoviruses in mammalian cells. The researchers surprisingly found a series of RNA molecules with noncontiguous sequences from the viral genome [14, 15]. Later, the intervening sequences (introns) had been found in many other genes and splicing of pre-mRNA had been observed *in vitro* [16, 17]. Pre-mRNA splicing takes place either co-transcriptionally or post-transcriptionally, and characterizes by the removal of introns and the ligation of exons into a contiguous mature RNA (mRNA) from the newly transcribed pre-mRNAs through two sequential phosphoryl-transfer reactions known as transesterifications, which were directed by small nuclear ribonucleoproteins (snRNPs) [18, 19]. snRNPs are RNA-protein complexes that play key roles in splice-site

recognition, branch-point formation and catalysis in the process of pre-mRNA splicing. In eukaryotes, snRNPs are RNA-protein complexes, which are classified by the association with the U-rich small nuclear RNA (snRNA, 100-200 nt), such as the most abundant U1, U2, U4, U5 and U6 [20]. snRNPs combine together to form a large RNP machinery called spliceosome. The ordered assembly of spliceosome on nascent RNA is essential for pre-mRNA splicing (Fig. 1). Pre-mRNA was spliced either by constitutive splicing or by alternative splicing.

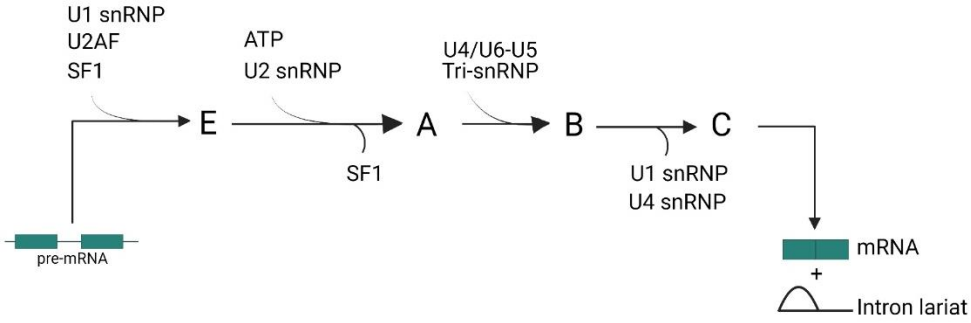

Figure 1. Stages of spliceosome assembly during the catalysis of pre-mRNA splicing.
The major snRNPs U1, U2, U4, U5 and U6 and auxiliary proteins assemble onto the intron of nascent pre-mRNA transcript in a step-wise fashion to carry out the splicing. Distinct H, E, A, B, and C complexes are intermediates during spliceosome assembly. During catalytic activation of the assembled spliceosome, the U1 and U4 snRNPs become destabilized and released from the spliceosome machinery. Thus, the catalytically active spliceosome consists of U2, U5, and U6 snRNPs. *(The figure was created with BioRender.com).*

In eukaryotic cells, most exons are thought to be constitutively spliced [21]. However, for certain exons, their inclusion in the transcripts is flexible, determined by the combined action of many factors, and can be changed by the intracellular and extracellular stimulations. This dynamic process refers to alternative splicing (AS) (Fig. 2). There are five main types of alternative splicing: mutually exclusive exons, cassette exon, alternative 3′ splice site, alternative 5′ splice site and intron retention [22]. By the inclusion or exclusion of alternative exons, a gene could generate multiple or even thousands of splice variants, which happens in approximately 95% of protein-coding genes in humans [23, 24]. AS plays an essential role in protein diversity and fine-tuning the complexity of biological functions [25]. Most AS events are tissue-dependent variation; 10-30% are individual-specific variations and affected by polymorphisms, subject to pronounced cell, tissue, or condition-specific regulation [24, 25].

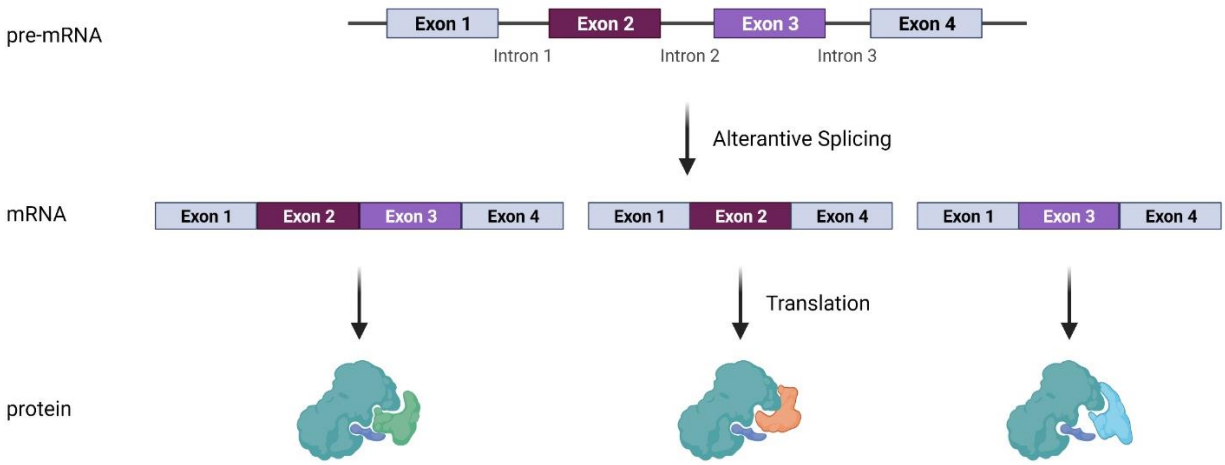

Figure 2. Diagram of alternative splicing.

In a pre-mRNA transcript, alternative exons 2 and 3 are both included in mRNA, or only exon 2 or 3 included in mRNA. Because of alternative splicing, one pre-mRNA transcript generates different protein isoforms with different biochemical properties. It is annotated as constitutive exon (exon 1 and 4), alternative exon (exon 2 and 3), intron (black straight line) and protein (colored irregular shape). *(The figure was created with BioRender.com).*

2.1 Molecular mechanisms of alternative splicing

The inclusion level of an alternative exon is mainly determined by the combined effect of cis-acting RNA elements and trans-acting protein (or RNA in some cases) factors, (1) Splice sites: these conserved sequences in the pre-mRNA begin with the dinucleotide GU at its 5′ end, ends with AG at its 3´ end, and include branch point located anywhere from 18 to 40 nucleotides upstream from the 3´ end of an intron [26]. They distinguish the intron/exon boundaries, provide binding sites for spliceosome assembly and guide the cleavage of introns. The strength of 5´ and 3´ splice sites contributes nearly equal roles in the exon recognition and exhibits their regulation in a combined way [27]. (2) Enhancers and silencers: also called splicing regulatory elements (SREs) and often located near splice sites either in exons or introns. They are cis-acting elements for specific binding of splicing activators (enhancer) or inhibitors (silencer), in turn, either promoting or inhibiting the recognition of splice sites and the assembly of spliceosome. There are three major classes of splicing regulatory proteins [28]:serine/arginine-rich proteins (SR proteins) [29-31], heterogeneous nuclear ribonucleoproteins (hnRNPs) [32-34], and tissue-specific RNA-binding proteins such as neuron-specific RNA-binding protein Nova [35]. SR proteins are a conserved family of regulatory RNA-binding proteins (RBPs) and mainly function in constitutive

and alternative splicing as splicing factors such as SRSF1 (previously called SF2/ASF) and SRSF2 (previously called SC35) [36]. The family of SR proteins shares a common structural organization containing one or two N-terminal RNA recognition motif (RRM) and a C-terminal variable-length domain enriched with Arginine and Serine amino acid residues (RS domain) that interact with other proteins mainly to recruit the splicing machinery [36, 37]. SR proteins used to be considered as splicing enhancers, while hnRNPs as splicing repressors [38]. The activity of SRSF1 under splicing conditions is antagonized by members of the hnRNP A/ B family of proteins in *in vitro* experiments [39]. However, in many cases, the effect of SR proteins and hnRNPs on splicing is highly complex and context-dependent [32, 40-42]. Recent studies showed that SR proteins actually could either activate or repress splicing events, which was confirmed by the depletion of individual SR proteins (8 of SR proteins were checked in total.) [43]. The regulation of AS by hnRNP protein hnRNP L will be discussed in more detail below.

Besides the interaction of cis-acting elements and trans-acting regulatory factors, other features that modulate exon usage are (1) Pre-mRNA secondary structure: including the formation of an RNA helix through RNA-RNA base paring, thiamine pyrophosphate (TPP)- or protein-mediated (such as PTB and hnRNP A1) RNA structural rearrangements [44-51]. (2) The kinetics of transcription: When this concept was first raised, it had been thought that slow elongation of RNA Polymerase II (RNA pol II) would favor the processing of co-transcriptional splicing at upstream sites, resulting in the inclusion of alternative cassette exons. In contrast, fast elongation was predicted to reduce the competitive advantage of upstream splice sites and favor exon skipping [52]. Later studies revised this concept and show that slow elongation will either increase or decrease the usage of splice sites depending on in part if it's regulated by an enhancer or silencer [53, 54]. Interestingly, elongation rate of RNA pol II also affects splicing fidelity. There's a difference of splicing error frequency between fast and slow transcript strains [55]. Moreover, DNA methylation [56, 57], DNA damage [58], mutation of RNA polymerase II [59, 60], chromatin remodeling factor SWI/SNF [61], or histone modifications [62], even splicing factor (such as serine/arginine-rich splicing factor SC35 [63]) could regulate the pre-mRNA splicing through affecting the transcription elongation rate. (3) In some specific genes, the length of intron and exon contribute to the exon usage: the shorter the exon and intron length (<500 bp), the higher the exon inclusion level in both invertebrates and vertebrates, such as the influence of intron length on CD44 splicing [64-67]. For example, a minimal intron length (>80 bp) is required for splicing the large

rabbit beta-globin intron and preventing the abnormal splicing of exons [68]. (4) Epigenetic modification: including histone and DNA modification, such as histone methylation, histone acetylation and DNA methylation [69]. This part will be discussed in more detail below.

2.2 The regulation of alternative splicing by splicing factor hnRNP L

The 65 kDa hnRNP L is a multifunctional RNA-binding protein containing four highly conserved RRMs: RRM1, RRM2, RRM3 and RRM4, which all contribute to RNA binding through the secondary structure of β-sheets [70]. hnRNP L is localized mainly within nuclear protein complexes in the nucleoplasm at steady state and enriched in the periphery of the nucleoli as a component of SLM/Sam68 Nuclear Bodies that link signaling pathways to RNA processing [71, 72]. hnRNP L possesses both a nuclear localization signal (NLS) and a nuclear export signal (NES)-like sequence [73, 74], which allows it to translocate into the nucleoplasm after translation and to be exported into the cytoplasm upon external stimuli. The phosphorylation of hnRNP L is a well-studied post-translational modification, which usually results in alteration in biological activities, such as promoting or inhibiting the alternative splicing of pre-mRNA by changing the affinity of RNA binding [75-77].

hnRNP L was first reported as a splicing regulator in the splicing of the eNOS gene through the specific binding to intronic CA repeat enhancer [78]. Subsequent studies showed that hnRNP L could bind specifically to exonic or intronic elements of the pre-mRNA and function as a splicing activator or repressor [78-82]. The binding preference of hnRNP L for CA-repeat or CA-rich motifs was confirmed by the *in vitro* binding SELEX analysis [80] and individual-nucleotide-resolution UV cross-linking and immunoprecipitation in combination with deep-sequencing (iCLIP-Seq) [81]. Genome-wide analysis of hnRNP L binding distribution by iCLIP-Seq showed that hnRNP L exhibited a binding preference for introns and 3´ untranslated regions (UTRs) [81].

Like other members of the hnRNP family, in most cases, hnRNPL acts as a splicing repressor but sometimes also exhibits an activating role in the pre-mRNA splicing depending on the local context of spliced exons. For example, hnRNP L repressed the inclusion of *CD45* exon 4 and 5 [79], STREX exon of *Slo1* gene (also named as potassium calcium-activated channel subfamily M Alpha1, *Kcnma1*) [75, 83], exon 20 of *TJP1* gene and exon 4 of *SLC2A2* gene [84] by blocking the assembly of spliceosome complex. Also, an RNAi knockdown assay showed that hnRNP L promoted the splicing of the NMD-sensitive exon 6a of itself by binding to a highly

conserved intronic CA-rich enhancer [82]. The regulation of hnRNP L on the pre-mRNA splicing is determined by: (1) The feature of the binding sequences: act as a splicing activator by binding to specific splicing enhancers, but as a repressor by binding to silencers [78, 85]. (2) The strength of nearby 5′ or 3′ splice sites (SS): hnRNP L represses strong splice sites but enhances weak splice sites (when the absolute level of exon inclusion < 2%) of the same exon by a minigene assay [79]. (3) The proximity of the CA motif to 5′ SS also affects the hnRNP L role in alternative 5′ SS selection [80, 86]. (4) Position-dependent regulation of hnRNP L: represses splicing when bound to an upstream intron of alternative exons (nearby 3′ SS) while enhancing splicing when bound to the downstream intron (nearby 5′ SS) [81]. The repression of alternative proximal 5' SS selection by hnRNP L could also be through the binding of exonic CA motifs by using a KLF6 pre-mRNA alternative splicing model [86]. Interestingly, this suppression effect of hnRNP L on alternative 5′ SS selection is independent of the CA-cassette locations on the proximal exon, no matter whether located near a proximal or distal 5′SS [86].

There are different mechanisms contributing to the repression of the pre-mRNA splicing by hnRNP L (Fig. 3). Firstly, hnRNP L directly blocks the assembly of the spliceosome complex at the splice sites of the regulated exons. (1) It does so by the typical mechanism of blocking the binding of U1 or U2 small nuclear ribonucleoproteins (snRNPs) to the splice sites (Fig. 3A). For example, hnRNP L represses splicing by interfering with 5′ splice site recognition of the U1 snRNP in exon 4 of *SLC2A2* gene and by interfering with the binding of U2AF65 to the polypyrimidine (Py) and 3′ splice site recognition in exon 20 of *TJP1* gene and STREX exon of *Slo1* gene [75, 84]. (2) It can also repress splicing by preventing progression to the U4–U6–U5 tri-snRNP–containing B complex after the ATP-dependent addition of the U1 and U2 snRNPs and inhibiting the formation of the spliceosome, such as the repression of the splicing of *PTPRC* (encoding CD45) exon 4 [87] (Fig. 3B). Secondly, hnRNP L represses the activity of the splicing enhancer of the regulated exons. For example, the binding site of hnRNP L is in the middle of an exonic splicing enhancer (ESE), which recruits the binding of splicing activator SRSF1 in *PTPRC* exon 5 (Fig. 3C). Therefore, hnRNP L inhibits the splicing of *PTPRC* exon 5 by interfering with the binding of SRSF1 to the neighboring ESE, hence preventing the recruitment of U2 snRNP to 3′ splice sites [79].

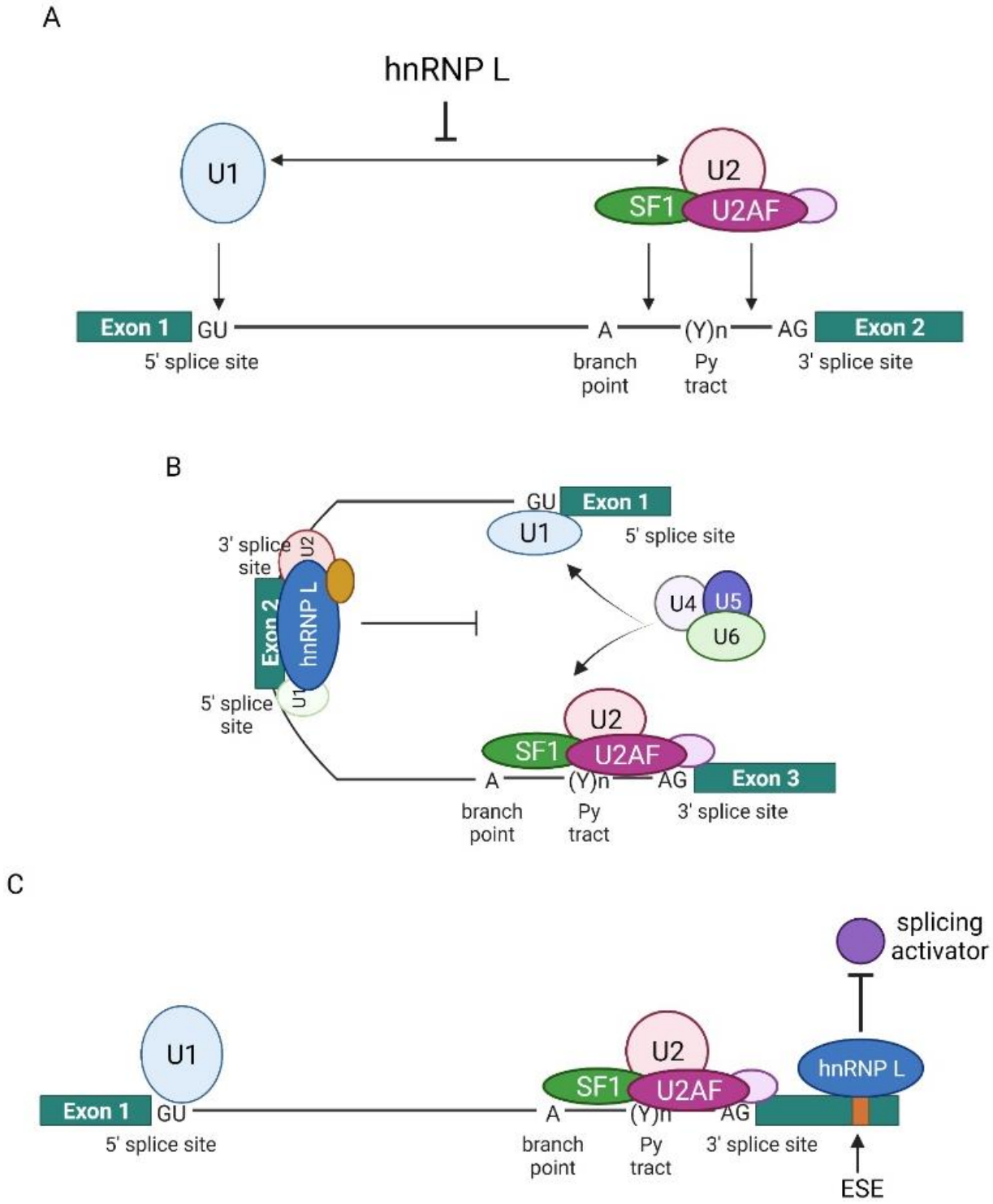

Figure 3. Molecular mechanisms behind the alternative splicing repression by hnRNP L. **A.** The typical mechanism: directly inhibiting the binding of U1 or U2 snRNPs to the splice sites. For example, in GH3 cells, hnRNP L binds to the specific element between the polypyrimidine (Py) and AG of the upstream 3´ splice site of the STREX exon of *Slo1* gene, blocking the binding of U2AF65 to the Py and resulting in the skipping of STREX. **B.** hnRNP L can also block the spliceosome assembly by preventing A complex progression to the U4–U6–U5 tri-snRNP–

containing B complex. For example, hnRNP L binds to exonic splicing silencer of *CD45* exon 4 and forms a stable U1 and U2 containing A complex across exon 4. This stable complex inhibits the binding of the U4–U6–U5 tri-snRNP, interferes with the formation of subsequent intermediate complex B and finally leads to the skipping of exon 4 *in vitro*. **C.** hnRNP L binds to an ESE (exonic splicing enhancer) and thus blocks the binding of splicing activator to the same ESE. For example, hnRNP L binds to the ESE of *PTPRC* exon 5, interferes with the binding of splicing activator SRSF1 to the ESE and leads to the skipping of *PTPRC* exon 5. *(The figure was created with BioRender.com).*

The regulation by hnRNP L on splicing is also affected by other splicing factors, such as hnRNP LL and hnRNP A1 [88-90]. HnRNP L and hnRNP LL could either cooperate or antagonistically modulate the regulation of alternative splicing of some exons [88, 89]. Based on the studies so far, the mechanisms underlying hnRNP L regulation of splicing include interference with spliceosome assembly as well as with enhancer activity of the regulated exons.

3. Activity-dependent splicing and cellular adaptation in endocrine and neuron cells

Excitable cells of many types, like neurons, endocrine, or muscle cells, have the capability to adapt their sensitivity to various kinds of extracellular physical, electrical, or chemical stimuli. Some non-excitable cells such as immunocytes also demonstrate the ability of adaptation in response to external stimuli. For example, adaptive immunity response is activated after an initial encounter with a specific pathogen and cells respond more rapidly and effectively to a subsequent encounter with the pathogen in the T lymphocytes. Numerous studies showed that the achievement of cellular adaptation is involved in the activity-dependent alterations of synapse-related proteins and ion channels in response to extracellular stimulation in the excitable cells, even in some of the non-excitable cells such as immunocytes [91]. These identified alterations occur at epigenetic, genetic [92], transcriptional [93], translational [94] and post-translational levels [95], referring to synapse plasticity, which contributes to learning and memory, stress adaptation and drug addiction.

At the epigenetic level, accumulating studies confirmed the role of epigenetic modifications in the regulation of cellular adaptation mainly through altering the transcriptome [96, 97]. For example, there is extensive evidence that DNA methylation, histone methylation, and acetylation are important for memory formation and maintenance [98]. The disruption of DNA methylation by DNMT blocker or Tet1 knockout (KO) impaired memory formation or induced memory extinction in mice [99, 100]. Interestingly, genome-wide DNA methylation was differentially changed between memory acquisition and maintenance (1h and 4 weeks of training

for contextual learning, respectively), demonstrating that there is a temporal correlation between DNA methylation and memory [101]. The DNA methylation change was significantly associated with the alteration of the expression and splicing of learning- and memory-related genes during memory formation [56, 101, 102]. It indicates that there may be an adaptive splicing change transcriptome-wide following the temporal dynamic of DNA methylation during memory formation, which may contribute another layer at the cellular and molecular level to the mechanism of memory formation.

Post-translational modification is the most well-investigated mechanism underlying cellular adaptation by altering protein functions and intracellular localization, which has been comprehensively reviewed by Davis and Müller, 2015; as well as Fernandes and Carvalho, 2016 [103, 104]. The regulation of cellular adaptation by post-translational modification is involved in learning and memory [105], drug addiction [106] and cell adaptation to hypoxic stress [107]. Recently, emerging evidence further highlights the importance of post-translational modification in the regulation of cellular adaptation and explores the mechanisms behind it. For example, Daniel Jacko et al. demonstrated the critical role of alpha-crystallin B phosphorylation in adaptation and de-adaptation to resistance exercise-induced loading in human skeletal muscle [108].

However, little has been explored about cellular adaptation related to alternative splicing (AS).

3.1 Activity-dependent alternative splicing and cellular adaptation

Is it possible that alternative splicing is also involved in cellular adaptation? Possible, based on the following evidence. Firstly, alternative splicing is not only regulated by intrinsic mechanisms in cell fate decisions but also regulated by extracellular stimuli. In 1999, Daoud et al. discovered the activity-dependent regulation of alternative splicing of the transformer-2-beta transcript in the rat brain [109]. Later numerous studies have demonstrated the activity-dependent alternative splicing of synapse-related proteins and ion channels, such as STREX exon of *Slo1* gene (also called *KCNMA1*, encoding BK channel) [110], exon 22 of *NMDAR* [111], mutually exclusive exon 5a, and exon 5b of *SNAP25* (synaptosomal protein of 25 kDa) [112], exon 18 of *NCAM* (neural cell adhesion molecule) [113], exon 11 of *NRXN2α* (encoding neurexin2 protein) [114] and exon 20 of *NRXN1* gene (encoding neurexin1 protein) [115].

Secondly, alternative splicing is a major factor that leads to protein diversity, generating protein isoforms with altered or even antagonistic properties. The various protein isoforms produced by alternative splicing contribute to the fine-tuning of protein functions and then cellular network. In neurons, the differential protein isoforms of synapse-related proteins and ion channels will lead to fine-tuning of neuronal properties, including cellular excitation, synapse formation, and synapse plasticity. This will finally result in the fine-tuning of biological activities, such as learning, memory, or drug addiction, in pathological activities. Here I will take the STREX exon of the *Slo1* gene as an example to explain how alternative splicing generates protein functional diversity and the potential role of activity-dependent splicing in cellular adaptation-related events.

Slo1 gene (also named *KCNMA1*) is the only known gene encoding the large-conductance calcium- and voltage-activated potassium BK channel α subunits. The pore-forming α subunits comprise a trans-membrane β coupling domain, a trans-membrane voltage sensor, a trans-membrane pore-forming loop and a long intracellular COOH terminus that forms a Ca^{2+} sensor important for activation of the channel [84]. This allows it to serve as a Ca^{2+}/voltage signal integrator in the regulation of cellular excitability by participating in the repolarization and after hyperpolarization of the action potential [116]. BK channel is associated with many cellular adaptation events, which refers to both non-neuronal and neuronal physiological processes, such as ethanol sensitivity [117-119], cognitive function [120, 121], neurotransmitter release [122] and fine-tuning of cochlear hair cell frequencies [123].

There are at least 27 constitutive exons and 10 alternative exons in the vertebrate *Slo1* gene [83]. These alternative exons are either cassette exons that could be included or excluded in Slo transcripts or exons containing alternative 5´ or 3´ splice sites. Combinations of alternative splicing in the *Slo1* gene could produce several hundreds of channel subunits, which could potentially form billions of BK channel heterotetramers comprising four different variant subunits, a, b, c and d [124]. Therefore, although they are coded by a single gene, the BK channels exhibit great diversity and different cellular properties.

Stress-axis regulated exon (STREX) is one of the alternative exons, which is located between constitutive exon 18 and 19 in the *Slo1* gene. It encodes a 59-residue cysteine-rich insert at the c2 position of alternative splicing in the C-terminus of mammalian BK_{Ca} channels. The STREX exon is widely expressed in excitable cells and regulated by membrane depolarization. Its

inclusion or exclusion results in the difference in BK_{Ca} channel excitable properties – in both kinetic and calcium sensitivity [125, 126]. $STREX^{-exon\ included}$ channels activate at more negative voltages than $STREX^{-exon\ excluded}$ channels, and STREX speeds activation and slows deactivation at a given test potential in cRNA-injected Xenopus oocytes [125]. A study of single-channel gating properties showed that the STREX deletion from BK channel did not affect the burst duration and number of openings per burst, confirming that the single-channel conductance was not significantly different from the wild type of BK channel [126]. However, the inclusion of STREX exon increases Ca^{2+} influx ($[Ca^{2+}]i$) sensitivity of the BK channel, making the channel functional at low physiological levels of $[Ca^{2+}]i$ [126]. The apparently functional difference in the BK channel induced by STREX inclusion or skipping indicates that alternative splicing of STREX exon of the *Slo1* gene affects cellular adaptation events that the *Slo1* gene participates in, as is described above.

Thirdly, the alternative splicing decision is not immutable but plastic and dynamic under precise temporal and spatial control. This is important. Since all cell types in a multicellular organism share the same DNA. The difference between different cell types and between different development stages is mainly caused by the synthesis and accumulation of different RNA products and protein molecules. As discussed above, alternative splicing contributes immensely to RNA and protein diversity. The spatiotemporal regulation of alternative splicing allows it to play an important role in the fine-tuning of cellular activity. In neurons, the dynamic regulation of alternative splicing could occur during neuron development, the formation of synapse plasticity, or the maintenance of drug addiction. For example, using quantitative real-time polymerase chain reaction (RT-PCR) Taqman™ assays, MacDonald, et al. reported the dynamic splicing of STREX exon from embryonic day 13 (E13) to 35-day old (P35) mice in the CNS during the brain development, which was observed in the spinal cord, midbrain, cerebellum, pons and medulla tissues. STREX splicing also demonstrated different patterns in different CNS regions (13 tissues were checked) at P35 mice [127]. Later, an RNA-sequencing analysis showed the transcriptome-wide developmental shift in splicing in the cerebellum and directed the axonal and synaptic formation, which includes the alternative splicing shift of *Ptprd* and *Nrxn1* genes [128]. These pieces of evidence demonstrate that alternative splicing is a flexible process that could be spatiotemporally and dynamically regulated in neurons. The dynamic regulation of alternative splicing allows it to be a potential mechanism of cellular adaptation.

Interestingly, emerging shreds of evidence have linked the alternative splicing to the regulation of cellular adaptation, although most studies are only limited to the discovery of different splice variants of the genes that demonstrate different functions in the cellular adaption activities. These studies referred to synaptic plasticity [129], which contributed to memory and learning, drug addiction [130], and cancer drug resistance [131, 132]. Firstly, by the inclusion or exclusion of exons, alternative splicing diversifies synapse-related proteins, such as ion channels [125, 133], channel receptors [134, 135], and other key neural proteins [136]. For example, a DAF-2 gene splice variant DAF-2c in the taste receptor neuron ASER is specifically able to rescue the loss of taste avoidance behavior in DAF-2 deleted *C. elegans* strains [136].

Also, alternative splicing is probably also involved in stress adaptation. Stress adaptation refers to a type of cellular adaptation in response to chronic stimulation. For example, the expression of 5,611 AS isoforms of 2,156 genes are differentially changed after consecutive 10 days air exposure as well as temperature and salinity challenge compared to the non-treated group in a genome-wide analysis of AS in the Pacific oyster, which was further validated using RT-PCR [137]. A similar result has been observed in shrimp in response to stress adaptation induced by virus or bacteria infection or low salinity stress [138].

Moreover, alternative splicing has demonstrated emerging importance in the regulation of drug addiction [139, 140]. Feng et al. showed that there were 2,998 genes that were differentially spliced in response to repeated cocaine treatments (daily intraperitoneal injections for seven consecutive days of cocaine) in mice. The prediction obtained from RNA-seq data was further confirmed by Nanostring validation. The splicing factor A2BP1 (also known as RBFOX1 or FOX-1) was involved in the cocaine-dependent regulation of alternative splicing since the protein levels of A2BP1 were increased (>2.5-fold) by repeated cocaine treatments [139]. Another example refers to the study of the decline of D2 receptor desensitization, which could be induced by drug exposure to cocaine [141] and alcohol [142], and resulted in reduced neuron excitability. Dopamine D2 receptor has two splice variants: D2S (short) and D2L (long), both of which are autoreceptors for the regulation of cellular excitability and dopamine release. A reduction in desensitization of D2 receptor was only observed in D2S-expressing neurons, but not in the D2L ones upon a single cocaine treatment by mice slice incubation [140]. The D2 receptor was regulated by calcium signaling with D2S and D2L splice variants differentially regulated [130]. It

suggests that calcium-induced alternative splicing is crucial for the cocaine-induced adaptation of the D2 receptor.

Taken together with the observed changes of RNA level of splicing factors [143] in the hippocampus memory process, the current evidence supports that alternative splicing is important to maintain cellular adaptative capacity. However, little has been known about the underlying mechanisms.

3.2 The regulation of activity-dependent alternative splicing

Depolarization of the plasma membrane describes a shift in the membrane potential to a less negative value inside the cell and results in eventual reversal of the transmembrane potential due to influx of positively charged ions, or in rare cases, efflux of chloride ion with a sudden chemical or electrical stimulus [144, 145]. The depolarization of the membrane induces calcium influx through the voltage-gate Ca^{2+} channel or ionotropic glutamate receptors because of the 10,000-fold gradient of free calcium concentration in cells (cytoplasm: 0.1 μM, extracellular: 1mM) [146].

In *in vitro* experiments, the membrane depolarization could be induced: (1) By increasing Ca^{2+} entry into target cells through voltage-gated Ca^{2+} channels, using such stimuli as potassium chloride (KCl), glycine [147], and GABA [148]. (2) By increasing Ca^{2+} entry into target cells through N-methyl-d-aspartate (NMDA) receptors, especially in neurons, which are glutamate-gated cation channels with high calcium permeability [149]. Some chemicals act as neuroexcitatory amino acid agonists could activate membrane depolarization through NMDA receptors, such as kainic acid (KA), an analog of excitotoxic glutamate [150]. Currently, KA is mainly used to activate neuron activity, model epilepsy and neurodegenerative states. (3) Some through Ca^{2+}-regulated Cl^- efflux, the beta-phorbol esters act in this way, such as 12-O-tetradecanoylphorbol-13-acetate (TPA) and phorbol 12,13-dibutyrate (PDBu) [145, 151]. (4) Through brief electrical stimulation by increasing the open probability of membrane voltage-gated channels and actively push ion flow across the membrane [152]. Also, the membrane depolarization could be blocked by: (1) The inhibition of voltage-gated Ca^{2+} channels. Based on physiological and pharmacological criteria, five types of voltage-gated Ca^{2+} channels are classified: L-type, N-type, P/Q type, R-type, and T-type [153]. L-type Ca^{2+} channel, widely expressed in neurons, endocrine, and muscle cells, is the one that couples membrane depolarization with a

cellular response and is inhibited by nifedipine [154]. (2) The inhibition of NMDA receptors by competitive and noncompetitive NMDA antagonists, such as by competitive (DL-2-amino-7-phosphonoheptanoate, AP7) and non-competitive (MK 801) blockers [155]. Besides the inhibition of Ca^{2+} influx, membrane depolarization could be reversibly blocked by some drugs, which act as nicotinic agonists and induce a prolonged depolarization state and prevent cells in response to the next stimuli, such as the neuromuscular blocking drugs including suxamethonium and decamethonium [156].

In 1939, Hodgkin and Huxley made the first intracellular recording of the electrical change that mediates the action potential [157]. Over 80 years' studies, it has been well demonstrated that depolarization controls numerous cellular activities and physiological processes. At the gene expression level, a wide range of alternative splicing (activity-dependent splicing) was regulated by membrane depolarization. During the past two decades, the underlying mechanisms of this widespread regulation of activity-dependent alternative splicing also have been well studied. Briefly, membrane depolarization controls activity-dependent splicing mainly through two mechanisms: (1) The post-translational modifications of splicing factors by different kinase signaling pathways, which consequently alters the protein-RNA binding affinity, or the nucleocytoplasmic distribution, or protein activities. (2) Epigenetic modification, including histone and DNA modification.

3.2.1 Control of post-translation modification of splicing factors by various kinase signaling pathways

At the post-translation level, splicing factors could be modified by phosphorylation, acetylation, ubiquitylation, methylation, sumoylation, and hydroxylation [158, 159], while depolarization-induced post-translational modification on splicing factors has mainly been involved in protein phosphorylation through the regulation of splicing factors or enzymes catalyzing other post-translation modifications (PTMs). In general, the addition of a phosphate group to proteins (including splicing factors) will affect the modified proteins through two ways: 1) the addition of extra two negative charges will attract or repulse a group of positively or negatively charged protein chains, respectively, thus affect protein activity; 2) the attached phosphate group will help to form a new binding site or mask an existing binding site, thus affect protein-protein interaction, protein-DNA interaction and protein-RNA interaction [160].

Depolarization-induced calcium influx could activate various signaling kinases in animals, including multi-functional calcium/calmodulin-dependent protein kinases (CaMKs), cAMP-dependent protein kinase A (PKA), protein kinase C (PKC), and MAPK/ERK [161-165], although in many cases the catalyzing enzyme as well as other molecular details, or the functional consequences have still been unclear.

3.2.1.1 CaMK IV signaling pathway

By far, the best-characterized example of calcium signaling-controlled splicing is through the multi-functional Ca/CaMKs pathway, which contains three enzymes referred to as CaM-kinases I, II, and IV [166]. More specifically, the regulation of splicing is mainly through the calcium/calmodulin (CaM)-dependent protein kinase IV (CaMK IV) pathway and seldom has been reported through CaMKI and CaMKII signaling pathways. CaMK IV is encoded by the *CAMK4* gene, which is a Ser/Thr kinase and a vital molecule for calcium signaling transduction to downstream effector proteins, including splicing regulatory proteins. CaMK IV can be activated by the calmodulin complex and the phosphorylation of Thr200 in the activation loop by the upstream CaMK kinase (CaMKK1 or 2) [167, 168].

In some cases, the phosphorylation of splicing factors by calcium signaling could alter their binding affinity to the specific splice sites and subsequently affect the assembly of the spliceosome complex, which will finally lead to the change in alternative splicing patterns. In a review article, Razanau and Xie provided a comprehensive summary of CaMK IV-regulated splicing of ion channel and synapse-related genes [169]. Here, I will summarize the main points of this review. In this review, the authors listed three examples of the splicing factors that were phosphorylated by CaMK IV kinase and the phosphorylation effects on the specific pre-mRNA splicing. The splicing factors are phosphorylated at Ser513 on hnRNP L, unknown site on hnRNP A1, and Ser20 on SAM68 (Src-associated in mitosis, 68 kDa). The phosphorylation of hnRNP A1, hnRNP L, and SAM68 all resulted in the skipping of exons in N-methyl-d-aspartate receptor 1 (*NMDAR1*), *Slo1*, and neurexin 1 (*Nrx1*) genes, respectively. For hnRNP L and hnRNP A1, the skipping effect was caused by the increase of the binding to the specific RNA elements, which were a CA-rich CaMK IV-responsive RNA element (CaRRE1) within its upstream 3´ splice site of STREX exon in *Slo1* gene for hnRNP L and the UAGG motifs of exon 21 in the *NMDAR1* gene for hnRNP A1,

respectively. However, the underlying mechanism of the skipping effect on exon 20 in *Nrx1* transcripts by the SAM68 phosphorylation has not been fully established.

In other cases, the phosphorylation activity of CaMK IV could affect the nucleocytoplasmic transport of the splicing factor, change its intracellular distribution, and finally affect the splicing decision of its targeted exons. For example, during the study of the regulation of homeostatic and Hebbian plasticity by alternative splicing, Li et al. found that Ca^{2+}/CaMK IV signaling phosphorylated the splicing factor Nova-2 at the sites of Ser25, Thr27, and Ser194 and reduced the nuclear location of the phosphorylated Nova-2 by driving it into the cytoplasm, which was responsible for the exclusion of exon 29 of BK channel [133].

Interestingly, by the inclusion or exclusion of the alternative exons of STREX or exon 29 in *Slo1* gene, exon 21 in the *NMDAR1* genes, and exon 20 in *Nrx1* genes, the generated ion channel and synapse-related proteins by different transcript variants possessed different properties and subsequently altered cellular activities. For example, the inclusion or exclusion of exon 29 in the *Slo1* gene could increase or dampen the K^+ current, shrink or widen the action potential duration, and finally affect the cellular firing frequency [133].

3.2.1.2 PKA signaling pathway

PKA regulates pre-mRNA splicing by the phosphorylation of splicing factors, including the SR protein serine/arginine-rich splicing factor 1 (SRSF1, previously designated SF2/ASF) [170-172], 9G8 [173] and SC-35 [174], polypyrimidine tract-binding protein (PTB, or hnRNP I) [175] and adenovirus L4-33K protein [176] *in vitro* and *in vivo* experiments, and by the interaction with SR-related splicing protein Arginine/Serine-rich 17A (SFRS17A) [177]. The PKA-phosphorylated splicing factors could either enhance or repress the proteins' capability to regulate alternative splicing. For example, in the regulation of alternative splicing of tau exon 10, PKA signaling enhanced the inclusion of tau exon 10 by promoting SRSF1 and SC35 binding to increase exon 10 inclusion but preventing 9G8 from inhibition of tau exon 10 inclusion through the phosphorylation of these three splicing factors in HEK-293T cells [172-174]. However, the underlying mechanisms, as well as the molecular details, have not been well characterized.

So far, two potential mechanisms have been demonstrated. Firstly, phosphorylation of splicing factors by PKA could affect their capability to interact with RNA elements. For example, PKA can phosphorylate SRSF1 at serine 119 *in vitro*. Mutation of Ser119 to alanine of SRSF1

reduced the RNA binding capability of SRSF1and affected the ability of SRSF1 to activate splicing of the Minx transcript *in vitro* [171]. It indicated that the PKA-induced phosphorylation of SRSF1 can enhance the binding of SRSF1 to RNA elements and therefore alter the decision of pre-mRNA splicing. Another potential mechanism contributing to the regulation of pre-mRNA splicing by PKA signaling may be through inducing nucleocytoplasmic distribution of splicing factors. Xie et al. have found that PKA directly phosphorylated the splicing factor polypyrimidine tract-binding protein (PTB) at Ser-16 *in vitro* and *in vivo*, which was abolished by the mutation of Ser-16 to alanine (S16A). Also, S16A mutant dramatically decreased the export of PTB from the nucleus to the cytoplasm in heterokaryon assays [175]. It confirmed the crucial role of PKA-induced phosphorylation in PTB shuttling between nuclei and cytoplasm, which was likely a promising molecular mechanism underlying the regulation of PTB-dependent alternative splicing. However, the downstream targets of the pathway have not been clarified.

Interestingly, through the phosphorylation of splicing factors, the PKA signaling pathway regulates the splicing of some specific alternative exons in combination with other signaling pathways. For example, both DNA-dependent protein kinase (DNA-PK) and PKA phosphorylated the splicing factor adenoviral L4-33K protein but with opposite effects on L1 alternative RNA splicing [176]. By the phosphorylation of L4-33K, DNA-PK inhibited L4-33K activated L1 alternative splicing, while PKA enhanced L4-33K regulatory effect on L1 splicing [176]. This confirmed that both PKA and DNA-PK controlled the phosphorylation of splicing factor L4-33K but with the opposite effect on it, suggesting the combinational phosphorylation of splicing factors by different signaling pathways may be a common regulatory principle in cells. However, it is still unclear how the L1 alternative splicing has been differentially regulated by DNA-PK and PKA signaling pathways. For example, we still do not know whether the differential splicing of L1 is through the phosphorylation of the differential sites of L4-33K.

3.2.1.3 PKC signaling pathway

Protein kinase C (PKC) belongs to a family of serine/threonine kinases and are grouped into three subfamilies based on their structure and dependence on second messengers: conventional PKC (α, the alternatively spliced βI and βII, and γ), which is physiologically activated by the increased the concentration of lipid second messenger diacylglycerol (DAG) and calcium ion (Ca^{2+}); novel PKC (δ, ε, θ, and η), which is physiologically dependent on DAG; and atypical

PKC (ζ, ι), whose activation depends on neither DAG nor calcium, but the binding of protein scaffolds [178, 179]. Here I mainly focus on the role of the Ca^{2+} -sensitive conventional PKC isozymes, which could be activated by membrane depolarization. This signaling pathway is essential for synapse plasticity and formation and can regulate alternative splicing of synapse-related genes [180, 181].

In the cellular study, the Ca^{2+} -sensitive conventional PKC isozymes can be activated by functional analogs of phorbol esters (such as phorbol 12-myristate 13-acetate) and inhibited by the relatively specific inhibitors bisindolylmaleimides Gö 6983 (also inhibits novel PKC isozymes) and Gö 6976 (also inhibits protein kinase D) [182]. By PKC inhibitor assay, it showed that the alternative splicing of *Bcl-x* was controlled by a signaling pathway that is dependent on PKC in EcrR-293 cells [183]. Pharmacological evidence further demonstrated the essential role of the calcium/ PKC/Rho-associated protein kinase II (ROCK II) pathway in the depolarization-induced splicing repression of specific exons of the neurexin 2α and neurexin 3α in rat cortical neurons [184]. This study stressed the contribution of PKC signaling to the depolarization-induced splicing regulation, although through mechanisms that were poorly understood. A recent study reported the disruption of embryonic to adult transitions of a set of 22 alternative splicing events in the diabetic heart by PKCα/β inhibitor BisIX (Ro-31-8220) through the alteration of the phosphorylation status and expression level of CELF1/Rbfox2 proteins [185]. These studies suggested the importance of conventional PKC in regulating alternative splicing and the depolarization-induced splicing response. However, little has been known about the involved mechanisms and splicing factors. Further exploration is needed to see if the change in phosphorylation state of splicing factors induced by PKC plays a role in the regulation of alternative splicing.

3.2.1.4 MAPK signaling pathway

MAPKs comprise a family of ubiquitous and highly conserved protein Ser/Thr kinases in eukaryotes, which guide cellular signaling in response to a variety of extracellular stimuli. In mammals, MAP kinases are grouped into three families: ERKs (extracellular-signal-regulated kinases), JNKs (Jun amino-terminal kinases), and p38/SAPKs (stress-activated protein kinases) [186].

In the early 90s, it was reported that depolarization-induced calcium influx through L-type calcium channels stimulated MAPK kinase MEKl and activated MAP Kinase via Ras activity in

PC12 cells. This study demonstrated an important link between MAPK and Ras pathway, which are two key mediators of nervous system signaling [146]. Later studies found that the membrane depolarization could activate multiple MAPKs and their substrates, such as extracellular signal-regulated kinase (ERK) [187-190], p38 MAPK [190], and mitogen-activated protein kinase-interacting kinases (MNKs) [191]. Interestingly, the pattern of membrane depolarization resulted in a different result referring to the duration of MAPK phosphorylation [192]. Briefly, compared to a single 3-min membrane depolarization induced by 90mM KCl treatment, the activation of MAPK signal lasts longer upon the space, repeated stimuli (four repeated 3-min 90mM KCl-induced depolarizations with 10-min intervals). Also, the persistence of phosphorylated MAPK evoked by repeated KCl treatments wasn't observed upon a prolonged 42-min depolarization in hippocampal neurons, which led to morphological alterations in hippocampal dendrites [192]. A similar phenomenon was also observed in the specific memory-stabilizing upon spaced training in behavioral experiments. Long-term behavioral sensitization was produced by space, repeated stimuli but not a single stimulus in *Aplysia california* [193]. In *Aplysia california*, spaced, repeated stimuli also increased MAPK activity in sensory neurons and consequently phosphorylated cAMP response element binding protein (CREB) that was required for long-term memory [194, 195]. It indicated that the activation of MPAKs could be evoked by membrane depolarization and the phosphorylated duration of MAPKs was determined by different depolarization fashions. The persistent activation of MAPK was only produced by spaced, repeated membrane depolarizations, which was essential for synapse plasticity and long-term memory in neurons. However, little has been known about the molecular mechanism underlying the differential memory fashion induced by a single depolarization and by spaced, repeated depolarizations.

The regulation of gene expression has been well studied by the depolarization-activated MAPK in mammals [189]. It is related to a wide range of cellular processes, such as neurotransmitter release [196], synaptic plasticity, and memory formation [187]. For example, MAPK/ERK signaling is responsible for activity-dependent expression alteration of a large number of genes in the mouse hippocampus, including *Arc/Arg3.1*, *Arl5b*, *Gadd45b*, *Homer1*, *Inhba* and *Zwint*, which is important for shaping neuronal connectivity [197].

Also, emerging evidence emphasized the role of MAPK catalytic cascades [198-200], and their substrates MNKs [201, 202], in the regulation of alternative splicing by phosphorylating

splicing factors. Splicing factors that were phosphorylated by MAPKs included heterogeneous nuclear ribonucleoprotein A1 (hnRNP A1), RNA-binding motif 20 (RBM20), and the serine/arginine-rich splicing factor 3 (SRSF3) [198-200]. MAPKs or MNKs could cause a change in nucleocytoplasmic distribution, or expression level, or maybe in some unknown properties/levels of splicing factors, all of which consequently resulted in the alteration in targeted alternative splicing. The first example showed that MAPK signaling pathways regulated alternative splicing of the E1A splicing reporter minigene through the alteration of the subcellular distribution of the splicing factor hnRNP A1 [198]. The activated p38 by stress stimuli increased the phosphorylation of splicing factor hnRNP A1 and led to the subcellular redistribution of hnRNP A1, which consequently resulted in a change in alternative splicing of an adenovirus E1A pre-mRNA by minigene splicing reporter assay. It confirmed that p38 MAPK signaling regulated stress-induced alternative splicing through the phosphorylation of a splicing factor that changes the nucleocytoplasmic transport of the splicing factor. Also, the MAPK signaling cascade altered the expression level of the splicing factor and modulated pre-mRNA splicing [200]. Cai et al. showed that the activation of the MAPK/ERK signaling pathway enhanced the expression level of RBM20 and influenced its targeted pre-mRNA alternative splicing of *titin*, LIM domain binding 3 (*Ldb3*), calcium/calmodulin-dependent protein kinase II gamma (*Camk2g*), and triadin (*Trdn*) in cardiomyocytes under both basal and osmotic stress-activated states. These studies clearly demonstrated the importance of MAPK signaling cascade in the regulation of pre-mRNA alternative splicing. Besides MAPKs, their substrate MNKs also regulation the phosphorylation splicing factors, such as hnRNP A1 and the polypyrimidine tract-binding protein (PTB)-associated splicing factor (PSF) [203]. These studies suggested that MAPK signaling cascade regulated alternative splicing under stress and disease conditions. However, little has been known about the regulation of MAPK signaling in alternative splicing upon membrane depolarization.

3.2.1.5 Protein tyrosine kinase signaling

In contrast to protein serine/threonine kinases, the protein tyrosine kinases (PTKs) are the other key group of signaling molecules, which comprise a large and diverse multigene family found only in multicellular organisms. In the human genome, 90 unique tyrosine kinase genes and five tyrosine kinase pseudogenes have been identified [204] to be involved in various biological activities, including synaptic plasticity, cognitive and memory processes [205, 206].

It has been reported that tyrosine phosphorylation and PTKs could be evoked by membrane depolarization. In the late 90s, it had been demonstrated that the tyrosine phosphorylation of the epidermal growth factor receptor (EGFR) was required for the activation of the Ras/MPAK pathway upon depolarization-induced calcium influx in neuronal cell types [207]. Later studies explored the PTKs that were activated by membrane depolarization, such as tropomyosin receptor kinase B (TrkB) [208, 209] and Ca^{2+}/CaM-dependent proline-rich tyrosine kinase 2 (Pyk2, also known as FAK2, CAKb, RAFTK and CADTK) [210, 211]. For example, the tyrosine kinase Pyk2 was implicated in the tyrosine phosphorylation of MAPK caused by membrane depolarization in neuronal cells [212, 213].

Tyrosine kinases can activate multiple signal transduction cascades, transmit extracellular signals into the cytoplasm and often to the nucleus, and thus regulate the gene expression process [214-216]. A recent study claimed that PTKs regulated alternative splicing through the phosphorylation of splicing factors [217]. Li et al. showed that TAR DNA-binding Protein 43 (TDP-43) was doubly phosphorylated by the MAPK/ERK kinase MEK at threonine 153 and tyrosine 155 (p-T153 and Y155) sites in human cells. TDP-43 could control the splicing regulation of more than 600 protein-encoding genes through GU-rich elements [218-220]. The increased phosphorylation of TDP-43 by MEK suppressed its splicing regulatory function in its target exon splicing [217]. However, the regulation of alternative splicing and depolarization-induced alternative splicing by tyrosine kinase signaling has not been well studied so far.

To explore the role of tyrosine kinase in the regulation of depolarization-induced splicing, tyrosine kinase inhibitors (TKIs) assay would be a good choice as a start. Protein tyrosine kinases (PTKs) are enzymes that catalyze tyrosine phosphorylation of specific target proteins by the transfer of phosphate groups on ATP to the tyrosine residues [221]. TKIs are also called tyrphostins, a term coined by Alexander Levitzki in 1988 for the short name of “tyrosine phosphorylation inhibitor,” which could directly inhibit receptor and non-receptor tyrosine kinases [222]. TKIs exhibit its inhibition effect mainly through the competition with ATP for the ATP binding site of PTKs, such as tyrphostin AG 1288 [223]. Until 2018, there were more than 20 kinds of highly specific TKI that had been launched on the market because of their anti-tumor effect [223]. As discussed above, alternative splicing is a widespread process in metazoan and is crucial for protein diversity as well as the fine-tuning of cellular properties. Further exploration of the relationship

between alternative splicing and tyrosine kinase would allow us to develop more specific and efficient TKIs.

3.2.2 Control of activity-dependent splicing by epigenetic modifications

Epigenetic modification refers to the heritable changes that could control gene expression but not involving changes in DNA sequence. It refers to the modifications that not only occurred in DNA but also in histone and RNA, such as DNA methylation, histone acetylation, chromatin remodeling, and nucleosome positioning, mRNA modifications, et al. [69, 224, 225]. However, currently, there is not and has not been any credible support for the heritability of RNA modifications, and it needs further exploration. Besides mRNA gene expression, epigenetic mechanisms also play an essential role in many other cellular processes, such as microRNA expression, DNA-protein interactions, suppression of transposable element mobility, X-chromosome inactivation and genomic imprinting [225]. At the gene expression level, the regulation of alternative splicing by epigenetic modification has been well-studied during recent decades. Interestingly, the emerging role of epigenetic modification in depolarization-induced splicing has also been demonstrated, such as histone modification.

3.2.2.1 Histone modification and activity-dependent splicing

A histone modification is an addition of a covalent post-translational modification (PTM) to histone proteins by their writers, which could be removed by the specific erasers, mainly at amino acids in the N-terminal tails [226]. In cells, there are 13 types of histone PTMs to date, such as acetylation, methylation, phosphorylation, ubiquitylation, and sumoylation. Histone acetylation and methylation are the most common and the most extensively studied ones in the regulation of alternative splicing [227]. Histone acetylation refers to the transfer of an acetyl group from acetyl-CoA to the conserved ε-N-acetyl lysine amino acids on histone proteins by histone acetyltransferases (HATs), which could be removed by histone deacetylases (HDACs) [228]. Histone methylation refers to the transfer of a methyl group from S-adenosylmethionine (SAM) to lysine (Lys or K) or arginine (Arg or R) residues of histone proteins by histone methyltransferases, which could be removed by histone demethylases [229].

Both histone acetylation and methylation are dynamic processes in response to various extracellular stimuli. They all play an essential role in the regulation of alternative splicing in response to depolarization/neural activity through the kinetic coupling of splicing and transcription

[113, 230, 231]. In 2009, the effect of change in histone acetylation on the splicing responses to membrane depolarization was firstly investigated by Schor et al. [113]. KCl-induced depolarization resulted in the exclusion of the neural cell adhesion molecule (*NCAM*) exon 18 by causing H3K9 hyper-acetylation in the specific region surrounding the targeted exon in murine neuroblastoma N2a cells. The mechanism behind this process is associated with the altered elongation rate of RNA polymerase II (pol II). Later, they further demonstrated that histone methylation could regulate the same exon (*NCAM* exon 18) but at different cellular contexts (not in depolarized cells) [232]. Interestingly, Sharma et al. linked protein kinase signaling CaMKIIδ or PKD1 with the regulation of alternative splicing by histone acetylation in response to membrane depolarization [230]. In brief, membrane depolarization led to changes in the histone acetylation through the activation of CaMKIIδ or PKD1 signaling pathways. The alteration of histone acetylation induced changes in alternative splicing of a group of depolarization-responsive exons, including *Nuclear factor I* (*NfI*) Exon 23a, by affecting the elongation rate of pol II in cardiomyocytes. Also, recently it has been shown that activity-induced histone methylation (H3K9me3) controlled the alternative splicing of the *Neurexin 1* (*Nrxn1*) gene through the AMP-activated protein kinase (AMPK) signaling pathway in memory-related neurons in mouse dentate gyrus [231].

These studies confirmed the importance of histone acetylation and methylation in the regulation of alternative splicing in response to membrane depolarization and investigated the calcium signaling pathway as the underlying mechanism. However, little has been known about how histone acetylation and methylation occur at specific regions surrounding the targeted exons instead of a general effect on the whole pre-mRNA. Interestingly, a recent study identified that P66α (official name Gatad2a: GATA Zinc Finger Domain Containing 2A) acted as an adaptor to recruit HDAC2 (Histone Deacetylase 2) and Suv39h1 (suppressor of variegation 3-9 homolog 1) and brought the enzymes to a TGATAA element within the targeted exon by a zinc-finger domain for sequence-specific binding [231]. The recruited HDAC2 and Suv39h subsequently caused changes in histone acetylation and methylation and finally resulted in changes in alternative splicing of *Nrxn1* exon 22 [231]. P66α is a critical component of the methyl-CpG-binding domain proteins MBD2 (Methyl-CpG Binding Domain Protein 2) -NuRD (nucleosome remodeling and deacetylase) complex, which is essential for ATP-dependent chromatin-remodeling and histone modifications [233, 234]. It indicated that the specificity of the regulation of alternative splicing

by histone modifications was related to some complex mechanisms. Some RNAs/proteins could act as adaptors to guide the recruitment of HATs (histone acetyltransferases) and HDACs to specific RNA elements surrounding the targeted alternative exons.

3.2.2.2 DNA methylation and activity-dependent splicing

The regulation of activity-dependent splicing by DNA methylation will be delineated in detail below (Please see section "4. DNA methylation, splicing, and neurodegenerative disease").

3.3 Adaptive activity-dependent splicing is likely a potential mechanism contributing to cellular adaptation

The signaling pathway in depolarization-induced AS changes by KCl has been well studied in our lab over the past 20 years [75, 83, 110, 125, 169]. By inducing cellular depolarization, it activates diverse secondary signaling molecules and regulates gene expression, including AS [169]. Calcium, the most important and well-studied secondary massagers in the regulation of splicing, is a key factor for a classic autoregulatory homeostatic feedback loop of cellular excitability. The concept of this feedback loop was proposed around 25 years ago [235-237] and was firstly summarized and demonstrated graphically by Tsien et al. [133]. This feedback loop is involved in such diverse cellular adaptation processes as synapse plasticity [110, 133, 238], stress adaptation [239-241], and drug addiction [242].

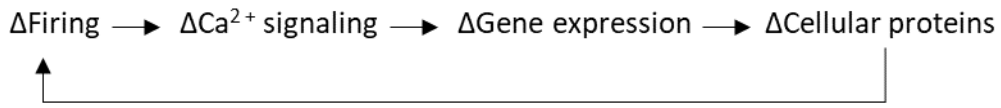

In 2001, Xie et al. explored the regulation of alternative splicing of ion channels by depolarization and provided the first evidence suggesting that alternative splicing is a novel dimension involved in the regulation of the feedback loop of cellular firing [110]. Briefly, the study found that KCl-induced depolarization activated Ca^{2+} signaling and resulted in the exclusion of stress axis-regulated exon (STREX) in the *Slo1* BK potassium channel gene in GH3 cells, generating BK channel proteins with lower sensitivity to calcium and voltage, and finally reduced the cellular excitability [110, 125, 126]. Since the BK channel controls the repolarization and fast after-hyperpolarization of action potentials and is important in setting the firing properties of neurons [110], it indicated that the activation of depolarization by extracellular stimuli could alter

the repolarization and after-hyperpolarization through the regulation of alternative splicing, which will consequently change the firing properties of later waves of action potentials.

Interestingly, recently Li et al. have made another interesting discovery related to the regulation of the autoregulatory homeostatic feedback loop of cellular excitability by alternative splicing. They showed that the chronic inactivity of sodium channels by tetrodotoxin (TTX) treatment broadened the action potential duration (APD), which was related to blunted afterhyperpolarization (AHP) instead of an altered depolarization, in cultured cortical cells [133]. More interestingly, alternative splicing of the BK channel by the exclusion of an alternative exon (exon 29) was responsible for this observation, which was regulated by the nuclear exit of Nova-2 through the CaMKIV signaling pathway upon the activation of the L-type Ca^{2+} channel [133]. This study provided a full-loop mechanism for the feedback loop by which chronic inactivity of sodium channel regulated APD and reset spike through the alternative splicing of BK channels. It shows that alternative splicing plays an essential role in the regulation of cellular adaptation and plasticity.

4. DNA methylation, splicing and neurodegenerative disease

4.1 DNA methylation, DNA methyltransferase (DNMT) and DNMT inhibitor

4.1.1 DNA methylation and its role in gene expression

DNA methylation is one of the most well-studied epigenetic modifications. In mammals, DNA methylation (the presence of 5-methylcytosine, 5mC) refers to the addition of a methyl group (-CH3) by DNA methyltransferases (DNMTs) from SAM to the C5 position of cytosine residues through covalent bonding.

DNA methylation occurs globally and covers the most CpG dinucleotides (70% - 80%) and the partial non-CpG sites, including CpHG (20%) and CpHH (<10%) sites, based on the genome-wide analysis of the human genome [243, 244]. The few unmethylated CpGs are mostly found in the promoter region of many genes where they densely cluster into ‘CpG islands’ (CGIs) [245]. It has been reported that only 4% to 25% of CpG islands have been shown to be methylated in normal tissues, depending on the definition used for CpG islands [246]. By analyzing previous studies, Siegfried et al. [246] proposed that the few unmethylated regions may be protected from methylation either by the protective effect of DNA binding proteins or by the presence of the modified histone H3K4Me2/Me3. Interestingly, high CpG density, which is the major difference

separating methylated regions from unmethylated ones, is not the reason that leads to the divergence of DNA methylation status, but a consequence of less DNA methylation due to the lower mutation rate of unmethylated cytosines [246].

The regulation of gene expression by DNA methylation was initially studied by exploring CGIs at the gene promoters, which usually are restricted to long-term, stable gene silencing [247]. In humans, whole-genome bisulfite sequencing of multiple individuals showed that the repression effect of promoter DNA methylation is clear only on genes with very high DNA methylation levels. Later, genome-scale DNA methylation analysis revealed that DNA methylation could occur at different genomic regions: transcriptional start sites (TSSs), gene bodies, regulatory elements, repetitive DNA sequences, as well as transposable and viral elements [247, 248]. The genomic positions of DNA methylation exert different influences on gene regulation based on its surrounding genomic context. For example, DNA in gene bodies is extensively methylated, and the gene body methylation is more prevalent than that in the promoters. Most of them are evenly distributed in the DNA sequences but not in the form of CGIs. Also, in contrast to the promoters, DNA methylation of gene bodies is not associated with gene repression but with gene activation, which has been confirmed in diverse animal genomes by bisulfite sequencing analysis [249, 250]. However, more recently, this positive linear relationship between DNA methylation of gene body and gene expression has been debated. Using four quantification measures, Lou et al. only observed a weak global positive relationship between gene-body methylation and gene expression for the mCG/length measure based on Spearman correlation in the human genome, but not the other three measures, including Pearson correlation [251]. Also, by a meta-analysis of human genome-wide methylation, the relationship between gene-body DNA methylation and gene expression levels displayed a bell-shaped curve, but not monotonic or linear [252]. That is, the lowest and highest gene expression level corresponds to the lowest DNA methylation level, while the middle expression level with the highest DNA methylation level. It suggested that the regulation of gene expression by gene-body DNA methylation is a complex process. Although in some specific DNA regions of specific tissues, there is a positive correlation between gene-body DNA methylation and the levels of gene expression, such as DNA methylation in the large partially methylated domains (PMDs) and highly methylated domains (HMDs) in the human placenta genome [253]. But in general, it is not a simple linear relationship between gene-body DNA

methylation and gene expression level, which may be determined by the combined effects of many other factors.

The importance of DNA methylation in the regulation of gene expression has been well studied and confirmed. The most extensively studied role of DNA methylation has been implicated in the control of DNA transcription, which was discussed above referring to the promoter and gene-body DNA methylation. DNA methylation of promoters could silence the transcription initiation of protein-coding genes, non-coding RNAs and protect the genome against transposons and transposon repeats [254-256]. The regulation of gene expression by gene-body methylation also has been known to preclude aberrant transcription for the protection of gene stability by the collaboration with H3K36me3 [257]. Besides the promoter and gene bodies, DNA methylation of other genomic regions also plays a role in modulating the initiation of transcription. For DNA methylation in repetitive elements (REs), it could silence repetitive DNA elements and suppress their mobility in order to maintain genome stability, such as the repression of retroviruses, long interspersed element-1 (LINE-1) elements, Alu elements, and others [258]. The disruption of repetitive elements (RE) methylation underlies the onset/development of a wide range of human diseases. The global hypomethylation of RE is closely related to tumorigenesis, which was viewed as a promising epigenetic cancer biomarker for cell-free DNA liquid biopsy [259-261]. The aberrant RE methylation was also widely observed in neurodegenerative diseases, such as Alzheimer's disease [262]. For intragenic DNA methylation, it could repress the initiation of intragenic genes to preclude aberrant and potentially deleterious transcription and to maintain the fidelity of gene transcription initiation [263].

The role of DNA methylation in the regulation of alternative splicing of pre-mRNA has attracted increasing interest from researchers, which will be discussed in detail below. Besides DNA transcription and alternative splicing, DNA methylation also plays a role in the regulation of alternative promoter usage, intragenic non-coding RNAs and transposable elements, alternative polyadenylation and enhancer activity [264]. Interestingly, recently another important role of DNA methylation has been discovered by Zhou et al.. By comparing the whole-genome sequences and sizes of 53 organisms, they found a positive correlation between genome size and the percentage of transposable elements (TEs) while a negative correlation between genome size and the CpG observed/expected ratio in both TEs and host DNA. DNA methylation increased the C-to-T

transition mutations via deamination in the TEs and host DNA, which decreased the proportion of CpG dinucleotides and finally led to the control of transposable elements by host genes over evolutionary time [265]. It suggests that host cells expanded their own genome size by DNA methylation of transposable elements.

4.1.2 DNA methyltransferases (DNMTs) and DNMT inhibitors

There are four known human DNA methyltransferases, DNMT1, DNMT2, DNMT3A, and DNMT3B, which use a highly conserved catalytic mechanism to methylate 5-cytosine residues in genomic DNA. Analysis of DNMT expression levels by semi-quantitative RT–PCR found that DNMT1, 3a and 3b are coordinately expressed in most normal human tissues, including the human brain [266]. DNMT1 is the most abundant DNMT involved in the maintenance of methylation. DNMT3A and DNMT3B function as de novo methyltransferases required to establish and maintain genomic methylation. Different from the above three DNMTs, which possess both the regulatory N-terminal region and C-terminal catalytic domain, DNMT2 is composed solely of the C-terminal domain and has the potential to methylate RNA instead of DNA. DNMT2 is believed to participate in recognition of DNA damage, DNA recombination, and mutation repair [267]. Therefore, multiple DNMT inhibitors that can efficiently deplete DNMT1, DNMT3a and DNMT3b together are needed to deplete DNMTs for DNA methylation.

5-azaCytidine (5-azaC), 5-aza-deoxycytidine (5-aza-dC), zebularine [268] and RG108 [269, 270] are the most commonly used DNMT inhibitors in previous studies *in vivo* or *in vitro*. They represent two different mechanisms of DNMT inhibition.

5-azaC belongs to nucleoside DNMT inhibitors that also include 5-aza-dC , 5-fluro-2'-deoxycytidine (5-fluro-dC), DHAC and zebularine [271]. These nucleoside DNMT inhibitors can insert into newly synthesized DNA chains at nuclear replication sites and form a covalent complex with DNMT and irreversibly trapping DNMT [272]. Among these nucleoside DNMT inhibitors, 5-azaC is a potent and stable inhibitor of DNMT 3a *in vitro*. For example, In 2004, Schneider-Stock et al. showed that transcription of DNMT3a was inhibited severely after 24h treated with 5-azaC (1 μM) in HCT 116 colon cancer cells [273]. This inhibition effect reaches a peak at 48h and persists more than 96h, although another study showed that the half-life of 5-azaC is 17h in neutral phosphate buffer at 37℃ [274].

5-azaC can also down-regulate transcription of DNMT1 efficiently [275]. This was illustrated using a DNA methyltransferase trapping assay by measuring immobilization of nucleoplasmic GFP-DNMT1 fusion after 5-azaC/5-aza-2'-deoxycytidine treatment. In this study, it was reported that time and dose dependence (30 μM, 100 μM, 300 μM respectively) of Dnmt1 immobilization after 5-azaC and 5-aza-dC treatment, and 5-aza-dC was more potent (around fivefold more potent in the same concentration-30 μM) than 5-azaC in depleting the nucleoplasmic pool of GFP-Dnmt1. With longer incubation times, the nucleoplasmic GFP-Dnmt1 pool became progressively immobilized in cells treated with 300 μM 5-azaC or 30uM 5-aza-dC until complete depletion was reached after about 90 min or 40 min, respectively. This is consistent with the fact that 5-aza-dC is directly incorporated into DNA, whereas 5-azaC has to be modified before incorporation and can also be incorporated into RNA.

In another study, it was observed that 5-azaC resulted in a strong depletion of DNMT1 and potentially also in a weaker reduction in DNMT3B levels in HCT 116 cells. It also showed that 5-azaC (10 μM) had shown an intermediate effect on HCT 116 cells, which decreased live HCT 116 cells to 50% within 5 days, and seemed to be highly toxic to NALM-6 cells, which reduced live NALM-6 cells to around 30% within 4 days [274]. Brueckner et al. showed that DNMT1 protein was completely depleted after 48h of 5-azaC treatment [276] but had no apparent inhibition effect on DNMT3b [273].

Similar to 5-azaC, 5-aza-dC and zebularine as stable and potent DNMT inhibitors also belong to nucleoside DNMT inhibitors and can trap DNMT. 5-aza-dC (2.5 μM) can cause 95% degradation in DNMT1 level after 12h treatment but has no significant effect on DNMT3a and DNMT3b level of mouse lymphosarcoma cells at this dose [277]. Another study shows that DNMT3a and DNMT3b could also be inhibited after 48h of 5-aza-dC (10 μM) exposure in Hela cells and HCT cells [278].

Zebularine (100 μM) is reported [279] to selectively deplete DNMT1 by day 1 of treatment, and the potent depletion effect persists up to 40 days in T24 cells. DNMT3a and 3b were also affected in T24 cells, and this was most pronounced after 3 days of continuous zebularine treatment, yet both proteins gradually recovered thereafter. Moreover, in 2002, Zhou et al. found that zebularine as a novel DNMT inhibitor exerts a strong inhibition effect on M.Hha I, which is a

bacterial cytosine-[C5]-specific DNA methyltransferase and has close molecular similarity with human DNMT2 protein [272].

Different from 5-azaC etc., RG108 belongs to non-nucleoside DNMT inhibitors, which also include curcumin, procaine, hydralazine, EGCG, psammaplin A, 3-Nitro-2-flavone and Δ2-isoxazoline. RG108 can block the active site of free DNMT proteins without the formation of covalent reaction intermediates [274]. Brueckner et al. showed that RG108 has a potent inhibition effect on purified recombinant CpG methylase M.SssI, which has significant structural similarity with the DNMT1 catalytic domain. Also, they found that RG108 is a stable DNMT inhibitor with a half-life of 20 days in neutral aqueous solutions at 37℃.

To investigate the regulation of DNA methylation or for therapeutical purposes, many artificial methods were explored to induce DNA methylation in cells, including drug [280, 281], siRNA [282], piRNA [283], and depolarization by KCl treatment [284]. Based on the study of Kawasaki in 2004, siRNAs targeted to CpG islands within the promoter of a specific gene can induce transcriptional gene silencing by means of DNA-methyltransferase-dependent methylation of DNA in human cells. In 2015, Itou et al. established an artificial piRNA production system by the concomitant expression of sense and antisense mRNAs in murine embryonic testes. This system made it possible to induce gene-specific DNA methylation by piRNAs in male germ cells. Depolarization-induced DNA methylation has been a well-characterized manipulation. Recently, Hannon et al. have found that moderate chronic depolarization induced by +10 mmol/L KCl at 10 DIV for 24h can cause DNA methylation in neuron cells. These changes are mediated by calcium entry through L-type CaV1 channels and/or downstream signaling via the calcium-dependent phosphatase calcineurin.

Except for a few invertebrate genomes, most animal genomes have moderately or even very high levels of DNA methylation in a mosaic pattern or in a way referred to as global methylation [285-287]. This widespread distribution of DNA methylation in animal genomes suggests its essential roles in cells, involving not only normal development and cell functions but also a number of important human diseases [288-291].

4.2 The relationship between splicing and DNA methylation

Generally, DNA methylation is associated with condensed heterochromatin state and inhibition of gene expression. Strictly, DNA methylation displays two opposite effects on gene

expression based on the methylation of different DNA regions [252]. Gene-body methylation, which is more prevalent than promoter methylation, has been observed to be positively correlated with gene expression levels [252]. However, the CpG methylation/demethylation in promoter regions lead to the hypothesis that DNA methylation/demethylation is associated with regulation of gene expression by either directly affecting the binding of some transcription factors with their recognition sequences or by changing in chromatin states that restrict/facilitate the accessibility to transcript factors to the gene promoter [245, 292].

It has been observed that the level of DNA methylation and histone methylation H3K36me3 [293] was elevated at actively spliced genes (intron-containing genes) compared with intronless genes. H3K36me3 refers to the tri-methylations of histone H3 at lysine 36 (H3K36), which is only catalyzed by histone-lysine N-methyltransferase SETD2 (SET Domain Containing 2) [294]. The control of H3K36me3 on gene expression has been well studied. It has been reported that the level of H3K36me3 is proportional to transcriptional activity. The level of H3K36me3 is also increased by alternative splicing activation of the intron-containing gene induced by the phorbol myristate acetate (PMA) treatment in Hela cells. The level of H3K36me3 is decreased by splicing inhibition of intron-containing gene, which is induced by the treatment of transcription inhibitor DRB [293]. Since DNA methylation is known to control DNA transcription [295], does it also play a role in the regulation of co-transcriptional splicing [296], just like the effect of H3K36me3?

The mainstream answer is yes. A genome-wide study in the honeybee [297] showed that exons included in transcription had significantly higher absolute DNA methylation level (mCG/length) than excluded exons, specifically in the exonic region. Also, methylated genes were positively associated with alternatively spliced genes. Furthermore, they observed that both methylated genes and alternatively spliced genes were associated with longer gene lengths.

Moreover, the Wong group [298] and Ast group [299] indicated that dynamic DNA methylation and demethylation state of exons played a role in the regulation of splicing. Using whole-genome bisulfite sequencing (WGBS) and deep mRNA sequencing, Wong and colleagues [298] observed that more than 50% of differentially methylated CpG sites (DMSs) were located at exons and introns compared between promyelocytes and granulocytes. Considering that WGBS won’t distinguish 5´-methylation from 5´-hydroxymethylation of cytosine, further analysis by

RRHP (Reduced Representation 5-Hydroxymethylcytosine Profiling) was done and showed that the average exonic DNA 5´-hydroxymethylation (5 hmC) is positively associated with the inclusion level of these exons. This study indicated that dynamic methylation status is involved in the regulation of splicing in the terminal stage of granulopoiesis. However, the underlying mechanism remains unclear.

Interestingly, Ast et al. reported that DNA methylation did regulate the inclusion level of alternative splicing [299]. Using the CRISPR technique, they methylated specific regions of EDI (extra domain I) minigenes by the cotransfection of sgRNAs (single guide RNAs) with dCas9-DNMT3A-DNMT3L (fusing the DNMT3A-DNMT3L protein to the deactivated form of Cas9) into HEK293 cells, respectively. EDI is the first alternatively spliced region of human fibronectin (*FN1*) gene (also known as EDA and EIIIA) and was usually used in the form of minigene to study the mechanisms underlying the regulation of alternative splicing events in *in vivo* experiments [59, 60, 300, 301]. Also, they demethylated specific regions of EDI minigenes by the co-transfection of sgRNAs with dCas9-TET1 into Met+ HEK293T cells. By BS-PCR, they found that the demethylation of alternative exon (from 100% to 84.6%) decreased its inclusion level (Index: from 1 to around 0.3), but not the demethylation of the flanking intron or constitutive exon. However, the hypermethylation of the alternative exon, constitutive exon, or their flanking intron did not significantly change the inclusion level of exons. This study indicated a direct relationship between exonic demethylation and the regulation of alternative splicing, but the relationship between hypermethylation and alternative splicing is still unclear.

Interestingly, an opposite conclusion of the relationship between DNA methylation and splicing has been raised recently. Nanan et al. reported that unlike the strong association of H3K36me3 with minigene splicing potential, DNA methylation status was irrespective of the minigene splicing capacity [302]. A panel of minigene platforms was generated for the study of the relationship between DNA methylation and splicing. It contained spliced two-exon minigenes with differentially splicing capabilities (splicing competent gDNA, splicing deficient ΔSS, splicing partially restored ΔSS+5´3´, intron deleted minigene) and unspliced one-exon minigenes (splicing deficient gDNA, modified gDNA with heterologous splice sites). They found that the highest H3K36me3 level at the gene body corresponded to the highest splicing capability. However, methylation-sensitive restriction enzymes-polymerase chain reaction (MSRE-PCR) and

bisulfite pyrosequencing analysis of specific methylation sites of minigenes showed that the *de novo* and maintenance of DNA methylation was not impacted by their splicing potential of constitutive exons.

Therefore, the relationship between DNA methylation and splicing is debatable. These opposite views will draw more attention to this issue, stimulating researchers for further investigations.

4.3 The known mechanisms that convey DNA methylation information into alternative splicing

In the past decade, two models have been proposed to explain the effect of DNA methylation on alternative splicing. Firstly, a kinetic model, also called the "window of opportunity" model, has long been proposed by Kornblihtt et al. to explain the impact of transcription elongation rate on splicing [62]. Researchers found that the elongation rate of transcription varied throughout the transcription process of a gene, from one gene to another. The highly dynamic transcription elongation rate impacted the cotranscriptional processes, including splicing [53, 59, 303]. The other model is the recruitment model, in which adaptor protein binds to DNA methylation regions and recruits splicing factors which will play diverse roles in alternative splicing.

Three adaptor factors have been studied in detail in the regulation of splicing by DNA methylation. One is CTCF. In 2011, Shukla et al. provided the first evidence that DNA methylation has an impact on the regulation of alternative splicing through DNA-binding factor CTCF (CCCTC-binding factor) in a kinetic model. They found that when DNA is unmethylated, CTCF can bind to the alternative exon and create a roadblock for RNA polymerase II elongation, which results in the inclusion of weak upstream exon on the mRNA. However, if the DNA binding site of CTCF is methylated, binding of CTCF is prevented and subsequently increases the rate of RNA polymerase II elongation, and thus leads to exon skipping. This pathway functions in a mammalian model system for alternative splicing of a specific exon in *CD45* gene, as well as alternative splicing in a genome-wide scale [56, 304].

Moreover, the methylcytosine dioxygenases TET proteins were involved in this process through the conversion of 5mC into 5-hydroxymethylcytosine (5hmC) [305, 306]. In a genome-wide scale, methylated DNA immunoprecipitation (MedIP) analysis showed that 5mC and 5hmC

reciprocally exchange strictly at CTCF-binding sites in CTCF-binding and the absence of CTCF binding cells, respectively. 5hmC was required for the inclusion of CTCF-regulated CD45 exon, while 5mC displayed an opposite function. This study indicated that the dynamics of DNA methylation contributed to an additional layer of the regulation of pre-mRNA splicing.

Interestingly, CTCF was required for the splicing of presynaptic CaV channel Cacna1b gene and preferred the CaV2.2 channel isoforms with increased opioid sensitivity in mice, likely through the hypomethylation of an alternative exon in CaV2.2 gene in DNMT inhibitor and TET assays [307]. Besides alternative splicing, CTCF linked the regulation of alternative polyadenylation to gene body CpG methylation through the recruitment of cohesion complex and the formation of chromatin loop to modulate transcriptome diversity [308]. These data indicated that CTCF was a splicing regulator required for the splicing of some exons, and also played an important role in opioid addiction. The regulation of splicing by CTCF was likely controlled by the DNA methylation status in the gene body or specific exon through a kinetic or/and a recruitment model. However, no direct evidence supports this speculation so far. We still do not know which splicing factors are involved in this machinery and how it works.

Another adaptor factor is MeCP2 (methyl-CpG binding protein 2). The regulation of splicing by MeCP2 was first reported by Zoghbi et al., as well as the observation of aberrant alternative splicing in Rett syndrome of mouse model [309]. Later, Maunakea et al. found that similar to CTCF, MeCP2 was also involved in the DNA methylation-mediated alternative splicing by regulating the elongation rate of RNA pol II. But the difference is that, with the presence of DNA methylation, MeCP2 binds to the exon and recruits enzymes with HDAC activity, which slows Pol II elongation and thus leads to elevation of exon inclusion in the mRNA. Since MeCP2 is enriched at the DNA level in a specific fraction of alternative exons, MeCP2 likely regulates alternative splicing of particular exons [57].

Secondly, it refers to a recruitment model. Interestingly, besides the kinetic model, MeCP2 could also regulate the alternative splicing by interaction with splicing factors in a cell line, primary neurons, and the brain [310-314]. Chang et al. [310] reported the interaction of MeCP2 with multiple splicing regulators, including TDP-43, LEDGF, DHX9, FUS, hnRNP H, and hnRNP F. Global splicing was disrupted in a mouse model of Rett syndrome with MeCP2 mutation, including the splicing of Gria2 flip/flop, which is related to synapse plasticity. The global splicing change

was accompanied by the dissociation of MeCP2-binding splicing regulator LEDGF, suggesting the potential impact of the interaction on the regulation of splicing, including Gria2 flip/flop. Moreover, Wong et al. showed that 5-azaC inhibition of DNA methylation or DNAMT3A and 3B knockout reduced the binding of MeCP2 near splice junctions flanking introns and facilitated intron retention, which was negatively associated with the occupancy of MeCP2-binding splicing factors Srsf family and Tra2b, but positively associated with RNA polymerase II stalling near the splicing junction of the retained intron in different primary cells and cell lines [311]. Thus, the kinetic model and recruitment model might work in combination to confer the effect of DNA methylation on pre-mRNA splicing. Interestingly, the regulation of splicing by MeCP2 was indirectly related to the impact of CTCF and TET on the learning-dependent alternative splicing of the brain-derived neurotrophic factor gene in turtle (tBDNF). MeCP2 knockdown did not affect the expression of CTCF but decreased its binding to tBDNF [312].

More interestingly, MeCP2 has been shown to regulate activity-dependent splicing in the mouse hippocampus tissue [315]. Upon the treatment of calcium signal-activating kainic acid, a potent neuroexcitatory amino acid agonist that acts by activating glutamate receptors, a group of exons of synapse-related genes displayed aberrant splicing in mice of the MeCP2 mutant group compared to that in the wild-type group. Oliveira et al. further showed that MeCP2 was required for the regulation of pre-mRNA splicing not only in basal conditions but also splicing response for spatial learning formation by RNA-Seq analysis [316].

Together, it indicates that MeCP2 is required to maintain the splicing in the transcriptome and to finetune splicing response to depolarization or learning activity, likely through the kinetic model and the recruitment model in combination. However, these data support the regulation of splicing by MeCP2 but did not provide direct evidence to prove the impact of DNA methylation on pre-mRNA splicing through MeCP2. Besides, the regulation of splicing has been argued to be not a major function of MeCP2 [314].

The third adaptor factor is HP1 (heterochromatin protein 1), another factor of the recruitment model. Both HP1α and HP1β have been involved in the regulation of alternative splicing by DNA methylation. Using the EDI minigene assay, it concludes that with the presence of H3K9 tri-methylation of chromatin, HP1 binds to the methylated chromatin of EDI gene and mediates DNA methylation’s effect on splicing by recruiting splicing factor SRSF3 to its

methylated form and enhancing SRSF3's role as a splicing silencer and thus lowering the inclusion level of target exon [317].

4.4 DNA methylation, pre-mRNA splicing and Rett syndrome

4.4.1 The impact of DNA methylation on various progressive diseases

Altered DNA methylation has been widely observed in numerous progressive diseases, which becomes worse over time, including immune-mediated diseases [318] (such as rheumatoid arthritis [319]), metabolic diseases [320] (such as type 2 diabetes mellitus [321]), cardiovascular disease [322] (such as dilated cardiomyopathy [323]), chronic kidney disease [324], neurodegenerative diseases [325] (such as Alzheimer's Disease [326]), genetic neurodegenerative diseases (such as Rett syndrome [327], mostly caused by MeCP2 mutation, and Huntington disease [328]), and some other rare diseases [329] (such as Hereditary Sensory Neuropathy [330], caused by DNMT1 mutation), and also linked to various tumors [331] (such as breast cancer [332]). However, the molecular mechanisms that link DNA methylation with the development of progressive diseases remain poorly understood.

Also, the aberrant RNA splicing of transcriptome-wide or specific genes has been reported in various progressive diseases, such as in rheumatoid arthritis [333], type 2 diabetes [334], dilated cardiomyopathy [335], chronic kidney disease [336], Alzheimer's Disease [337], Rett syndrome [338], and Huntington disease [339]. As discussed above, the regulation of DNA methylation on pre-mRNA splicing has been widely reported in *in vitro* experiments, although some opposite views were also proposed. The concurrent aberrations in DNA methylation and alternative splicing shed new light on the mechanisms that link DNA methylation with the development of progressive diseases, with an emerging realization that the implication of DNA methylation on the development of these progressive diseases may rely heavily on its regulation of pre-mRNA splicing.

Neurodegenerative diseases are a group of chronic, progressive disorders 'characterized by slow progressive loss of neurons in the central nervous system (CNS), which leads to deficits in specific brain functions (e.g., memory, movement, cognition) performed by the affected CNS region'[340], including Parkinson's disease (PD), Alzheimer's disease (AD), Huntington's disease, amyotrophic lateral sclerosis (ALS), Rett syndrome, etc.. The regulation of neurodegenerative diseases at the gene expression level by DNA methylation has been well studied, such as in

Alzheimer's disease, Parkinson's disease, amyotrophic lateral sclerosis, Huntington's disease, and hereditary ataxias [341, 342]. For example, it has been reported that there were more relevant in terms of the correlation between DNA methylation and dendritic spine density in the cortical layer in non-psychiatric controls compared with that in schizophrenia (SZ) subjects via DNA methylation genome-wide analysis of postmortem brain, including BAIAP2 and DLG1 gene. Specifically, they observed that 43.2% of DNA methylation sites of the BAIAP2 gene were significantly hypomethylated in SZ subjects [343].

4.4.2 DNA methylation, pre-mRNA splicing and Rett syndrome

Rett syndrome (RTT, MIM 312750) is a rare genetic and postnatal progressive neurodevelopmental disease, which is typically recognized in early childhood (6 to 18 months). RTT usually leads to shortened life expectancy, which is determined by the age when symptoms first started and their severity [344]. RTT is one of the most common causes of mental retardation and severe intellectual disability in females. A broad array of symptoms is caused by RTT, which includes 'the loss of language skills, fine and gross motor skills, communication skills, deceleration of head growth, and the development of stereotypic hand movements occurring after a period of apparently normal development [344].

RTT occurs almost exclusively in girls and is only rarely seen in boys since it's an X-linked dominant disorder with lethality in hemizygous males. RTT is caused by mutations in the X-linked *MECP2* gene, encoding the canonical methylated CpG (5mCpG) binding protein, which was first identified in 1999 [345]. More than 95% of individuals with typical RTT present at least one mutation in MeCP2 [346]. Notably, besides RTT, MeCP2 mutations have also been reported in other neurodevelopmental diseases, such as Angelman syndrome [347] and non-specific mental retardation [348]. It suggests that MeCP2 mutation is not the only determinant of the disease, and other factors should be involved in the onset and the development of RTT.

The most common RTT-associated missense mutation is MeCP2 T158M (547C→T), which was firstly reported in 1999, together with other mutation types, including the missense mutations of F155S (538T→C), R133C (471C→T), and R106W (390C→T), as well as nonsense mutation (837C→T) and an insertion (694insT) at codon 208 shifts the reading frame [345]. Until now, more than 200 MeCP2 unique mutations have been discovered as the cause of RTT (Rettbase; http://mecp2.chw.edu.au/). MeCp2 mutation types have been reported to be a strong predictor of

disease severity [349, 350]. For example, particular mutations such as p.Arg133Cys, p.Arg294X, p.Arg306Cys, 3´ truncations, and other point mutations were significantly less severe than p.Arg106Trp, p.Arg168X, p.Arg255X, p.Arg270X, splice sites, deletions, insertions and deletions [350]. It explained the drastic differences in disease severity between the RTT cases. However, the underlying mechanism has still been unclear. The investigation of the relationship between MeCP2 mutation types and disease severity would provide a potential target for RTT drug study.

Interestingly, a recent study found that the elevated MeCP2 T158M expression is accompanied by increased binding of MeCP2 T158M to DNA and ameliorated multiple RTT-like features in both males and females MeCP2 T158M–knockin ($Mecp2^{T158M}$) mice. It indicates that MeCP2 T158M mutation leads to functional impairment compared to wild type, and the overexpression of MeCP2 T158M may work as an alternative therapeutic approach for RTT patients [351].

As discussed in the above section, MeCP2 acts as a DNA methylation reader, mediating the regulation of gene expression, including chromatin organization, transcription and alternative splicing. The MeCP2 mutation would result in alterations in gene expression level in the RTT brain, which was confirmed with solid pieces of evidence [309, 315]. At the RNA splicing level, it has been reported that there was aberrant splicing of endogenous genes in the cerebral cortex in a mouse model of RTT ($Mecp2^{308/Y}$ mice) based on transcriptome-wide analysis [309]. Later, researchers reported activity-dependent aberrant gene expression and alternative splicing in the mouse model of RTT (Mecp2-Null mice) [315]. These aberrations in mRNA level and alternative splicing were induced by neuron activity in the mice's RTT brain. It is consistent with the increase of clinical severity with age. However, we do not know how extracellular stimulation has been converted into signals that lead to aberrant gene expression with the MeCP2 deficiency. Is it involved in the dynamics of DNA methylation? Do other factors or molecules play a role in this signaling pathway? Further exploration is needed to answer these questions.

In the following chapters, I will present our investigation on adaptive splicing and its control by DNA methylation. Contents in these chapters have integrated most of the manuscript that has been submitted for peer review in *Nucleic Acids Research* (Ling Liu, Hai Nguyen, Urmi Das, Jian-Kun Yu, Lei Lei, Matthew Kung, Shervin Pejhan, Mojgan Rastegar, Jiuyong Xie.

Control of Adaptive Splicing by DNA Methylation.). The relative contributions of other authors are as follows.

- Hai Nguyen: wrote scripts and mapped DNA bisulfite sequencing reads into the reference genome by BSmap program and to exons in the genome.
- Urmi Das: mapped RNA sequencing reads into the reference genome by DEXSeq or MATS program.
- Jian-Kun Yu: carried out the experiments in Fig. 11E-F ans S_Fig. 4.
- Lei Lei: carried out the hnRNP L and hnRNP LL knockdown experiments in the previous study, the data from which was reanalyzed by Ling Liu and used in the Fig. 11A, and help to refine the graph of Fig. 14.
- Matthew Kung: analyzed the hnRNP L/LL target exons and contributed to Fig. 11B.
- Shervin Pejhan: collected the samples of hippocampus and cerebella tissue of Rett syndrome patients and extracted RNA from the collected tissues.
- Mojgan Rastegar: collaborating principal investigator for the project providing the hippocampus and cerebella tissues of Rett syndrome patients.
- Jiuyong Xie: proposed the hypothesis of the thesis, helped to design the experiments, guided Ling Liu to carry out the experiments and to revise the paper writing, and coordinated the collaboration with Prof. Mojan Rastegar's lab and other authors.

CHAPTER II Rationale and Hypothesis

Rationale:

In adaptation to changing environments, animals or cells respond differently to repeated stimulations from that to a single stimulation by addictive drugs, exercises, hypoxia, etc., which often involves gene regulation [352-357]. Among the many steps of regulation, alternative pre-mRNA splicing [28], a common way to diversify the transcriptomes and proteomes in metazoans [358, 359], should play an important role in this process. Based on the previous studies, alternative splicing is not an immutable but plastic and dynamic process under precise temporal and spatial control. More interestingly, it dynamically responds to the various extracellular stimulations, which is a process involved in multiple signal transduction pathways and molecules, and controlled by the combined effects of specific RNA elements, cis- and trans-acting factors, epigenetic modifications as well as other regulatory factors. Consequently, the highly diverse and dynamic splice variants in the mammalian transcriptomes allow for the fine-tuning of gene functions in response to the changing environment. However, little has been known about the role of alternative splicing in this process, no matter the potential mechanisms behind the possible regulation of alternative splicing in the face of environmental changes.

We have found that the stress hormone axis-regulated exon (STREX) of the BK potassium channel gene is regulated by depolarizing concentrations of KCl [110]. The regulation predicted adaptive splicing for the fine-tuning of cellular electrical properties by repeated stimulations differently from that by the first-time stimulation [110, 169]. Interestingly, chronic inactivity- or depolarization-induced alternative splicing of the BK channel, AMPA receptor, or neurexin gene is critical for the homeostasis of electrical properties or synaptic formation [115, 133, 134, 169]. Moreover, the regulation is mediated by the Ca^{++}/calmodulin-dependent protein kinase IV (CaMKIV) and its downstream splicing factors hnRNP L/LL [75, 83, 110, 169, 360], Sam68 [115], or Nova-2 [133], depending on the target exons. In particular, hnRNP L binds a CA-rich CaMKIV-responsive RNA element (CaRRE) upstream of the STREX exon to inhibit U2AF65 binding [75, 110, 361]. In addition, histone modifications also regulate depolarization-induced splicing [113, 169, 362]. Importantly, the depolarization effect on splicing is reversible [360]. However, adaptive splicing, i.e., a distinct splicing response to repeated stimulations differently from a one-time stimulation, remains to be clearly demonstrated at both specific exon and transcriptome levels.

DNA methylation, an epigenetic modification, plays an important role in adaptation [101, 357, 363]. DNA methylation levels are correlated with exon inclusion in the genome/transcriptome [297, 364], which is supported by some [299, 317], but against by others [302]. For some studies, methylated DNA interacts with some adaptor proteins, such as Methyl-DNA-binding protein MeCP2, methyl-free DNA-binding CTCF and methyl-lysine chromatin-binding HP1, to control splicing through different mechanisms [57, 307, 309, 317]. In particular, MeCP2 binds the methyl-CpG, hmCA or mCAC di- or tri-nucleotides [365, 366], and regulates gene transcription and splicing [57, 309, 367, 368]. *MECP2* mutations are found in 92% cases of typical Rett syndrome [345, 346, 369], a severe, progressive neurodevelopmental disorder with autistic features [344, 370], to which progressive, abnormal brain activities including epilepsy often contribute to clinical severity [371, 372]. In a *Mecp2*-null mouse model of Rett syndrome, the expression of long genes tends to be preferentially affected [366, 367, 373], and the splicing response of synaptic exons is aggravated in the hippocampus upon treatment by the calcium signal-activating kainic acid [315]. Interestingly, both DNA methyltransferase DNMT3a and MeCP2 are regulated by calcium singling: DNMT3a recruited by the CaMKIV-regulated cAMP-responsive element modulator (CREM)α in T lymphocytes [374-376], and MeCP2 phosphorylated by CaMKII in hippocampal neurons [377]. MeCP2 likely controls alternative splicing through its recruitment by methylated DNA [57], and interaction with splicing factors including YB-1 [309-311, 313, 378]. However, a recent bioinformatics analysis reported only minimal effects of DNMTs and MeCP2 on alternative splicing globally through experimental evidence yet to be provided [379]. The various reported effects of DNA methylation or MeCP2 on splicing demands clarification using side-by-side global methylation and splicing analysis and/or direct methylation of exon DNA for splicing assays.

Based on the previous studies, I proposed that if treated by two or more KCl treatments, cells will display adaptively desensitized excitability, thus, leading to an adaptive change in splicing response to KCl. However, do all alternative exons have the adaptive splicing response upon repeated KCl treatments with the same concentration in the transcriptome-wide scale? Will these adaptive splicing responses of exons induced by repeated cellular excitations try to maintain homeostasis (adaptive desensitization) or boost the original splicing response induced by single cellular excitation (adaptive hypersensitivity)? Moreover, if there is adaptive splicing upon repeated cellular activities, what mechanisms and molecules may contribute to this process? Is DNA methylation involved in the regulation of this process?

Therefore, the focus of this thesis project is on investigating if alternative splicing contributes to an extra layer to the underlying mechanism of cellular adaptation in response to repeated stimuli in the form of adaptive splicing, and the role of DNA methylation in the control of alternative splicing and adaptive splicing in response to extracellular stimulations, as well as its correlation with pathophysiological activity or disease.

Hypothesis:

I hypothesize that there's transcriptome-wide adaptive splicing upon repeated extracellular stimulations, which is under the regulation of DNA methylation.

Thesis work overview:

Using our established inducible splicing system, I first delineated the impact of repeated depolarization and exon DNA methylation on adaptive splicing in pituitary cells. The inclusion level of most of the detected exons did not change substantially between the repeated treatments and a single treatment upon membrane depolarization, supporting the strong homeostatic expression of the majority of exons and characteristic genes during the experiment. Interestingly, the inclusion of a specific group of synaptic exons was changed adaptively upon repeated stimulations.

Next, I investigated the effect of DNA methylation on the splicing, splicing response to membrane depolarization, and adaptive splicing induced by repeated extracellular stimulations. The exon inclusion, splicing response to KCl-induced depolarization, and adaptive splicing was disrupted globally by the DNA methylation modulator 5-azaCazacytidine. Methyl-CpG-dependent augmentation of the inducible splicing was confirmed using both whole-genome bisulfite DNA sequencing (WGBS) and RNA-Seq in combination with *in vitro* methylated reporter exons for transient splicing assays. Moreover, aberrant splicing of the synaptic exons also occurred upon 5-azaC treatment of the pituitary cells, or upon mutations, particularly within the methyl-C- or splicing factor-binding domain of the MeCP2 in the hippocampus of Rett syndrome patients. Thus, exon DNA methylation controls adaptive pre-mRNA splicing upon repeated cell excitations, and disruption of this regulation contributes to the aberrant splicing of neurological diseases.

CHAPTER III Materials and Methods

Materials

Mammalian cell lines

GH3	rat pituitary tumor cells, derived from female pituitary gland
HEK293T	human embryonic kidney cells, derived from female fetal kidney
LA-N-5	human neuroblastoma cells, derived from bone marrow of a male patient suffering from neuroblastoma
N1E	male mouse neuroblast cells
PC12	rat pheochromocytoma cells, derived from male adrenal gland

Materials for cell culture

Material	Manufacturer
B-27® Supplement (50×), serum-free	Fisher Scientific
Cell culture plate	Falcon
CO_2 gas	Welders Supplies
Disposable latex gloves	Ocean Pacific
Disposable Petri Dishes, Sterile	Falcon
Disposable serological pipets	Falcon
F-10 Nutrient Mixture (Ham) (1×), liquid	Invitrogen
Fetal Bovine Serum (FBS)	Invitrogen or Sigma
Gibco® Dulbecco's Modified Eagle Medium (D-MEM) powder	Invitrogen
Gibco® Penicillin-Streptomycin, 100X Solution	Invitrogen
GlutaMAX™ Supplement	Fisher Scientific
Horse serum (HS)	Invitrogen
L-Glutamine, 200mM Solution	Invitrogen
Neurobasal®-A Medium	Invitrogen/Gibco
Opti-MEM™ I Reduced Serum Medium	Gibco
Phosphate Buffered Saline (PBS) Tablet	MP Biomedicals
Polypropylene centrifuge tubes	BD FALCON
Polypropylene tubes with snap cap	VWR

Pipet Tips	VWR
Trypsin, 2.5%	Cellgro

***E.coli* strains**

DH5α	Xie lab

Antibodies

Anti-hnRNP L (4D11)	Santa Cruz
Anti-Ser16-PTB	Xie lab
Anti-YB-1	Xie lab

Chemicals and reagents

2-mercaptoethanol	Sigma-Aldrich
Agarose Powder	VWR
Agarose-GPL/LE	American Bioanalytical
Ampicillin	Fisher Scientific
Bovine serum albumin, RNase free	Fisher Scientific
Diluted SAM	NEB
Dimethyl Sulfoxide (DMSO)	Fisher Scientific
Dithioreitol (DTT)	Fisher Scientific
Ethanol (95%)	Fisher Scientific
Ethidium bromide (EtBr)	Sigma-Aldrich
Ethylenediamine Tetraacetic Acid (EDTA)	Fisher Scientific
Gibco® D-Glucose	Sigma-Aldrich
Glycerol	Fisher Scientific
Glycine	Fisher Scientific
Hydrogen chloride	ACROS Organics
Instant skim milk powder	Nestle
Isopropanol	Fisher Scientific

LB Agar	Fisher Scientific
LB Broth	Fisher Scientific
Lipofectamine® 3000	Invitrogen
Magnesium chloride ($MgCl_2$)	Fisher Scientific
Methanol	Fisher Scientific
Neurobasal®-A Medium	Invitrogen/Gibco
Nifedipine	Sigma-Aldrich
Igepal CA-630	Fisher Scientific
Oligoes & Primers Designed	IDT (Integrated DNA Technologies)
P3000™ Reagent	Invitrogen
Phenylmethylsulfonyl fluoride (PMSF)	Fisher Scientific
Phosphate Buffered Saline (PBS) Tablet	MP Biomedicals
Polybrene (Hexadimethrine bromide)	Sigma-Aldrich
Polyoxyethylene-20-sorbitan Monolaurate (Tween 20)	Fisher Scientific
Potassium chloride (KCl)	Fisher Scientific
Sodium chloride (NaCl)	Fisher Scientific
Sodium dodecyl sulfate (SDS)	Fisher Scientific
Sodium Orthovanadate (Na_3VO_4)	Fisher Scientific
Tris base	Fisher Scientific (J.T. baker)

Enzymes and buffers

10 × Buffer B	Invitrogen
10 × Buffer O	Invitrogen
5 × First strand buffer	Invitrogen
5 × Forward buffer	Invitrogen
ApaI	Invitrogen
BglII	Invitrogen
BstUI	NEB
CpG Methyltransferase (M.SssI)	NEB

dNTP set	Invitrogen
DTT, 0.1M	Invitrogen
Methyltransferase Reaction Buffer	NEB
M-MLV Reverse Transcriptase	Invitrogen
RNase inhibitors	BIO BASIC INC
T4 DNA ligase	Invitrogen
T4 DNA ligase reaction buffer	Invitrogen
Taq DNA polymerase	Xie lab

Kits

GenElute Mammalian Total RNA Miniprep Kit	Sigma-Aldrich
Plasmid Midi Kit	QIAGEN
Plasmid Mini Kit	QIAGEN
QIAEX II Gel Extraction Kit	QIAGEN
QIAquick Gel Extraction Kit	QIAGEN

Others

Filter (0.22 μm)	NALGENE
Aluminum Foil	Fisher/ Fisherbrand
Dry ice (solid CO_2)	Praxair
Kimwipes	Fisher
Lambda DNA/EcoRI + HindIII Markers	Xie Lab
PBS-MspI DNA Marker	Xie Lab
Plasmid sequencing	Robarts Research Institute
Polyvinyl Wrapping Film	Fisher
Strips of Eight Tubes and Caps	VWR (Axygen)
Western blotting detection reagent	GE Healthcare

Buffers and solutions

0.5 M EDTA·2Na

EDTA·2Na·2H_2O	37.224 g
Nanopure H_2O	150 ml
Adjust pH to 8.0 with NaOH pellets.	
Fill up with nanopure H_2O to 200 ml, autoclave, stored at 4 ˚C.	

1 M Tris·HCl

Tris base	60.57 g
Nanopure H_2O	400 ml
Adjust pH to 7.5 with 6 N HCl.	
Fill up with nanopure H_2O to 500 ml, autoclave, stored at 4 ˚C.	

1 × TE Buffer

10 mM Tris·HCl	2.0 ml
1 mM EDTA	0.4 ml
Fill up with nanopure H_2O to 200 ml, autoclave, stored at 4 ˚C.	

10 × TBS Solution

5 M	NaCl	292.5 g
0.2 M	Tris·HCl (pH 7.5)	200 ml
Fill up with nanopure H_2O to 1 L, through 0.45 μm filter, stored at room temperature		

10 × PCR Buffer (40 ml)

200 mM	Tris·HCl (pH 8.3)	8.0 ml
15 mM	$MgCl_2$	6.0 ml
250 mM	KCl	2.5 ml

0.5%	Tween-20	667 µl
1 mg/ml	BSA (Inactivated)	800 µl
	nanopure H_2O	22.033 ml
Stored in aliquots at -20 ˚C.		

PCR Mix I (21.64 ml)

	10 × PCR buffer	2.5 ml
100mM	dNTP (dATP, dTTP, dGTP, dCTP)	50 µl each
100mM	$MgCl_2$	125 µl
	nanopure H_2O	18.815 ml
Together with the Mg^{2+} contained in 10 × PCR buffer, the final concentration of Mg^{2+} in PCR reaction is 2mM.		
Stored in aliquots at -20 ˚C.		

NP-40 Buffer (Nonidet-P40)

150 mM	NaCl	4 M
10 mM	Tris· HCl (pH 7.5)	1 M
1 mM	EDTA·2Na	0.5 M
0.325%	Igepal CA-630	20%
Fill up with nanopure H2O to 200 ml, autoclave, stored at 4 ˚C.		

RT Mix I

5 × First strand buffer	400 µl
dNTP (100 mM, dATP, dTTP, dGTP, dCTP)	2.5 µl each
DTT (0.1 M)	200 µl
nanopure H_2O	90 µl
Mix well, stored at -20 ˚C.	

Methods

Cell culture

Rat GH3 pituitary cells were cultured at 37 °C with 5% CO2 in Ham's F10 nutrient mixture with 10% horse serum (HS), 5% fetal bovine serum (FBS), mouse N1E and human LA-N-5 neuroblastoma cells in Dulbecco's Modified Eagle's Medium (DMEM) with 10% HS, rat adrenal phaeochromocytoma (PC12) cells in DMEM with 10% HS, plus 2.5% FBS, and human embryonic kidney (HEK) 293T cells in DMEM with 10% FBS. Penicillin-streptomycin-glutamine solution was added to all cultures except GH3 (without glutamine). Adhesive cells were dispersed by trypsin (0.05%, w/v) - EDTA (0.53 mM) solution during subculture.

Cell growth evaluation

Before measurement, cell clusters were pipetted into separated single cells. Mix 1 part of 0.4% trypan blue [380] and 1 part cell suspension. Incubate the mixture ∼3 min at room temperature. The total number of cells that have clear cytoplasm (viable cells) were counted on day 0, day 2 and day 5.

Repeated chemical treatments

For the repeated KCl treatment group, cell cultures were treated with KCl (50mM) for 6h, then washed and supplied with fresh complete culture medium, followed by incubation for 18h, completing the 1st round (day) of the KCl treatment, and the treatment was repeated up to the 6th time (6th KCl). For the single KCl treatment group (1st KCl), cells went through the same medium change process except that the KCl (50mM) was added on the 6th day together with the 6th KCl group. In some experiments (1st or 6th KCl), 5-azacytidine or DMSO (1nm, 1μm, 10 μm, 20μm or 50μm) was added to fresh culture medium for 18h in total. Cell density was maintained throughout the experiment by splitting them into extra dishes. Total or Cytoplasmic RNA were collected before and after the 1^{st} and 6^{th} KCl treatments using GenElute Mammalian Total RNA Miniprep Kit (QIAGEN) or QIAquick Gel Extraction Kit (QIAGEN), respectively.

For cytoplasmic RNA, cells were lysed in 0.325% NP-40 buffer (the details shown in the ‘CHAPTER III Materials and Methods’). Based on preliminary tests, 0.325% NP-40 buffer can break the cell membrane but not the nuclear membrane. Cytoplasm suspensions and nuclear pellets were separated by centrifugation at 14,000 rpm for 5 min. The cytoplasm suspensions were used

for the RNA extraction by QIAquick Gel Extraction Kit (QIAGEN), while the nuclear pellets were stored at -20°C for the subsequent DNA extraction.

RNA-Seq and WGBS analyses

RNA-Seq analyses were performed the same as our previous procedures [89], except that the Illumina HiSeq4000 paired-end 100-bp sequencing was used for the total RNA of non-treated (NT), 1st KCl, or 6th KCl samples, and the Illumina NovaSeq 6000 S2 paired-end 100-bp sequencing was used for the cytoplasmic RNA of the 6th KCl samples with or without 24h pre-treatment by 5-azaC (50μm). The DEXSeq identifies alternative exons, alternative transcription starts and alternative polyadenylation [89, 381]. MATS identifies alternative splice junctions [382].

For WGBS analyses, approximately 1 μg of gDNA each sample was subject to bisulfite conversion for shotgun library construction (NEB Ultra II) and Illumina HiSeqX PE150 sequencing, yielding 150-bp paired-end reads. DNA quality control, library preparation, Illumina library quality control and Illumina HiSeqX PE150 sequencing were conducted at the McGill University Génome Québec Innovation Centre (Montréal, Québec, Canada). We obtained an average of 66 ± 4 million of paired-end reads. The sequence quality was verified using FastQC [383], with the high-quality reads mapped to the rat genome assembly Rnor_6.0.84 (GH3 samples) or mouse assembly GRCm38 (mm10, hippocampus tissue samples), using BSMAP [384], allowing a maximum of 2 mismatches. The DNA methylation status of individual cytosines of each exon was obtained by filtering the BSMAP output list with the genomic coordinates within the DEXSeq list of changed exons. The total DNA methylation level of an exon (mCpG or mCpH, (CpG methylation or CpH methylation, respectively)) was calculated by multiplying the average methylation ratio of CpG or CpH cytosines with the total number of mCpG or mCpH sites, respectively, in the sense strand of each exon.

For both RNASeq and WGBS, visualization of genomic sequencing data was explored by Integrative Genomics Viewer (IGV) (developed at the Broad Institute of MIT and Harvard, available for download from https://software.broadinstitute.org/software/igv/) [385]. To understand the biological meaning behind a large list of significant genes, functional annotation of these genes was performed by the Database for Annotation, Visualization and Integrated Discovery (DAVID) (developed at the U.S. National Institute of Allergy and Infectious Diseases, available on the Internet at https://david.ncifcrf.gov/) [386].

Semi-quantitative RT-PCR

RT-PCR was performed based on our previous procedures [75, 89]. Briefly, for reverse transcription, 300ng of cytoplasmic RNA was used in a 10ul- reaction and incubated at 45°C for 50min. For PCR, 1ul of RT product was amplified in a 12.5ul-reaction for 28 -32 cycles. PCR products were resolved in 2-2.5% agarose gels containing ethidium bromide (EtBr), visualized under UV light and captured by a digital camera. Percentages of the splice variants were calculated based on band intensities quantified using ImageJ (National Institutes of Health).

Table 1. Primers for RT-PCR analysis

Table1.1 Primers for RT-PCR analysis using Rattus norvegicus (Norway rat) genome assembly

Targeted Sequences	**IGV Location (RGSC 6.0/rn6)**	**Primers (5´->3´)**
Rims2 Exon 21	7:78453733-78453775	F: TGTCCAGACCAGTCCGTCAAG
		R: CATCACTGTCCGAGGATTTAG
Rps24 Last Exon	16:762006-762075	F: TGAGCCTAAACACAGACTTGCG
		R1: GCCATACTATGGAAACCGTC
		R2: AGTCACCGTAGAACTACTCC
Ehmt2 Exon 9	20:4584122-4584223	F: TGAAGCCATCCAGGAAACGG
		R: ACTTTCGGTGGCCATACACTTG
STREX	15:923843-924016	F: CACATTGGAGTCCATGTTGTC
		R: AGTGCCTTCGTGGGTCTGTCC
Epb41l3 Exon 15	9:117650309-117650344	F: TGATGGAGAGACCAGTGCCAC
		R: CAGGTACAAGTGGCTCAATCATGG
Dlg1 Exon 20a	11:72200684-72200784	F: GGTCCTAATATGATGACTGGTCGG
		R: CAGATGGTGAGAGTGACGAAG
Kidins220 Exon 26	6:44312349-44312382	F: CAGAGATCAGAACAATGGCCT
		R: AGGCATCATGCTCTGGTCCAG
Mapt Exon 7a	10:92359109-92359306	F: CGTAAGCAAAGACAGGACAGGAAAT
		R: ATCCTGGTGGCATTGGATGTG
Phldb1 Exon 10	8:49009516-49009560	F: ATGCTGTCCGAACTCTCCAGG

		R: GAATGGCACCAGTAGTCTCC
Nrg1 Exon 12	16:64055275-64055417	F: TGCTGACAATTACTGGCATCTG
		R: TGGTCATGGCTGATACATAC
Gphn Exon 6a	6:101614684-101614792	F: CGACAGAAGATAGTTCCTCATC
		R: TGAAGGCTTTGTCCATAGAC
Nsmf Exon 9	3:2267381-2267470	F: GAACTTCCGCAAACACCTG
		R: CTGGCAGAAAATCAGCATCTTCC
Gipr Intron 10	1:80066679-80066806	F: TTCAGCCTGTTCCTCGGTCAC
		R: AAGCCATTTGGTGGATCATTCGCAC
Gh1 Exon 1-5	10:94486204-94488181	F: CAGGTCCTGTGGACAGATCAC
		R: TGGCAGTTGCCAGAGTACAG
Prl Exon 1-5	17:39814238-39824299	F: CAGTGGTCATCACCATGAACAG
		R: TGCTGAAAGTTGTAATGCAAATAGAAC
Gapdh Exon 3-4	NA	F: CTTCATTGACCTCAACTACATGGTT
		R: GCTCCTGGAAGATGGTGATG
Actb Exon 3-4	NA	F: TGGGACGATATGGAGAAGATTTG
		R: CCATCACAATGCCAGTGGTAC
Upf3b Exon 10	X:123720295-123720333	F: CATCCTTCAGTTCGACATCAG
		R: GAGCTTCCTGAAGAACAAGC
Eif4a2 Exon 13	11:81379641-81379871	F: TCATCAACTGCCGCTATCGAC
		R: AATTCCGATCAGGGTCAAGCCG
APP Exon 12	11:24508928-24508984	F: AGGTACTTGTCGACTGCGTC
		R: TGCTCTGAACAAGCTGAGACC
PTBP1 Exon12	7:12668238-12668275	F: CTCCATGGACATTAGGAACAGAG
		R: ACAATGCCTGCTGCACGCTG
hnRNPa2b1 First Exon	4:81241244-81241282	F: AGAGCAGCATGAGCGGATATG
		R1: CCATGGAGTTAAGTCAGAGTC
		R2: ATTCACGCCCATAGATGCACG
Cacna1d Exon 7	16:6120153-6120179	AACTGTCATCCTCACAGCACTC
		AACGGCCATTACTCCTACAAGC

Rimbp2 Exon 14	12:31580978-31581688	F: TGTCGGACATCATGGAGGAAG
		R: AATACCTTCGGCTCACATGC
Cacna2d1 Exon 22	4:15741164-15741184	F: AACCCGCATCCAGCAAGATTC
		R: TGGCCTTGGTATTGCCAACCTAC
Ehmt2 Exon 13	20:4584122-4584223	F: TGAAGCCATCCAGGAAACGG
		R: ACTTTCGGTGGCCATACACTTG
Pak6 Exon 1	3:110442637-110443078	F: AGACCTCAGCTGGCAGAATAC
		R: TCCAGGATGTTCTGCCATTGTG
Cacna1d Exon 50	16:6193496-6193555	F: AGACTTCACAGCTGCCCTGCATC
		R: TAGCATGCCCACCAGTGAGACC
Ank3 Exon 4	20:20259263-20259364	F: TGGAGTGGACGTCAACATCTG
		R: ATTGGTGTCGTTCTGTAGGAGC
COL25A1 Exon 8	2:235664469-235664514	F: GAGCCACTGAGATCATAGACTAC
		R: CTTTGGTCCAGGAAGTCC
Sptan1 Exon 42	3:8582820-8582834	GATGAGATTGAAGCCTGGATCAG
		TAACTCCACGGATTCGGTCAG
Numbl Exon 4	1:84075985-84076059	F: AGCCAGCCTATGTGCCTGAG
		R: GAGAATGCCTTGTCCAGGTTGC
Dnm1l Exon 14	11:88875171-88875248	F: TGCCATAGTTGAAGTAGTGAC
		R: GTTGTCGGTTCCTGACCAC
Rps6kb1 Exon 5	10:73841502-73841652	F: CTTGGTGATTAAGCATGATG
		R: TGAGCTACTTCGGGTACTTGG
Syn2 Exon 3	4:147147591-147147686	F: TTCTTCAGCTCGCTGCGCAAG
		R: AGACTTCGTGCTCATCCGACAG
Ica1 Exon 12	4:34656370-34656432	F: CTGGAAGTGCTGAAGATC
		R: CAGCCATCCATGAGAGCTTC
Unc13a Exon 38	16:20063831-20063841	F: CCTTCAGTTTGGACAGCT
		R: GTGACATCCTAAGCCAAGTG
Sec31a Exon 24	14:10894315-10894407	F: TGTCCAGAGTTCAAAGTCAGC
		R: CTGTTGAGGTCGATAAACTGC

Cd44 Exon 14	3:92728727-92728852	F: TGAATGGATCGGGTTCCAC
		R: TTCACAGCCTACTGGAGAC
Slc25a3 Exon 8	7:31822243-31822367	F: AGAGCCCTTGCATGGAATAG
		R: ACAGTTGTGAATTTGGCTCC
Baiap2 Exon 14	10:109183753-109183801	F: GGTCTGGATGACTACGGG
		R: ATCTGTCATTGGTCACTGTTGG
APP Exon 12	11:24508928-24508984	F: AGGTACTTGTCGACTGCGTC
		R: TGCTCTGAACAAGCTGAGACC
RBM3 Exon 5	X:15100060-15100698	F: GACTGACTGACAACACTTCC
		R: CCTCCTGAGTAGCGGTCATAG

Table1.2 Primers for RT-PCR analysis using Homo sapiens (human) genome assembly

Targeted Sequences	**IGV Location GRCh38 (hg38)**	**Primers (5´->3´)**
MAPT Exon 4a	17:45983172-45983931	F: CTGAAGAAGCAGGCATTGGAG
		R: GCTTTTACTGACCATGCGAG
MAPT Exon 10	17:45989877-45990075	F: AAGGTGGCAGTGGTCCGTAC
		R: GCTCAGGTCAACTGGTTTGTAGAC
DLG1 Exon 20a	3:197042560-197298576	F: CAGGCAGGTTACACCAGATG
		R: TAGGTCCCAATATGATCACTGGTC
EPB41L3 Exon 15	18:5407699-5407738	F: CATTCATTCGTTACGGCAGTG
		R: ACTGACAGTGAGCGCACGGAC
KIDINS220 Exon 26	2:8747144-8747201	F: ACTGAGGCAGCATACTCTGG
		R: TCACAGCAGCTATTACAGCG
GPHN Exon 8	14:66924194-66924293	F: GCTTCAACAGAAGATAGTTCCTC
		R: AGTCATCTCCAGGACTGTG
GAPDH Exon3-4	NA	F: CTTCATTGACCTCAACTACATGGTT
		R: GCTCCTGGAAGATGGTGATG

Image Data Analysis

TIFF images were quantitated by Image J software [a Java-based image processing program developed at the National Institutes of Health and the Laboratory for Optical and Computational Instrumentation (LOCI, University of Wisconsin) and available on the Internet at https://imagej.nih.gov/ij/download.html] to measure the intensity of nucleic acid (RNA, DNA or PCR products) [387].

***In vitro* transcription, nuclear extract preparation and UV crosslinking-immunoprecipitation (carried out by Dr. Jian-kun Yu)**

These procedures were carried out as in our previous reports[75, 83]. The wild type and mutant RNA probes for the 3´SS of rat *Mapt* exon 6 were based on 42 nt of the upstream 3´SS of the rat equivalent exon of human *MAPT* exon 4a (5´-ccggccuuuccgaagcccgccaccacugcguaucuc**cacacag**-3´, with the 3´ AG underlined) in front of the 5´ 86nt of the DUP175 exon [110]. The 3´SS cacaca is the only CA triplet in the probe. The RNA probes were synthesized by *in vitro* transcription with T7 RNA polymerase [83].

Genome/transcriptome analysis of the published datasets of wild type or Rett syndrome mice

We analyzed the DNA methylation or alternative splicing of the hippocampal tissue samples of wild-type or Rett syndrome mice using the raw reads from two published datasets[315, 388]. Briefly, we analyzed the raw reads of RNA-Seq sequences from the total RNA of the hippocampi of male littermate mice (wild type and Mecp2 null mice) at 7-weeks of age upon KA treatment by intraperitoneal injection [315], and the raw reads of WGBS from gDNA of the hippocampal dentate gyri of 8-10 week-old male mice (C57BL/6, same as the Mecp2-null background) [388]. The reads were quality-controlled by FASTQC, trimmed and mapped to the mouse assembly GRCm38 (mm10) for DEXSeq or BSMAP analyses.

RNA samples from Rett syndrome patients (provided by Shervin Perjhan from Dr. Mojgan Rastegar's lab)

Usage of the patient samples in the study was under the approval of the Health Research Ethics Board of the University of Manitoba to our project collaborator Dr. Mojgan Rastegar's lab. Total RNA samples were isolated from the human hippocampus and cerebellar tissues using TRIzol (Life Technologies), as we reported [389-391]. Briefly, 0.5 mL of TRIzol was added to the frozen brain powders of about 50 mg in each tube, then homogenized and incubated for 5 min at

room temperature. We then added 0.1 mL chloroform, incubated it for another 3 min, and centrifuged for 15 min (12,000xg, 4°C). We collected the aqueous phase and added 5 µg RNase-free glycogen and 0.25 mL isopropanol, incubated it for 10 min at room temperature, and centrifuged for 10 min (12,000xg, 4°C). We washed the pellet with 0.5 mL of 75% ethanol and centrifuged for 5 min, 12,000xg, 4°C. RNA pellets were air-dried and re-suspended in 30µl of RNase-free water, quantified by NanoDrop 2000 micro-volume spectrophotometer, and stored at -80°C before RT-PCR. The Rett Syndrome human brain tissues used in this study are:

NIH#	RTT	Age (years)	Sex	PMD
*	T158M	13	F	< 6 h
*	A201V	19	F	24 h
4516	R255X	21	F	9 h
1815	IVS3-2A>G	18	F	5 h
5723	Not Available	22	F	6 h

*Donated brain tissues to the Rastegar lab for research [389, 390]. NIH: National Institutes of Health, RTT: Rett syndrome, PMD: postmortem delay (time).

Statistical tests

For the RT-PCR products, we used a two-tailed Student's t-test unless otherwise noted. The DEXSeq uses Fisher's test [381].

Establishment of an *in vitro* exonic DNA methylation splicing reporter assay

In order to investigate the regulation of alternative splicing by DNA methylation, splicing response to CaMKIV signaling, a splicing reporter assay were designed by using insert oligos with different exon methylation capacities, which were further classified into two subgroups with different methylation status: unmethylated or methylated insert oligo groups (see 'splicing reporter assay' at Chapter II Materials and Methods).

M.SssI CpG methyltransferase (M.SssI MTase) is an enzyme isolated from a strain of *E. coli* in NEB, which contains the gene coding for a DNA methylase from Spiroplasma sp. strain MQ1 (M.SssI) [392]. *In vitro*, CpG sequences could be completely and exclusively methylated by M.SssI MTase by the transfer of the methyl group from S-adenosyl-L-methionine (SAM) to

cytosine nucleotides (C^5) in double-stranded DNA [393]. Currently, M.SssI MTase has been used for the *in vitro* methylation of the gene promoter in promoter-reporter constructs [394] since its specificity on CpG sites is consistent with the endogenous DNA methylation [395]. However, no reports have demonstrated the methods of *in vitro* exonic DNA methylation by M.SssI MTase for splicing reporter assays. Here, I took *Baiap2* Exon 14 as an example to establish methylation on how to completely and exclusively methylate exon DNA, which was used for splicing reporter constructs, *in vitro* by M.SssI MTase as illustrated (Fig. 4). This established an exon DNA methylation-splicing reporter assay system for splicing researchers to conveniently examine the methylation effect on splicing by mutagenesis.

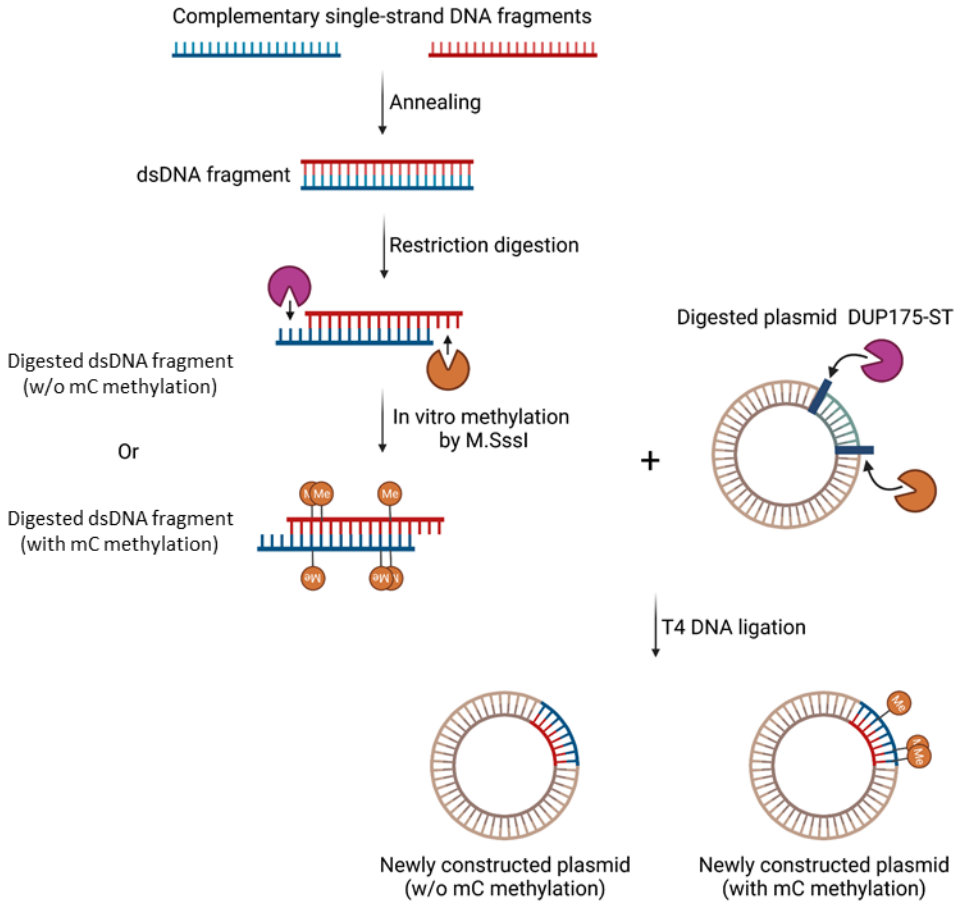

Figure 4. Outline of the *in vitro* exonic DNA methylation of Baiap2 Exon 14.
Complementary single-stranded oligos were denatured at 95°C, 5min and annealed at 60°C 30min before restriction digestion and ligation into the vector of the splicing reporter. Each insert dsDNA fragment was digested by ApaI (#ER1415, Thermo Fisher Scientific, US) and BglII (#ER0082, Thermo Fisher Scientific, US), fractionated in 1% agarose gel, excised and purified using the QIAquick Gel Extraction Kit (#28706, QIAGEN, Germany). Half of the DNA was methylated *in*

vitro with the CpG methyltransferase M.SssI (M0226L, New England Biolabs, USA) using S-adenosylmethionine (SAM) as a methyl group donor, and the methylation efficiency was verified by the CpG methylation-sensitive restriction enzyme BstUI (restriction site: CpG↓CpG, #R0518S, New England Biolabs, USA). The insert DNA fragments with or without methylation were ligated with the same double-digested splicing reporter vector DUP175[10], by T4 DNA ligase (Cat. # 15224-041, Invitrogen, US) at 14°C-16°C overnight. *(The figure was created with BioRender.com)*

Protocol

Equipment and kits

- Qiagen Plasmid Midi kit (Qiagen)
- QIAquick gel extraction kit (Qiagen)
- Agarose gel electrophoresis apparatus
- Water baths

Reagents

- Restriction endonucleases to excise fragment: Apa I (10U/μl, Invitrogen) and BglII (10U/μl, Fisher)
- REACT 4 Invitrogen, Buffer Composition (1× concentration): 20 mM Tris-HCl (pH 7.4), 5 mM MgCl2, 50 mM KCl.
- Buffer O (with BSA, Fisher), Buffer Composition (1× concentration): 50 mM Tris-HCl (pH 7.5 at 37°C), 10 mM MgCl2, 100 mM NaCl, 0.1 mg/ml BSA.
- M.SssI methyltransferase 4U/μl (New England Biolabs)
- 200× S-adenosylmethionine (SAM) (32 mM, New England Biolabs)
- NE buffer 2 (New England Biolabs)
- T4 DNA ligase, 1U/μl (Invitrogen)
- 5× T4 DNA ligase buffer (Invitrogen): 250 mM Tris-HCl (pH 7.6), 50 mM $MgCl_2$, 5 mM ATP, 5 mM DTT, 25% (w/v) polyethylene glycol-8000.
- DUP175-ST (Xie Lab)

Methods

1. Preparation of the insert fragment:

1.1 Synthesized both complementary single strands of *Baiap2* exon 14 and its partial flanking introns of DNA fragments (IDT, Integrated DNA Technologies), labeled as Baiap2E14 below. The sequences of GGGCCC (5′ – 3′, the restriction site for ApaI enzyme) and AGATCT (5′ – 3′, the

restriction site for BglII enzyme) were added to the 5´ and 3´ ends of the single strand of Baiap2E14, respectively. There is no CpG site in the partial flanking introns of *Baiap2* exon 14. Three complementary pairs of oligo inserts were listed below with different exon methylation capacities (CpG sites underlined) were synthesized using the *mBaiap2* exon 14 as a template: $(CpG)_{x3}$, $(CpG)_{x7}$, and $(GC)_{x7m}$, containing 3, 7 and 3 CpG sites, respectively, harboring the 48bp exon (uppercases) and partial flanking introns (lowercases) with ApaI (5´-GGGCC↓C-3´) and BglII (5´-A↓GATCT-3´) restriction sites at the 5´ and 3´ ends, respectively. Complementary single-stranded oligos were denatured at 95°C, 5min and annealed at 60°C 30min before restriction digestion and ligation into the vector of the splicing reporter.

$(CpG)_{x3}$: 5´-

gcgggccctgaccttgtgtttccttacagCGCGGATGTCGAAGTGGCCAGATTTTGAGCTGCCCCTG

ACTAGAGTTAgtaagttgagatctatgc-3´

$(CpG)_{x7}$: 5´-

gcgggccctgaccttgtgtttccttacagCGCGGATGTCGAAGTGGCGCGATTTTGAGCTGCCCGCG

ACTAGAGTTAgtaagttgagatctatgc-3´

$(CpG)_{x7m:}$ 5´-

gcgggccctgaccttgtgtttccttacagCGCGGATGTCGAAGTGGCCAGATTTTGAGCTGGGCCTG

ACTAGAGTTAgtaagttgagatctatgc-3´

1.2 Diluted the powder of two DNA oligos with nanopureH_2O into 1 μg/μl, respectively, store @-20C.

2. Annealing of two complementary single-strands to get double-strand DNA oligos *(labeled as dsBaiap2E14 below).*

2.1 Annealing reaction: prepare the following reaction mixture.

Annealing reaction	**Volume**
One single-strand of *Baiap2* DNA fragment	6 μg
The complementary single strand of *Baiap2* DNA fragment	6 μg
10× REact 4 buffer (Invitrogen)	12 μl

nanopureH_2O	Up to 120 μl

Incubate @ 94 °C 5min, then drop to 60 °C 30min, hold at 4 °C on ice.

Note: 10× React4 buffer (Invitrogen) was used as reaction buffer in this annealing reaction since it was the reaction buffer for the next step: ApaI digestion reaction. It was not necessary to purify the newly synthesized double-strand DNA oligos before the next step.

2.2 Electrophoresis of 3% agarose gel

After the annealing reaction, I ran the newly synthesized dsBaiap2E14 DNA oligos (200 ng) on 3% agarose gel to check the efficiency of the annealing reaction.

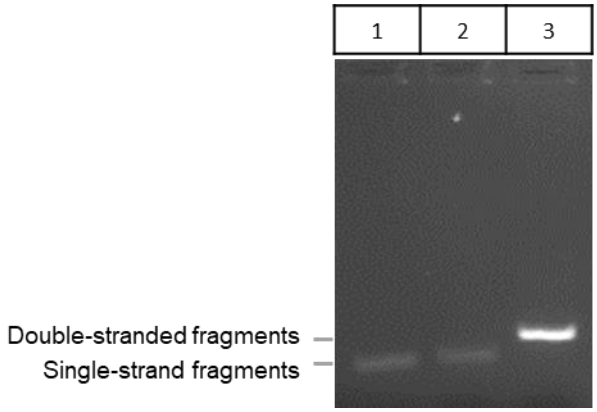

Figure 5. Electrophoresis of 3% agarose gel to check the efficiency of the annealing reaction. 1: one single-strand of Baiap2 DNA oligos, 2: the complementary single-strand of Baiap2 DNA fragment, 3: the annealed dsBaiap2E14.

The annealed dsBaiap2E14 (lane 3) ran slower than both of the Baiap2 single-strand oligos (lane 1 and lane 2), which indicated that the dsBaiap2E14 were near completely annealed.

3. Prepared plasmid DNA DUP175-ST. It contained restriction sites for both ApaI and BglII enzymes.

4. ApaI-BglII restriction enzyme digestion

Because of the salt difference between the reaction buffers of ApaI and BglII enzyme, the restriction enzyme digestion of ApaI and BglII was carried out separately. In both reactions, the

final concentration of the ApaI and BglII enzyme was 2.5U/μg DNA, and the total volume for each microgram DNA was 50 μl.

4.1 ApaI restriction enzyme digestion: prepare the following reaction mixture.

ApaI digestion of inserted DNA	**Volume**
dsBaiap2E14 (12 μg)	110 μl in total after evaporation in annealing and use for running a gel
10× REact 4 buffer (Invitrogen, 11μl)	
nanopureH_2O	
+ ApaI (10 U/μl)	3 μl
+10× REact 4 buffer (Invitrogen)	49 μl
+nanopureH2O	Up to 600 μl

ApaI digestion of plasmids	**Volume**
DUP175-ST	12.8 μg in 102 μl nanopureH_2O
ApaI (10 U/μl, Invitrogen)	3 μl
10× REact 4 buffer (Invitrogen)	60 μl
nanopureH_2O	Up to 600 μl

Mixed the above mixture gently by pipetting and incubated at 37 °C for 3h.

4.2 BglII restriction enzyme digestion

After the ApaI digestion, BglII restriction enzyme digestion was performed for both digested dsBaiap2E14-ApaI oligos and DUP175-ST-ApaI plasmids. The following materials were directly added into the tubes used for the ApaI restriction enzyme digestion above.

+BglII (10 U/ul, #ER0082, Fisher Scientific)	3 μl
+10× BufferO (with BSA, #B05, Fisher Scientific)	67 μl

Therefore, the total volume for the BglII digestion reaction was 670µl.

4.3 Concentrated double-digested DNA from the big volume reaction

4.3.1 Ran 200ng DUP175 plasmid on 1% agarose gel to check the digestion effect. If it is digested well, concentrated the double-digested DNAs (dsBaiap2E14-ApaI-BglII DNA oligos and DUP175-ST-ApaI-BglII plasmid DNA).

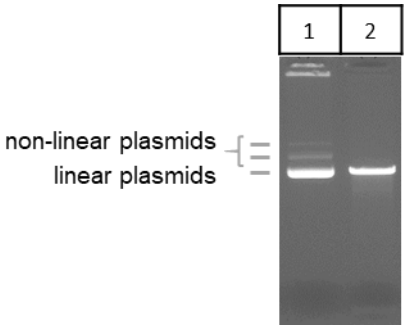

Figure 6. Electrophoresis of 1% agarose gel to check the efficiency of the restriction enzyme. The linear DUP175 is the major band of DUP175-ST after double-enzyme digestion. It indicates that the DUP175-ST plasmids were completely digested by ApaI and BglII enzymes. Notably, in some cases, the short DNA sequences that were cut off from the plasmid can also be observed on the gel when there are a large number of DUP175-ST plasmids loaded.1: undigested plasmids, 2: plasmids digested by ApaI and BglII restriction enzymes

4.3.2 After ApaI-BglII digestion, narrowed down the volume of the double-digested DNA (both dsBaiap2E14-ApaI- BglII oligos and DUP175-ST-ApaI- BglII plasmid DNA) using QIAquick Gel Extraction Kit (Cat. No. 28706, Qiagen).

5. *In vitro* methylation by M.SssI CpG Methyltransferase

5.1 The *in vitro* CpG methylation reaction: diluted supplied SAM (200×, 32 mM) to 1600 µM by nuclease-free water and prepared the following reaction mixture.

CpG methylation	**Volume**
10 × NEB buffer 2 (B7002S)	50 µl
Diluted SAM (1600 µM, 10×, NEB)	50 µl
dsBaiap2E14-ApaI-BglII	9.0 µg in 62 µl nanopure H_2O
M.SssI (4 U/µl, M0226S, NEB)	10 µl

nanopure H_2O	Up to 500 µl

Mixed well, pipette up and down more than 10 times using the 1000µl tips.

5.2 Incubated the mixtures at 37°C.

In one group, the incubation time was as in the previous study [394]. That is, incubated at 37°C overnight (around 15 - 18h), then added another 8µl M.Sssi (4U/µl) and 56µl 10× SAM (1600µM) into the tubes used for the *in vitro* CpG methylation reaction. Incubated at 37°C for another 4h. It's labeled as the 18h + 4h group.

In another group, 4h incubation was added before the overnight incubation. That is, incubate the mixtures 37°C for 4h, then added another 8µl M.Sssi (4U/µl) and 56 µl 10× SAM (1600 µM), incubated at 37°C overnight (around 15 - 18h), then added another 8µl M.Sssi (4 U/µl) and 56 µl 10× SAM (1600 µM) into the tubes used for the *in vitro* CpG methylation reaction. Incubated at 37°C for another 4h. It was labeled as the 4h + 18h + 4h group.

6. Methylation sensitive enzyme digestion to confirm methylation

6.1 Extracted DNA from 50 µl of the mixtures of the above reaction using the QIAquick Gel Extraction Kit (Cat. 28706, Qiagen). Half of the extracted DNA was used for the methylation confirmation by digestion using the methylation-sensitive enzyme BstUI, and the other half was used as the control in the agarose gel electrophoresis.

6.2 BstUI digestion: prepared the following reaction mixture.

BstUI digestion	**Methylated oligos**	**Unmethylated oligos**
BstUI(10 U/µl, NEB)	1 µl	1 µl
dsBaiap2E14-ApaI-BglII-M.SssI	1 µg	600 ng in 5 µl nanopure H2O
CutSmart Buffer (10x, NEB)	5 µl	5 µl
deionized H2O	Up to 50 µl	Up to 50 µl

Incubated the mixtures at 60°C, 3h.

The methylated oligos were labeled as dsBaiap2E14-ApaI-BglII-M.SssI and the un-methylated oligos were labeled as dsBaiap2E14-ApaI-BglII stored at -20°C for subsequent usage. Around 80% of DNA fragments were recollected by the QIAquick Gel Extraction Kit (Cat. 28706, Qiagen).

6.3 Electrophoresis of 3% agarose gel

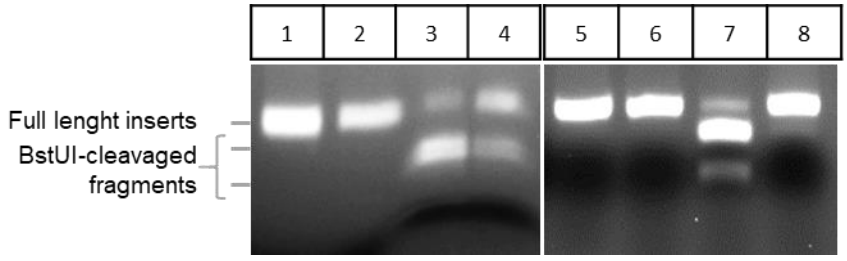

Figure 7. Confirmation of methylation by methylation-sensitive restriction enzyme BstUI digestion and 3% agarose gel electrophoresis.

The lanes 1-8 in the figure represented (The image containing lanes 5-8 was also used in figure 10B, which is the same image):

M.SssI	-	+	-	+
BstUI	-	-	+	+
18h + 4h	1	2	3	4
4h + 18h + 4h	5	6	7	8

The agarose gel showed that there was a difference in the methylation efficiency in the two different groups. In the 18h + 4h group, the methylation ration was 48.72%, while it was up to 92.29% in the 4h + 18h + 4h group. It showed that the methylation ratio in the 4h + 18h + 4h group was incredibly increased compared to the 18h + 4h group.

Undigested inserts %	w/o M.SssI	with M.SssI
18h + 4h	11.93	60.65
4h + 18h + 4h	6.06	98.35

6.4 After the confirmation of the methylation efficiency, extracted the left of the methylated dsBaiap2E14-ApaI-BglII-M.SssI oligos from the mixtures using the QIAquick Gel Extraction Kit (Cat. 28706, Qiagen).

7. Ligated DNA inserts into the splicing-reporter construct

7.1 Set up the following reaction in a microcentrifuge tube on ice

Component	Unmethylated inserts	Methylated inserts
5× T4 DNA ligase reaction buffer (Invitrogen, P/N y90001)	120 µl	120 µl
DUP175-ApaI-BglII	4.8 µg in 20 µl nanopure H_2O	4.8 µg in 20 µl nanopure H_2O
ds-strand DNA oligoes	2 µg in 20 µl nanopure H_2O	2 µg in 15 µl nanopure H_2O
T4 DNA ligase (Cat. # 15224-017, Invitrogen)	6.8 µl	6.8 µl
nanopure H2O	Up to 600 µl	Up to 600 µl

Notably, the concentration ratio of the insert (ds-strand DNA oligos) to vector (DUP175-ApaI-BglI ratio was 2:1 – 3:1.

7.2 Incubated the mixture 13-17°C, overnight.

Put some ice into the room temperature water until the temperature of the water was around 13°C. Floated tubes in the water baths and sealed the box tightly with a lid. After incubation overnight (16-18h), the temperature of the water was around 17°C in the morning.

8. Plasmid construction and cell transfection

The insert DNA fragments with or without methylation were ligated with the same double-digested splicing reporter vector DUP175[1], by T4 DNA ligase (Cat. # 15224-041, Invitrogen, US) at 14°C-16°C overnight. The ligated splicing reporters containing the methylated or unmethylated exons were concentrated using the QIAquick Gel Extraction Kit and co-transfected directly with the Flag-CaMKIV-dCT (CaMKIV) or –dCT-K75E (CaMKIVm) expression plasmid [1, 152, 366], into HEK295T cells using LipoFectamine 3000 (#L3000008, Invitrogen, US) and incubated overnight (16-18h) before RNA extraction.

Chapter IV Results and Discussion

The thesis research present in this chapter has been submitted for peer review in *Nucleic Acids Research* (Ling Liu, Hai Nguyen, Urmi Das, Jian-Kun Yu, Lei Lei, Matthew Kung, Shervin Pejhan, Mojgan Rastegar, Jiuyong Xie. Control of Adaptive Splicing by DNA Methylation.).

Results

1. Adaptive splicing of a specific group of synaptic exons upon repeated stimulation of cells by membrane depolarization

To determine if there is adaptive splicing in the GH_3 cells where we had found the depolarization regulated STREX splicing [75], we treated the pituitary cells once or six times with depolarizing concentrations of KCl (50mM, Fig. 8A) to identify exons with different responses between the two groups. The treatment scheme was based on the pre-determined time course of the splicing changes/recovery of the STREX exon, which was repressed 6h after KCl addition and recovered completely 18h after washing off KCl (Supplementary _Fig. 1). It did not change the cell growth curve after the repeated KCl treatment/wash-off cycles (Fig. 8B).

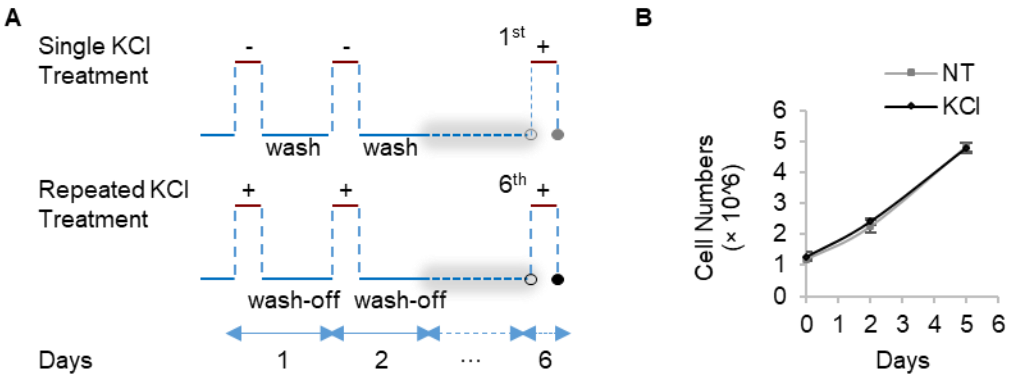

Figure 8. Adaptive splicing of a specific group of exons upon repeated membrane depolarization by KCl treatment.
A-B:
A. Scheme of the single or repeated KCl (50mM, 6h) treatments of GH3 pituitary cells (See also Materials and Methods). **B.** Growth curves of the GH3 cells throughout the repeated KCl treatments. NT: not treated. Cells were counted with a hemocytometer. (-): without KCl treatment, (+) with KCl treatment, 1^{st}: the 1^{st} KCl treatment, 6^{th}: the 6^{th} KCl treatment.

We searched for differentially spliced exons among cells untreated (NT), KCl-treated once only (1^{st} KCl), or KCl-treated 6 times (6^{th} KCl), using DEXSeq and MATS analysis of their RNA-Seq reads [89, 381, 382]. The inclusion level of most (99%) of the detected 145 thousand

exons/bins (hereafter called exons for simplicity) including the STREX did not change substantially between the 6th and 1st KCl-treated samples. Neither did the transcript level of the growth hormone (*Gh1*) and prolactin (*Prl*) genes characteristic of the rat GH3 pituitary cells (see below). These observations together with the growth curves (Fig. 8B) support strong homeostatic expression of the majority of exons and characteristic genes during the experiment. In contrast, the inclusion level of a smaller group of 1,878 (~1.3%) exons of 1,204 genes changed substantially between the 6th and 1st KCl groups (Fig. 8C), including ones (~25%) that barely responded to the 1st KCl treatment. The majority (81%) of these are alternative exons and the rest are the 1st or last exons from alternative transcription start or polyadenylation sites without involving alternative splicing. Thus, there is likely adaptive response of a specific group of exons during pre-mRNA processing, especially splicing, after repeated depolarization.

The top five clustered functions of the host genes ranged from 'synapse' to 'RNA recognition' by DAVID functional annotation clustering analysis (Fig. 8D). The synaptic genes include *Mapt* (microtubule-associated protein tau), *Nrg1* (neuregulin 1), *Epb41l3* (erythrocyte membrane protein band 4.1 like 3) and *Kidins220* (kinase D interacting substrate 220). They function in synapse formation[396], and plasticity[397-399], or hormone secretion[400].

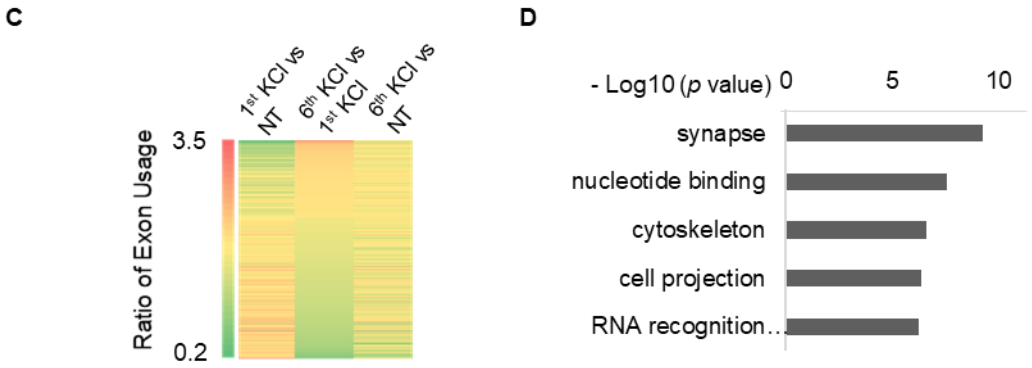

Figure 8. Adaptive splicing of a specific group of exons upon repeated membrane depolarization by KCl treatment. C-D:
C. Heatmap of splicing changes (by ratios of exon usage) of 720 exons between the 6th and 1st KCl treated samples, using DEXSeq analysis. **D.** DAVID functional clustering analysis of 1,204 genes whose exons changed between the 6th- and 1st KCl-treated samples based on DEXSeq and MATS analysis, ranked by -Log10 of the p values. DEXSeq filtered criteria: exon base mean >20, average base mean >20, normalized ratio (relative to the highest exon base mean of the gene) >0.002 and <1, fold change: >0.91 or <1.1, p-value <0.01. MATS filtered criteria: p-value <0.01, FDR (False Discovery Rate) <0.01.

After manual examination of the top-cluster exons in the Integrative Genomics Viewer (IGV)[385], we were able to validate the adaptive splicing by the different responses to the 6th and 1st KCl-treatment for 18 of 23 alternative exons (78.3%) by semi-quantitative reverse transcription-polymerase chain reaction (RT-PCR, Fig. 8E and below), supporting our relatively accurate prediction of the adaptive exons. After repeated treatments, in most cases their net changes of exon usage by depolarization were either reduced (desensitized, e.g., the proximal terminal exon of *Rps24*, Fig. 8E) or increased (hypersensitized, e.g., *Ehmt2* exon 10), and in one case (*Mapt* exon 6), the depolarization effect was reversed.

Besides the GH3 pituitary cells, we also examined adaptive splicing similarly by RT-PCR of the STREX exon in the LA-N-5 human neuroblastoma, N1E mouse neuroblastoma, and PC12 rat adrenal phaeochromocytoma cells. Though its repression by depolarization was not changed significantly after the repeated treatment scheme in the GH_3 cells (Fig. 8A & 5F), the repression was slightly dampened in LA-N-5, lost in N1E, and significantly augmented in PC12 cells after the 6th treatment (Fig. F). Thus, the repeated depolarization-induced adaptive splicing is cell-dependent.

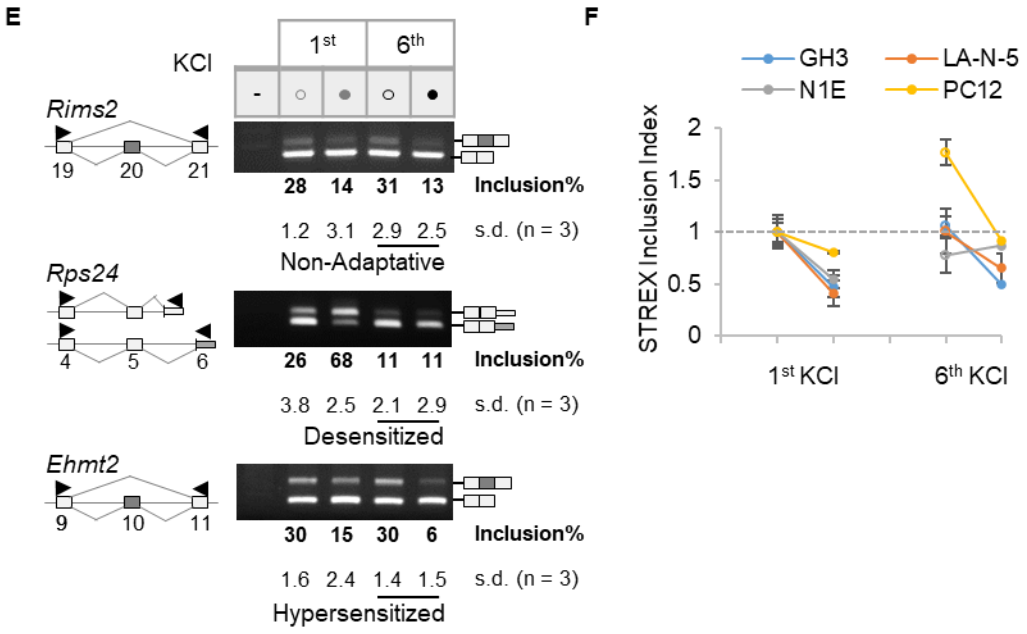

Figure 8. Adaptive splicing of a specific group of exons upon repeated membrane depolarization by KCl treatment. E-F:
E. Representative agarose gels of RT-PCR-validated exons of different splicing patterns upon repeated KCl treatments. The non-adaptive exon is a negative control. The 'desensitized' or

'hypersensitized' refers to the 6th versus the 1st KCl treatment effect on exon usage. 'Non-adaptive' means no change of this effect. Grey box: alternative exons, white box: constitutive exons, black arrow: primers. Open circle: before KCl treatment, dots: after KCl treatment. *Rims2* exon 21, NM_053945.2; *Rps24* last exons, FN801636(upper band) & NM_031112.1(lower band); *Ehmt2* exon 9, NM_212463.1, with the reference transcript IDs from the Rat Jul. 2014 (RGSC 6.0/rn6) Assembly. **F.** Cell-dependent adaptive splicing of STREX upon repeated KCl treatments. For the STREX inclusion index, its inclusion level (%) before the 1st KCl treatment (open circles) was taken as 1 (mean ± SD, n = 3). All others including the KCl-treated (filled circles) are relative to this baseline.

Together, these observations indicate that, although there is a strong homeostatic mechanism for the majority of exons upon repeated depolarization, there is indeed also adaptive splicing of a specific group of exons of genes in key cellular functions, in a cell-dependent manner. Moreover, the exon- and cell-dependence suggests the involvement of both *cis*-acting sequence/elements and *trans*-acting factors.

2. Concomitant global changes of DNA methylation and disruption of adaptive splicing by 5-azaCytidine

To identify the essential pathways mediating the adaptive splicing, we tested and observed effects by the NMDA receptor antagonist nifedipine on a CaMKIV-responsive reporter exon in the more transfectable N1E cells (S_Fig. 2), as in cerebellar neurons[361]. More interestingly, we also observed robust effects by 5-azaCytidine (5-azaC), a reported 'inhibitor' of DNA methyltransferases (DNMT) [401, 402], on endogenous exons of the GH3 cells (Fig. 9). Considering the role of DNA methylation in adaptation in other systems[101, 363], we chose to focus on the 5-azaC effects and DNA methylation in this study.

To investigate the global relationship between DNA methylation and adaptive splicing, we carried out both RNA-Seq of the cytoplasmic RNA and whole-genome bisulfite sequencing (WGBS) of corresponding nuclear genomic DNA (gDNA) of the 6th KCl-treated samples with or without pre-treatment by 5-azaC (50μM, 18h). This concentration allowed inhibition of DNA methylation substantially without causing cell death. Using DEXSeq or BSMAP analysis, we obtained differentially used exons between the two groups (*padj* < 0.05), and the corresponding exon DNA methylation levels of mCpG or mCpH (H: C, A or T), respectively (Fig. 9A). Interestingly, the 5-azaC-caused ratio changes of exon usage were inversely correlated with the total methylation levels of mCs: the bigger changes of exon usage (ratio < 0.5 or > 2) were limited

to the less methylated (< 100, mCpG or < 10, mCpH) exons and the highly methylated (> 100, mCpG or > 10, mCpH) ones limited to the smaller ratio changes of exon usage (0.5 < ratio < 2), while as the changes of the other exons were in various intermediate states. A similar inverse relationship was also observed after the methylation levels were normalized to exon lengths (per kilobases, S_Fig. 3A).

The methylation level (per kilobases) was reduced for about half of the exons but uninhibited for the others by the 50-µM 5-azaC treatment, in an exon-dependent way in the four quadrants of the plot against the ratio changes of exon usage (Fig. 9B, mCpG or mCpH). Similar DNA methylation changes were also observed in our separate analysis, using BSmooth [403]. Importantly, the net changes of DNA methylation correlate with the ratio changes of exon usage similarly as does the total level of exon DNA methylation in Fig. 9A.

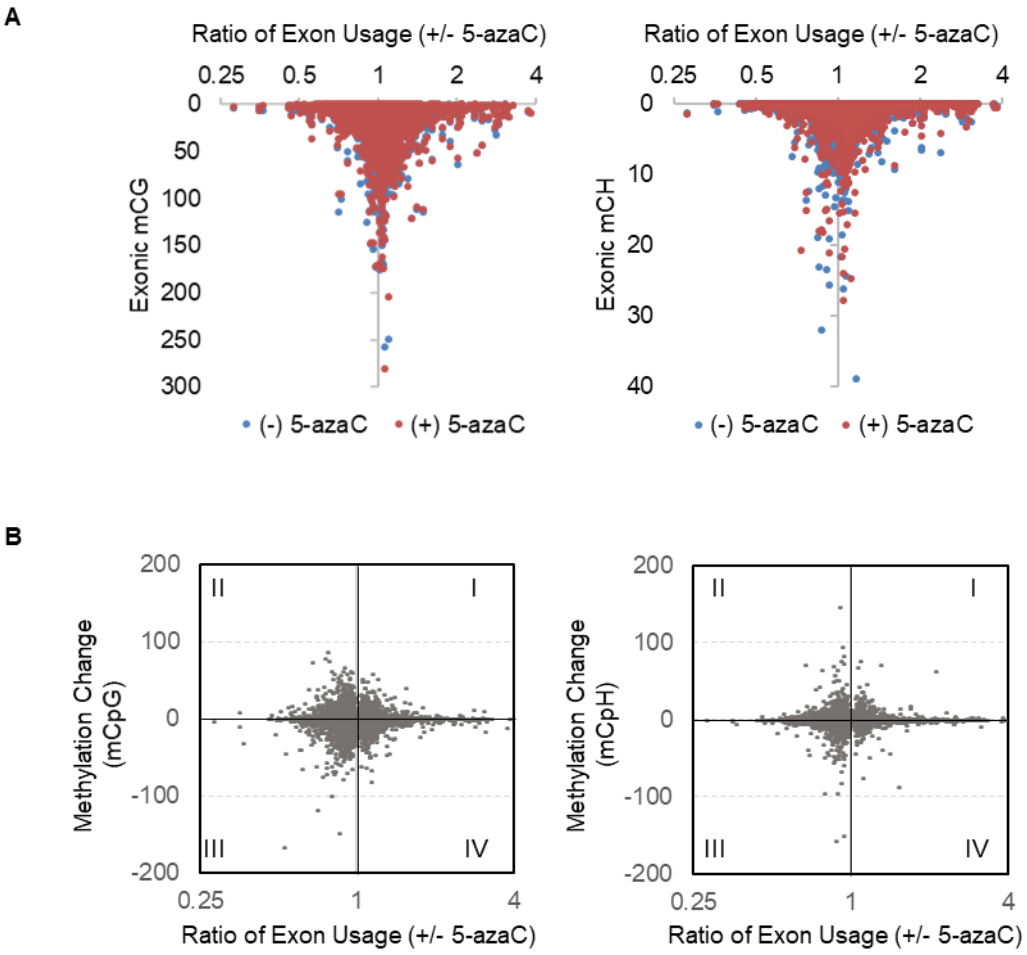

Figure 9. Disruption of the depolarization-induced adaptive splicing and exonic DNA methylation by 5-azaC in GH3 cells.
A-B:
A-B. Scatter plots of the genome-/transcriptome-wide exon DNA methylation levels (**A**) or their index of net changes (**B,** per kilobases of exon DNA) versus the ratios of their exon usage with/without 5-azaC (X-axis, in log2 scale) in the 6th KCl-treated GH3 cells. n = 22,361 exons for mCpG and 28,077 for mCpH. The total methylation level of exonic DNA mCpG or mCpH was calculated by the average methylation ratio (0-1) of CpG or CpH multiplied by the total number of CpG or CpH sites in each exon.

Of the top 114 exons with highly adaptive responses, the usage of nearly half (52) of them was also strongly changed by 5-azaC by more than 1.5 folds. In particular, changes of 40 (~77%) of them by the 6th KCl were prevented by the 5-azaC pre-treatment (Fig. 9C). The most significantly clustered functions of the host genes of the 52 exons, including the *Mapt, Dlg1* and *Kindins220* exons, are also synaptic functions (p = 8.5E-04). We thus examined these and above synaptic exons by RT-PCR as shown in Fig. 9D-E (also S_Fig. 3B). Their adaptive splicing was abolished (*Mapt* exons 6 and 10, *Nrg1* exon 12, *Epb41l3* exon 15 and *Kidins220* exon 26) or reversed (e.g., *Phldb1* exon 10) by 5-azaC. Interestingly, two previously non-adaptive exons (*Mapt* exon 7a and *Dlg1* exon 20a) became adaptive after the 5-azaC treatment. Moreover, these 5-azaC effects on adaptive splicing were accompanied by its disruption of exon DNA methylation (Fig. 9E, Right panels, mCpG and/or mCpH, and 2F). Importantly, changes of DNA methylation by the depolarization treatments were also observed in the 1st and 6th KCl-treated samples, concomitant with their splicing changes (Fig. 9G).

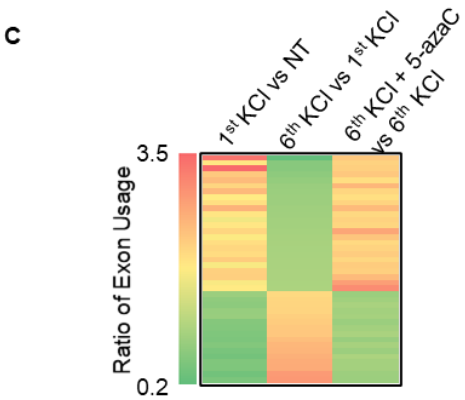

Figure 9. Disruption of the depolarization-induced adaptive splicing and exonic DNA methylation by 5-azaC in GH3 cells. C:
C. Heatmap of the splicing changes of 40 exons with adaptive responses to the 6th KCl highly different from the 1st KCl treatment and their changes prevented by 5-azaC (both > 1.5 folds).

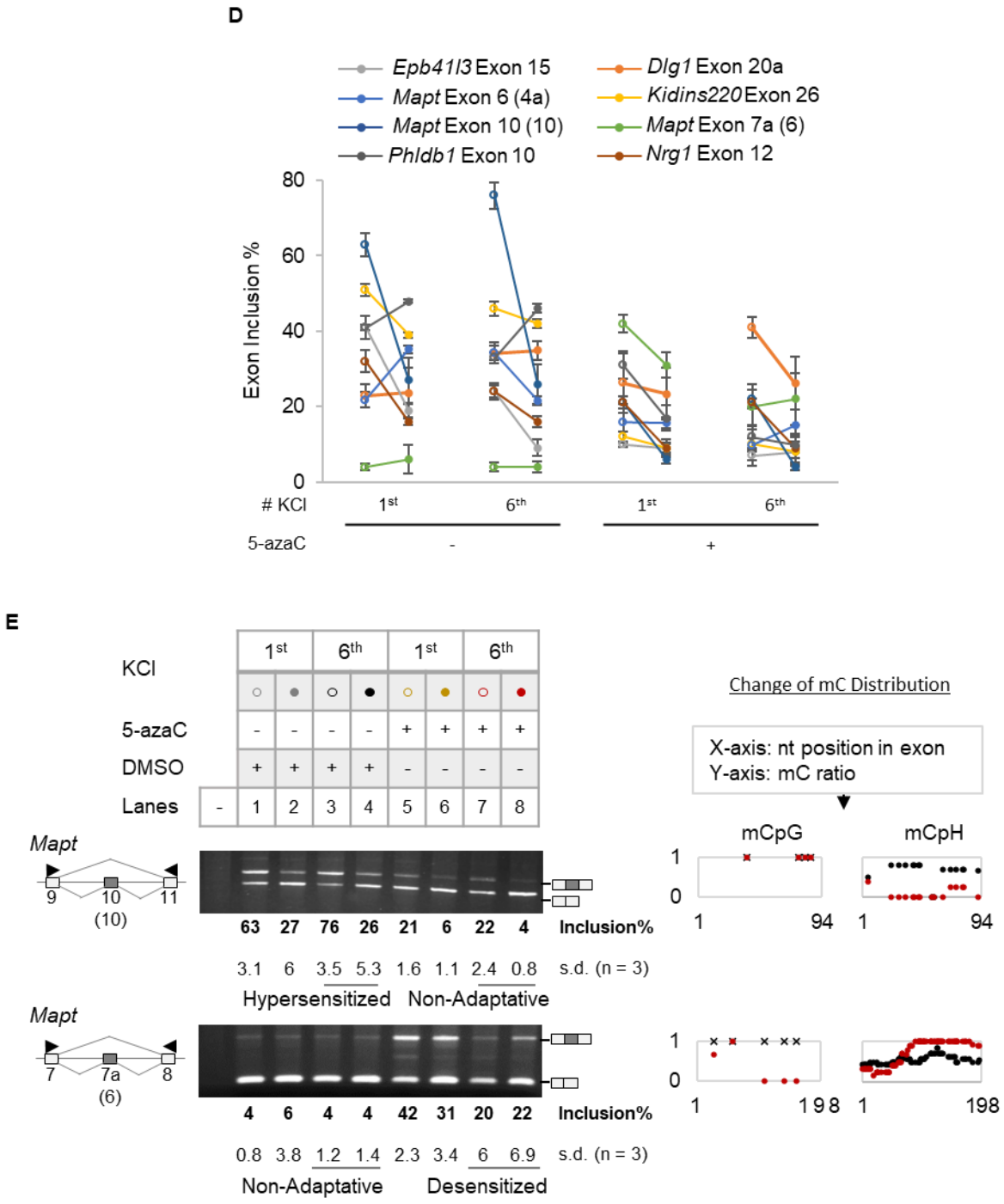

Figure 9. Disruption of the depolarization-induced adaptive splicing and exonic DNA methylation by 5-azaC in GH3 cells. D-G:

D-E. Representative examples of the disruption of activity-dependent adaptive splicing and the corresponding exonic DNA methylation change of synaptic exons by 5-azaC. The rat exon numbers are based on the following transcripts of the RGSC 6.0/rn6 Assembly: *Epb41l3* exon 15, NM_053927.1; *Mapt* exon 6, M84156, equivalent to human *MAPT* exon 4a (NM_001123066.3, GRCh38/hg38); *Mapt* exon 7a, M84156, between exons 7 and 8, equivalent to human *MAPT* exon

6 (NM_001123066.3, GRCh38/hg38); *Mapt* exon 10, M84156, equivalent to human *MAPT* exon 10 (NM_001123066.3, GRCh38/hg38); *Phldb1* exon 10, X74226; *Dlg1* exon 20a, NM_012788.1, between exons 20 and 21; *Kidins220* exon 26, NM_053795.1; *Nrg1* exon 12, NM_001271128.1. In the brackets are the commonly referenced human exon numbers. In **D** is a graph for the changes of percent inclusion (mean ± SD, n ≥ 3) of adaptive synaptic exons in the absence or presence of 5-azaC. In **E** are representative agarose gels of RT-PCR products (Left panel) of the major patterns of 5-azaC effects on the inclusion level, splicing response to depolarization, adaptive splicing to repeated depolarization of the synaptic exons in **D**. Please refer to Fig. 8E for the definition of 'non-adaptive', 'desensitized' or 'hypersensitized'. To the left of the gels are the splicing pathways (bracketed are the corresponding human exon numbers). Grey box: alternative exon; white box: constitutive exons; black arrow: primers. To the right are the corresponding levels of individual mC methylation (mCpG and/or mCpH) of each exon upon the 6th KCl treatment with (red) or without (black) 5-azaC treatment. The flanking introns (± 10nt) of exons always had the same methylation level as the corresponding exon ends.

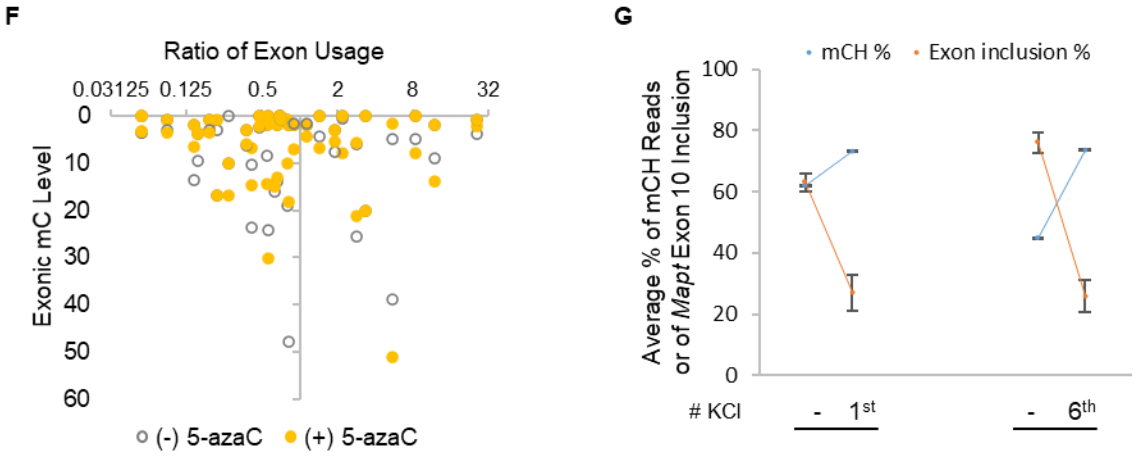

Figure 9. Disruption of the depolarization-induced adaptive splicing and exonic DNA methylation by 5-azaC in GH3 cells. F-G:
F. Scatter plot of the exon mC (mCpG or mCpH) levels and corresponding ratios of exon usage (log2) by RT-PCR results, with/without 5-azaC in the 6th KCl-treated GH3 samples (n = 31 exons in total). **G**. An example (*Mapt* exon 10) of DNA methylation changes by the 1st and 6th depolarization treatment, with its exon inclusion level plotted alongside. Here the methylation level is in percentage scale to be plotted alongside the exon percentages. The exon DNA mCG level did not change as in 2E. The KCl-induced methylation changes are inversely correlated with the splicing changes in a way similar to those exons in the quadrant II of 2B (Right).

Besides its effect on DNA methylation, 5-azaC also incorporates into RNA transcripts (mainly tRNA and non-protein coding RNA though mRNA also reported)[404, 405], causing frequent C to G transversions that can be identified in the RNA-Seq reads aligned to the genome [405]. We thus manually examined the RNA-Seq reads of 30 exons for the transversions (3,429 nt in total). We identified only one such transversion (read) in a 5-azaC-treated sample, allowing an

estimated 5-azaC incorporation rate at less than 1×10^{-4} of cytosines in the aligned reads. Therefore, we concluded that 5-azaC incorporation into mRNA had little effect on the observed splicing changes.

Taken together, these data suggest a critical role of DNA methylation in the adaptive splicing *of a group of synaptic exons upon repeated stimulation by depolarization.*

3. Methyl-CpG-dependent augmentation of CaMKIV-inducible alternative splicing by hypermethylation of exon DNA

To verify the direct effect of DNA methylation on the altered splicing response to cell activities, we established a mini-gene splicing reporter system for unmethylated or methylated exons in response to co-expressed CaMKIV (Fig. 10), a critical mediator of depolarization-induced splicing[75, 110, 115, 133, 361]. For the reporter, we synthesized a short exon of the brain-specific angiogenesis inhibitor 1-associated protein 2 (*Baiap2*) gene likely involved in autism [406]. The exon is methylated in the hippocampus of wild type mice and also regulated by kainic acid in *Mecp2*-null mice [315, 388]. We inserted the mouse exon with its partial flanking introns into the human beta-globin mini-gene DUP175 [110]. Besides its 3 CpG sites in the wild type $(CpG)_{\times3}$ reporter, we created 4 more CpG or their mutant sites in the $(CpG)_{\times7}$ or $(CpG)_{\times7m}$ reporter to examine the methyl-Cytosine effect (Fig. 10A). The inserts were ligated with the vector with or without prior CpG-specific *in vitro* methylation by the M. SssI CpG methyltransferase [392], after verification by methylation-sensitive restriction enzyme (MSREs) BstUI assays (Fig. 10B).

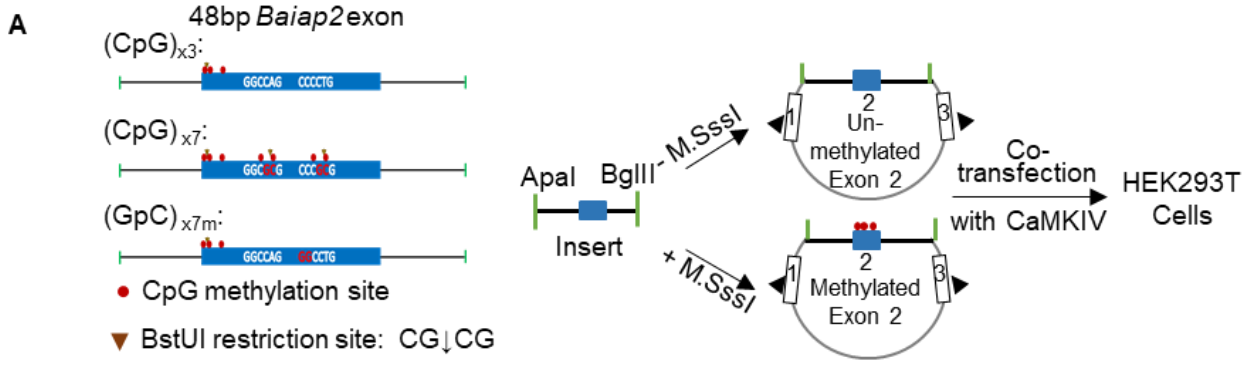

Figure 10. Effects of DNA hypermethylation of a reporter exon on its splicing response to CaMKIV.

A. Diagram of the reporter exons (Left) based on the exon 14 (48nt) and partial flanking introns of the mouse *Baiap2* gene. The subscripts of $(CpG)_{x3}$ and $(CpG)_{x7}$ denote the number of exonic CpG sites; no CpG sites are in the flanking introns. The mutated nucleotides are in red. In $(CpG)_{x7m}$, the mutated nucleotides of 'GGCGCG' were changed back to 'GGCCAG' or of 'CCCGCG' changed to 'GGCCTG'. **Right,** Diagram of the splicing reporter minigene system for unmethylated or methylated exons. The synthetic reporter exon inserts, unmethylated or *in vitro* methylated, were ligated with the vector DUP175 (curved lines, open boxes: constitutive beta-globin exons, arrowheads: PCR primer locations/directions, exons numbered according to the spliced mRNA), to obtain splicing reporters DUP175-$(CpG)_{\times 3}$, -$(CpG)_{\times 7}$, or -$(CpG)_{\times 7m}$, and co-transfected with constitutively active Flag-CaMKIV-dCT or its kinase-dead mutant Flag-CaMKIVm-dCT into HEK293T cells, and incubated overnight (16-18h) before RNA extraction.

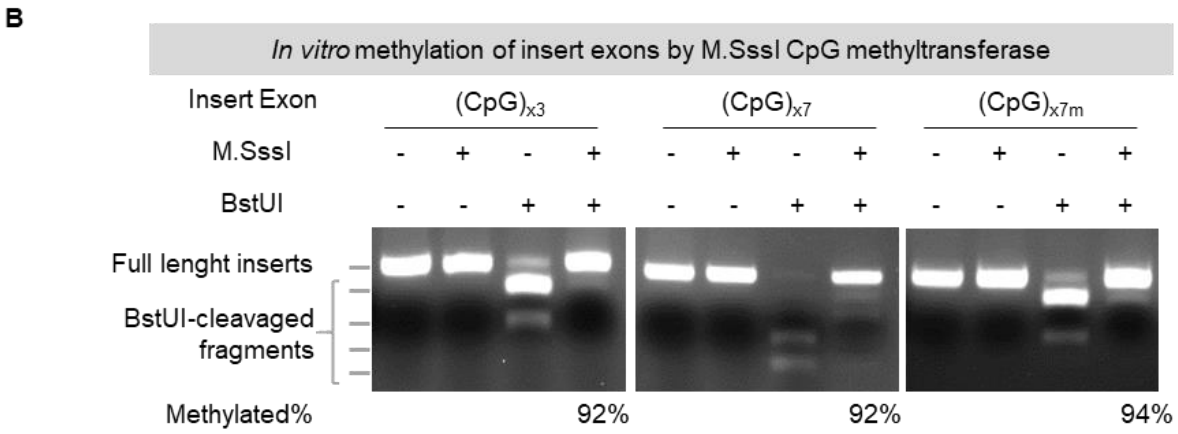

Figure 10. Effects of DNA hypermethylation of a reporter exon on its splicing response to CaMKIV. B

B. The *in vitro* methylation efficiency of the reporter exon inserts [$(CpG)_{x3}$, $(CpG)_{x7}$ or $(CpG)_{x7m}$] by M. SssI CpG methyltransferase, verified to be at least 92% by restriction enzyme digestion using the CpG methylation-sensitive BstUI (restriction site: CpG↓CpG). The percentage of the full-length insert (minus the uncleaved full-length inserts in the preceding lane) out of all fragments in each lane was taken as the methylation efficiency. **Note** that the re-appearance of the strong band of the cleaved mutant fragment indicates the loss of the two additional CGCG BstUI sites, extra targets for hypermethylation of the exon by M. SssI.

The ligated splicing reporters DUP175-$(CpG)_{\times 3}$, -$(CpG)_{\times 7}$, or -$(CpG)_{\times 7m}$ with unmethylated or methylated middle exons were co-transfected with constitutively active Flag-CaMKIV-dCT or its kinase-dead mutant Flag-CaMKIVm-dCT, as in our previous reports[110, 360, 361], into HEK293T cells and incubated overnight (~18h). Semi-quantitative RT-PCR of the

spliced mRNA showed that the co-expressed CaMKIV repressed both the unmethylated and methylated exons of the $(CpG)_{\times 3}$ and $(CpG)_{\times 7}$ reporters by a similar 3 folds (Fig. 10C, lanes 1-8). Interestingly, M. SssI methylation of the $(CpG)_{\times 7}$ reporter exon increased its inclusion from 51% to 64% (Fig. 10C, lane 7 vs. lane 5), in a way similar to those methylation-splicing changes in the quadrant I of Fig. 9B (Left). The hypermethylated exon was repressed by CaMKIV by a significantly larger extent (51% net reduction or about 5 folds, Fig. 10C, lanes 7-8) than its unmethylated exon (34% or 3 folds, Fig. 10C, lanes 5-6), suggesting augmentation of the CaMKIV effect by the hypermethylation. In contrast, mutating the extra 4 CpG dinucleotides abolished the hypermethylation effect on the basal splicing as well as its augmentation of the CaMKIV effect (Fig. 10C, lanes 9-12). Thus, the reporter exon DNA hypermethylation is required and sufficient to augment splicing response to CaMKIV, a critical mediator of the activity-dependent splicing[75, 110, 115, 133]. This assay not only mimicked the altered splicing response (adaptive splicing) after repeated depolarizations but also confirmed the essential role of DNA methylation in the response.

C

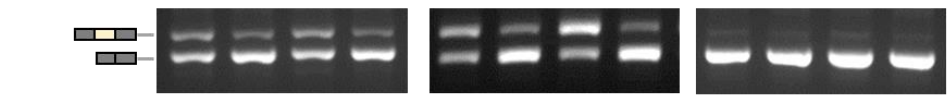

Lanes:	1	2	3	4	5	6	7	8	9	10	11	12
Inclusion%	29	11	30	10	51	17	64	13	1.8	1.5	1.4	1.9
s.d. (n = 4)	5.4	1.8	4.2	2.5	2.7	1.3	4.0	2.9	0.3	0.4	0.1	0.9

Figure 10. Effects of DNA hypermethylation of a reporter exon on its splicing response to CaMKIV. C:
C. Agarose gels of semi-quantitative RT-PCR products of the spliced products of the three minigene reporters, DUP175-$(CpG)_{x3}$, $(CpG)_{x7}$, and $(CpG)_{x7m}$ with different methylation profiles of the exon DNA, co-transfected with Flag-CaMKIV-dCT (CaMKIV) or Flag-CaMKIVm-dCT (CaMKIVm).

4. Regulation of the 5-azaC-disrupted synaptic exons by hnRNP L

We have previously identified hnRNP L in the depolarization/CaMKIV-regulated splicing and hormone production[75, 83, 89, 407]. A number of observations suggested it also as a regulator

of some 5-azaC-disrupted exons: (1) shL (short hairpin RNA against hnRNP L) - target exons/genes in synapse functions [89]; (2) methylation of the corresponding DNA of the hnRNP L-preferred CA dinucleotides (Fig. 9E & Fig. 11); (3) co-immunoprecipitation of hnRNP L with MeCP2[313]; (4) some shL target exons also affected by 5-azaC and specifically enriched among synaptic genes (Fig. 11A), with a CA-rich consensus CAGCAG (Fig. 11B); and (5) 15 of the synaptic exons changed by shL in IGV of the RNA-Seq reads (Fig. 11C and Table 2).

We verified the role of hnRNP L in knockdown/rescue assays of the exons of *Nrg1* and *Mapt* (S_Figs. 3B, 4 & Fig. 11D-F), genes involved in neurological disorders[397, 398, 408]. The repression of the *Nrg1* exon by depolarization was dampened upon repeated KCl treatment and the adaptive change was abolished by 5-azaC (Fig. 9D and S_Fig. 3B). The exon usage was enhanced by shL and further by shL plus shLL (S_Fig. 4). Importantly, the shL effect was abolished by the expression of Flag-hnRNP L, and the exon repression by depolarization requires the CaMKIV phospho-target serine Ser513 of hnRNP L, similarly as for the STREX exon [75, 407].

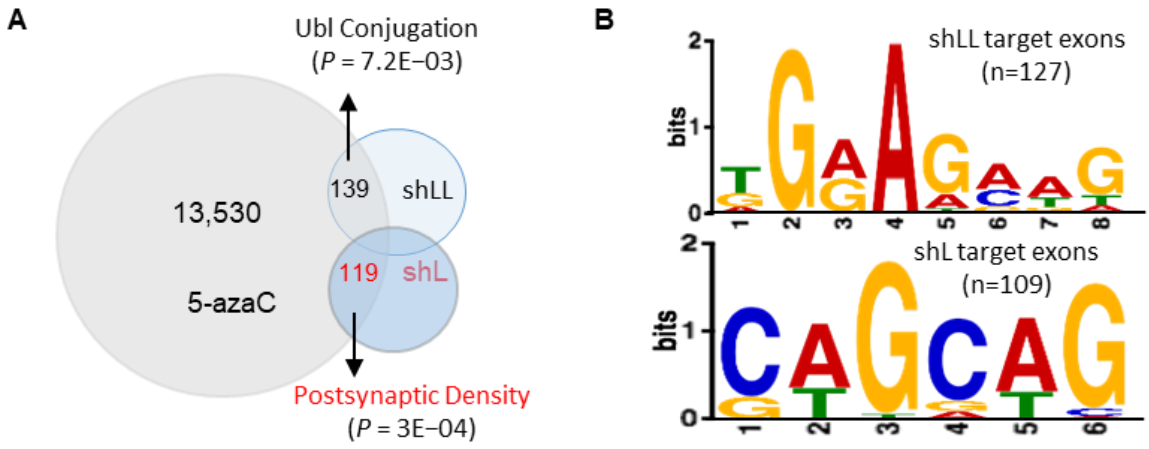

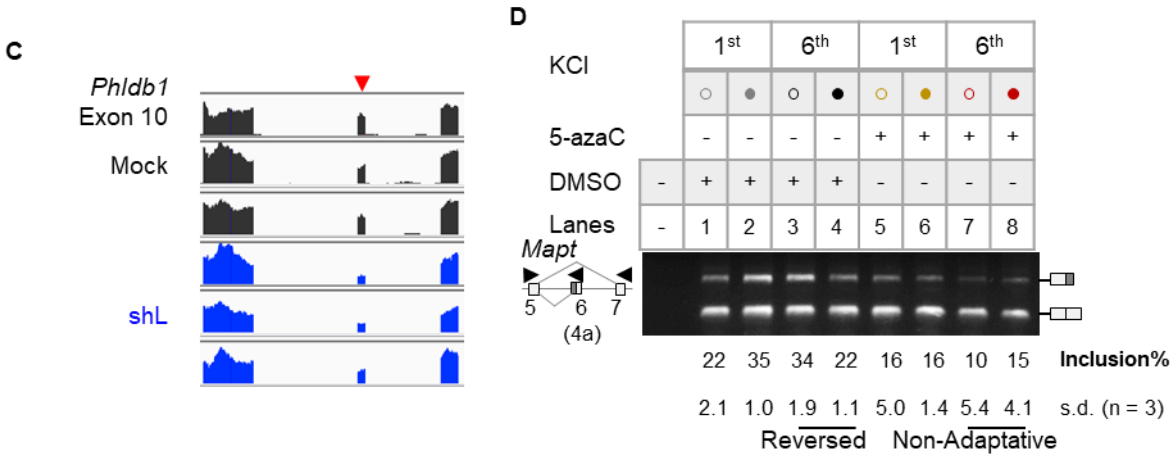

Figure 11. Essential role of hnRNP L in controlling a group of adaptively spliced synaptic exons disrupted by 5-azaC.
A-D:
A. Diagram of overlapped differentially spliced exons in the GH3 transcriptome upon 5-azaC treatment or lentiviral shL/shLL expression. **B.** Consensus motifs of shLL- or shL-changed exons that were also affected by 5-azaC, identified by MEME analysis. **C**. A representative example of the IGV profiles of the RNA-Seq reads of 5-azaC-affected, adaptive synaptic exons (Red arrowhead) changed by shL. Peaks of sequencing reads in black: mock, in blue: shL. **D**. Agarose gels of RT-PCR validation of the splicing changes of *Mapt* E6 (reference transcript GenBank #M84156) upon repeated membrane depolarization with or without 5-azaC. E4a: the human equivalent exon name. 'Reversed' or 'Non-adaptive' refers to the effect of the 6th versus the 1st KCl treatment on E6 usage.

Inclusion of the *Mapt* exon 6, equivalent to the human exon 4a in the Big tau in the peripheral nervous system [409], was enhanced by the 1st KCl but repressed upon the 6th KCl treatment, and the adaptive change was also abolished by the 5-azaC treatment (Figs. 9D and 11D). The exon usage was increased slightly by shL (Fig. 11E, n = 6) and importantly, restored to its basal level upon Flag-hnRNP L co-expression. Therefore, hnRNP L is a repressor of the adaptive synaptic exon 6 as well.

The sequence features of the exon suggested the location for hnRNP L binding and DNA methylation. The 762nt rat exon 6 and its flanking 20nt intron sequences contain 66 CA dinucleotides. Interestingly, a cacacag (underlined: 3´AG) at the 3´ splice site (3´SS) conserved in human, mouse and rat genes resembles the consensus CAGCAG of the shL target exons (Fig. 11B). It locates similarly as the hnRNP L-binding CaRRE at the upstream 3´SS of STREX and other exons[75, 89]. Moreover, its DNA methylation, together with 9 mCpHs (where H = A, C, or T) at

the 5´ 53bp of the exon, was reduced from 75% to 54% by the 1st KCl but increased from 66% to 100% by the 6th KCl treatment in BSMAP analysis, correlating inversely with the splicing changes. The methylation increase was strongly reduced by 5-azaC, back to only 29%. Thus, the 3´SS CA-rich motif is likely a target of hnRNP L and DNA methylation in the repeated depolarization-induced adaptive splicing of the *Mapt* exon 6.

UV-crosslinking-immunoprecipitation and CA to CG mutation assay indicated that the wild type (WT) 3´SS RNA probe cross-linked to hnRNP L in a CA-dependent way in HeLa nuclear extracts (Fig. 11F, lanes 3-5). Therefore, hnRNP L indeed binds the upstream 3´SS CA dinucleotides, likely to control splicing in a similar way as the CaRRE elements of the STREX and other exons [75, 361, 384].

YB-1, which interacts with MeCP2 at the transcription repressor domain (TRD) and A/C-rich motifs to regulate splicing [309, 410], was also pulled down (by anti-YB-1, lane 6), providing another possible physical link between the *Mapt* exon 6, MeCP2 and the methylated DNA. The binding of multiple splicing factors (Fig. 11F) to the 3´SS of exon 6, as well as the overlapping role of hnRNP LL (S_Fig. 4) [75, 89, 407], could explain the weak effect when only hnRNP L was knocked down (Fig. 11E). The finding of both MeCP2-interacting splicing factors here (hnRNP L and YB-1), plus MeCP2 phosphorylation by CaMKII [377], suggested to us that the hnRNP L together with the methyl-C-binding MeCP2 play a role in the splicing of these 5-azaC-affected adaptive synaptic exons.

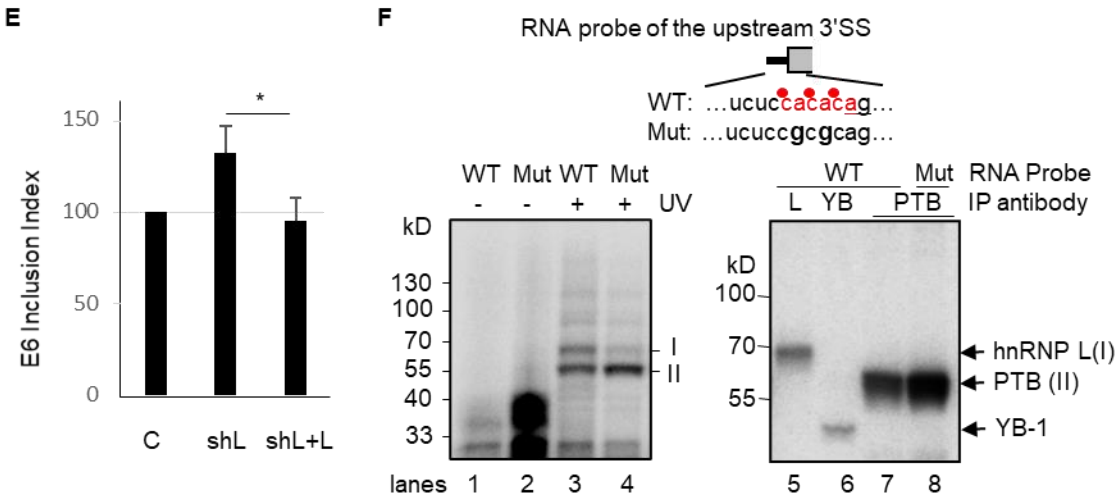

Figure 11. Essential role of hnRNP L in controlling a group of adaptively spliced synaptic exons disrupted by 5-azaC. E-F:
E. Bar graph of the index level (mean ± SEM, n = 6) of *Mapt* E6 inclusion in GH3 cells without (C) or with hnRNP L (shL) knockdown, or with shL plus hnRNP L (L) expression. ***: $p < 0.001$.
F. UV crosslinking of wild type (WT) CA repeat or CG mutant (Mut) RNA probes in HeLa nuclear extracts. Upper: diagram of the probes containing the 3´SS cacaca WT or cgcgca Mut motifs. Red dots: Corresponding DNA mCpAs whose methylation levels were reduced by 5-azaC. Underlined: 3´ AG. Lower: a phosphorimage of proteins crosslinked to the probes and resolved in SDS-PAGE gels. Immunoprecipitating antibody is against hnRNP L (L), YB-1 (YB) or PTB (PTBP1). A sixth of the crosslinking mix for immunoprecipitation was loaded in lanes 3 and 4.
(Data in the Fig. 11E-F were collected by Jian-kun Yu.)

Table 2. Exons of synaptic genes regulated by both hnRNP L and 5-azaC in DEXSeq analysis. (bold: the disruption of adaptive splicing by 5-azaC were confirmed by RT-PCR, underlined: aberrant splicing confirmed in Rett Syndrome patients, +: % Exon Usage increased, or decreased (-). Hypo: mC level reduced, and Hyper: mC level increased after 5-azaC treatment). *: exon reads relative to flanking exons changed by shL expression observed in IGV of RNA-Seq. In the brackets are the commonly referenced exon numbers of human *MAPT*.

Gene Name	Exon#	Gene Bank	5-azaC Regulation	shL Regulation	Exonic mCpH level	Exonic mCpG level	hnRNP L effect by
Cacna1d	E46	NM_017298.1	Down	Down	hyper	0	IGV
Cacna1d	E34	NM_017298.1	Down	Down	hyper	0	IGV
Clasp2	E17	NM_053722.2	Down	Down	hypo	0	IGV
Dlg1	**E20a**	NM_012788.1	Down	Up	hyper	0	IGV
Epb41l3	**E15**	NM_053927.1	Down	Down	hyper	0	IGV
Gabbr1	E19	NM_031028.3	Up	Up	hypo	0	IGV
Gphn	**E6a**	NM_022865.3	Down	Up	hypo	0	IGV
Kifc2	E14	NM_198752.3	Down	Down	hypo	hypo	IGV
Mapt	**E7a (6)**	M84156	Up	Down	hyper	hypo	IGV
Mapt	**E6 (4a)**	M84156	Down	Up	hyper	hyper	IGV & RT-PCR
Nrg1	**E12**	NM_001271128.1	Down	Up	hyper	0	IGV & RT-PCR
Phldb1	**E10**	X74226	Down	Down	0	hypo	IGV
Snap91	E29	NM_031728.1	Down	Down	NA	NA	IGV
Syne1	E90	MK681777	Up	Down	hyper	0	IGV
Syne1	E89	MK681777	Up	Down	hyper	0	IGV
Syne1	E88	MK681777	Up	Down	hyper	0	IGV

5. Aberrant splicing induced by 5-azaC and its aggravation by repeated depolarization

Interestingly, the 5-azaC treatment also caused aberrant splicing of a group of synaptic genes, including the *Dlg1* exons 20 and 21 (Fig. 12A and Table 2), *Nsmf* exon 9, *Gphn* exon 7a, and *Gipr* intron 10 (S_Fig. 5). In particular, the *Dlg1* and others even skipped constitutive exons or retained introns upon 5-azaC (or plus KCl) treatment.

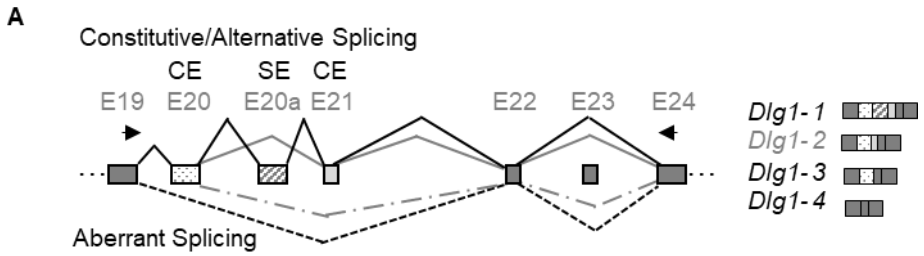

Figure 12. An example of the aberrant splicing of constitutive exons upon disruption of DNA methylation by 5-azaC and its aggravation by repeated depolarization in GH3 cells.
A. Diagram of the *Dlg1* splicing patterns observed after 5-zazC and repeated KCl treatments of GH3 cells. *Dlg1* exon numbering is based on the reference sequence NM_012788.1 of the RGSC 6.0/rn6 Assembly. *Dlg1* exon 20a is an alternative exon, while exons 19, 20, 21, 22, and 24 are constitutive exons in untreated GH3 cells. Solid grey box: constitutive exon, box with pattern: alternative exon.

For the *Dlg1* gene, whose genetic variants are associated with schizophrenia and autism spectrum disorders[411], its exon 20a is alternatively spliced and exons 19, 20, 21, 22 and 24 constitutively in the GH3 cells to generate *Dlg1-1* and *Dlg1-2* transcript variants (Fig. 12A). Interestingly, even the constitutive exons 20 and/or 21 were skipped upon 5-azaC treatment (Fig. 12A and Fig. 12B, lanes 5 and 7, *Dlg1-3* & *Dlg1-4*). The effect was enhanced by the 1st KCl treatment (lane 6) and more pronouncedly after the 6th KCl treatment (lane 8). Moreover, the 5-azaC effect was dose-dependent (1nM - 50μM) upon repeated KCl treatment (Fig. 12C).

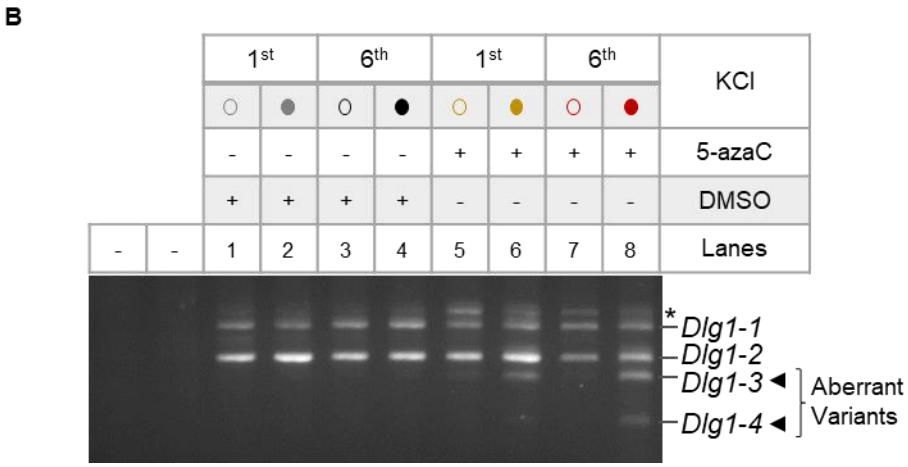

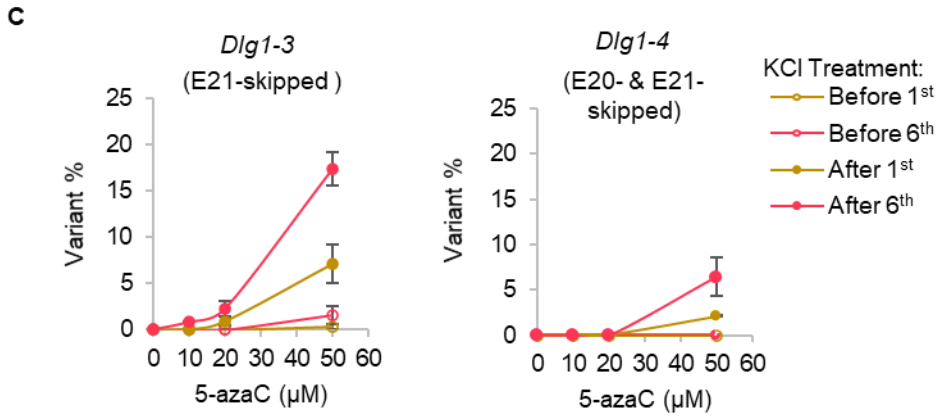

Figure 12. An example of the aberrant splicing of constitutive exons upon disruption of DNA methylation by 5-azaC and its aggravation by repeated depolarization in GH3 cells. B-C: **B.** Agarose gels of RT-PCR products upon repeated KCl treatments with/without 5-azaC (50μM). Asterisk: Heteroduplex of *Dlg1-1* and *Dlg1-2*. Products were confirmed by Sanger sequencing. Circle or hollow triangle: before KCl treatment; dots or solid triangle: after KCl treatment; for example, black dot: after 6th KCl treatment w/o 5-azaC, red solid triangle: after the 6th KCl treatment with 5-azaC. **C.** Dose-dependent effects on the aberrant splicing of *Dlg1* constitutive exons 21 (*Dlg1*-3 variant) and 20 (*Dlg1*-4 variant) induced by increasing concentrations of 5-azaC (0, 1nM, 1μM, 10μM, 20μM and 50μM).

The methylation level of the corresponding gDNA of the aberrantly skipped exons was also changed by 5-azaC: the mCpH methylation of exon 20 increased from 0.645 to 0.985 on average (n = 14 mCpH, p = 1.4E-8), and of exon 21 reduced from 0.443 to 0.262 (n = 9 mCpH, p = 1.2E-5) (Fig. 12D).

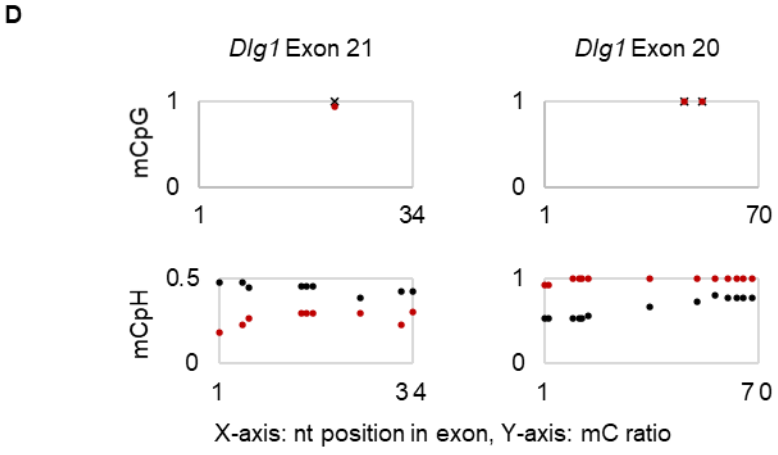

Figure 12. An example of the aberrant splicing of constitutive exons upon disruption of DNA methylation by 5-azaC and its aggravation by repeated depolarization in GH3 cells. D:

D. Changes of the exonic DNA methylation (upper: mCpG, lower: mCpH) of the *Dlg1* constitutive exons in the 6th KCl-treated cells with (black) or without (red) 5-azaC (50μM) treatment.

In further support of this 5-azaC effect on aberrant splicing, we also observed the aberrant skipping of the constitutive exons of *Prolactin* (*Prl*), a signature hormone gene of the GH3 cells, accompanied by reduced *Prl* transcript levels and exon methylation changes upon treatment by 5-azaC and KCl (S_Fig. 6). Similarly, the reduction was aggravated by repeated depolarization.

Therefore, 5-azaC also causes aberrant splicing, which can be aggravated by repeated depolarization treatments.

6. Aberrant splicing of the adaptive synaptic exons in the hippocampus upon mutations in the protein interaction or methyl-DNA binding domains of *MECP2* protein in Rett syndrome patients

Particularly relevant to the 5-azaC- or DNA methylation-regulated adaptive or aberrant splicing of synaptic exons are the important role of neuronal activities for synapse development[412], aggravated, activity-dependent aberrant splicing in *Mecp2*-null mice[315], and moreover, the abnormal neuronal activities or synaptic plasticity associated with the progressive severity of the Rett syndrome after birth[344, 370, 371, 413, 414]. We thus examined these exons in MeCP2-defective samples to determine if their splicing is also affected by mutations of the methyl-C binding protein gene, particularly those affecting the splicing factor- or mC-binding domains.

We first examined the exon DNA methylation and corresponding splicing changes in the hippocampus of *Mecp2*-null mice upon treatment by the calcium signal-activating kainic acid (KA)[315, 388]. The splicing changes by kainic acid were aggravated overall in the mutant mice as expected [315]. More interestingly, we found that the splicing changes were inversely correlated with exon DNA methylation (Fig. 13A): the higher change ratios were limited to the least methylated exons and the highly methylated exons limited to the least change ratios, similarly as in the 5-azaC-treated GH3 cells (Fig. 13A). These included 8 of the above 52 highly adaptive exons affected by 5-azaC (Fig. 13C). Thus, a similar correlation between exon DNA methylation and splicing changes exists in the *MeCP2*-null mice as in the 5-azaC-treated GH3 cells (Fig. 13).

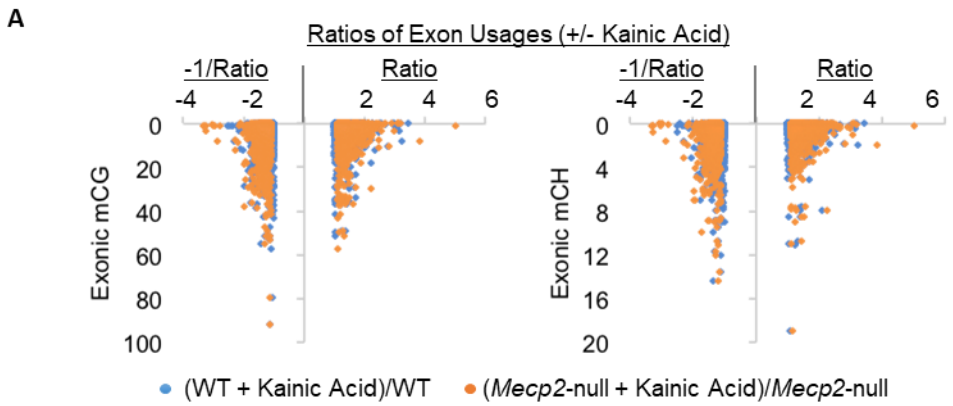

Figure 13. Aberrant splicing of the 5-azaC-affected, adaptive synaptic exons in the hippocampus of a mouse model of Rett syndrome and Rett syndrome patient samples with *MECP2* mutations.
A. Scatter plots of the mCpG (Left) or mCpH (Right) methylation levels of exonic DNA of wild type mice and ratios of corresponding exon usage with/without kainic acid treatment in the hippocampus of wild type (blue) or *Mecp2*-null (brown) mice, through analysis of the raw reads from two separate datasets by Osenberg or Guo respectively. The ratios less than one are displayed as -1/ratio to illustrate the shift from 1 (or -1) in the *Mecp2*-null mice. Note the further shift of brown (mutant) dots overall away from the midline compared to the blues WT ones of the same group of exons. n = 1,719 exons for both mCpG and mCpH.

We then examined the adaptive synaptic exons in human patients of Rett syndrome, carrying mutations of the *MECP2* gene affecting the methyl-DNA binding or transcription repressor/splicing factor-interaction domains (MDB or TRD) [344, 345, 415]. RT-PCR of 6 exons of the synaptic genes identified three of them, *EPB41L3* exon 15, *KIDINS220* exon 26 and *MAPT* exon 10 that changed significantly in the patient samples (Fig. 13B). Specifically, usage of the *EPB41L3* exon 15 increased from 7.41% in normal to 55.95% ($p < 0.001$, n = 5 hippocampi) in the patients. Usage of both the *KIDINS220* exon 26 and *MAPT* exon 10 decreased. Additionally, the average level of a *GPHN* (gephryin) exon was also decreased (Fig. 13D). In contrast, these aberrant splicing events were not observed in the cerebella of the same patients, supporting hippocampus-specific aberrant splicing.

Interestingly, samples of the TRD mutants R255X, A201V and MDB mutant T158M consistently exhibited higher splicing changes than did the IVS3-2A>G (Fig. 13D). Taken together with the essential role of the two domains for MeCP2 interaction with splicing or other factors and the methyl-C of DNA[309, 416], respectively, this *MECP2* mutation-dependent effect suggests a critical role of the splicing factor interaction or mC-binding by MeCP2 to maintain proper splicing.

Moreover, patients with the R255X or T158M mutation also have higher Rett concordant scores than with the IVS3-2A>G mutation [417], consistent with a potential correlation between the splicing aberration and Rett concordance.

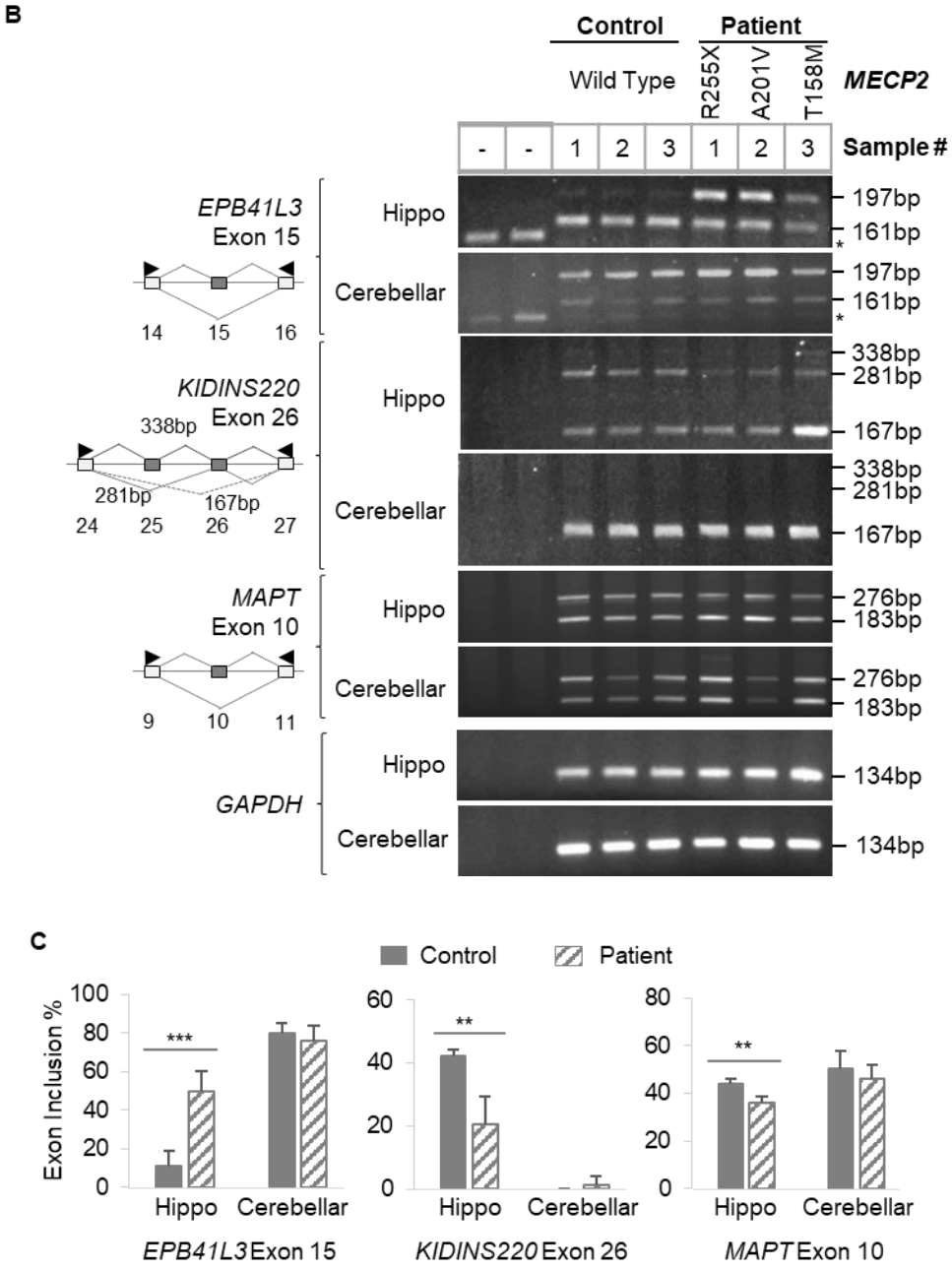

Figure 13. Aberrant splicing of the 5-azaC-affected, adaptive synaptic exons in the hippocampus of a mouse model of Rett syndrome and Rett syndrome patient samples with *MECP2* mutations. B-C:

B. Agarose gel RT-PCR products of three 5-azaC-affected adaptive synaptic exons in the hippocampal tissues (Hippo) of Rett syndrome patients and healthy controls. Cerebellar tissues of the same patients are included as controls. *GAPDH*, RNA loading control. Black arrowheads: location/direction of PCR primers. Gray boxes: alternative exons, white boxes: constitutive exons. *: Products from primers without cDNA. The size of each *KIDINS220* gene product is indicated next to the splicing pathway diagrammed to the left of the gel. **C**. Bar graphs of the percentages (mean ± SD) of exon inclusion levels based on the RT-PCR result of 5 Rett syndrome patients and 4 controls. ***: $p < 0.001$, **: $p < 0.002$.

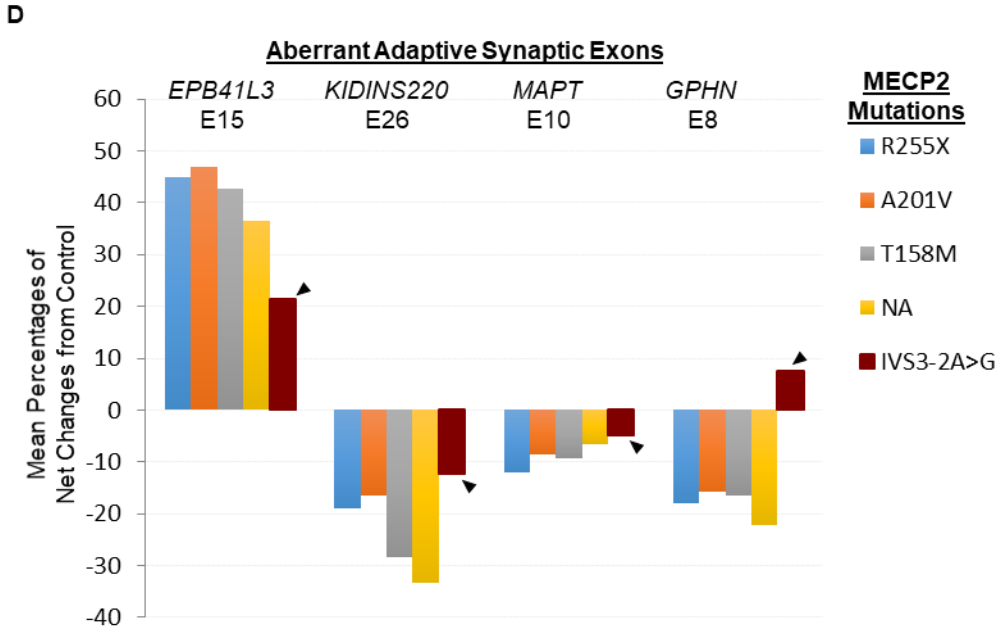

Figure 13. Aberrant splicing of the 5-azaC-affected, adaptive synaptic exons in the hippocampus of a mouse model of Rett syndrome and Rett syndrome patient samples with *MECP2* mutations. D:
D. Bar graph of the net percent changes of each exon usage of patients from the mean percentages of the control samples in the presence of their respective *MECP2* mutations. NA: mutation information not available. Arrowhead: IVS3-2A->G samples. The numbering of human exons is based on the following transcripts: *EPB41L3* exon 15, NM_012307.4, equivalent to the *Epb41l3* exon 15 (NM_053927.1); *KIDINS220* exon 26, NM_001348729.2, equivalent to the *Kidins220* exon 26 (NM_053795.1); *MAPT* exon 10, NM_001123066.3, equivalent to *Mapt* exon 10 (M84156); *GPHN* exon 8, NM_020806.4, equivalent to *Gphn* exon 6a (NM_022865.3).

Thus, *MECP2* mutations, particularly of the splicing factor and mC-binding domains, cause aberrant splicing of the adaptive synaptic exons specifically in the hippocampus of Rett syndrome patients.

We therefore conclude that DNA methylation controls adaptive splicing of synaptic exons upon repeated cellular excitations (Fig. 14), and deregulation of the exons by disrupting DNA methylation or the splicing factor- or mC-binding domain of MeCP2 likely contributes to their aggravated aberrant splicing, specifically in the hippocampus of Rett syndrome patients.

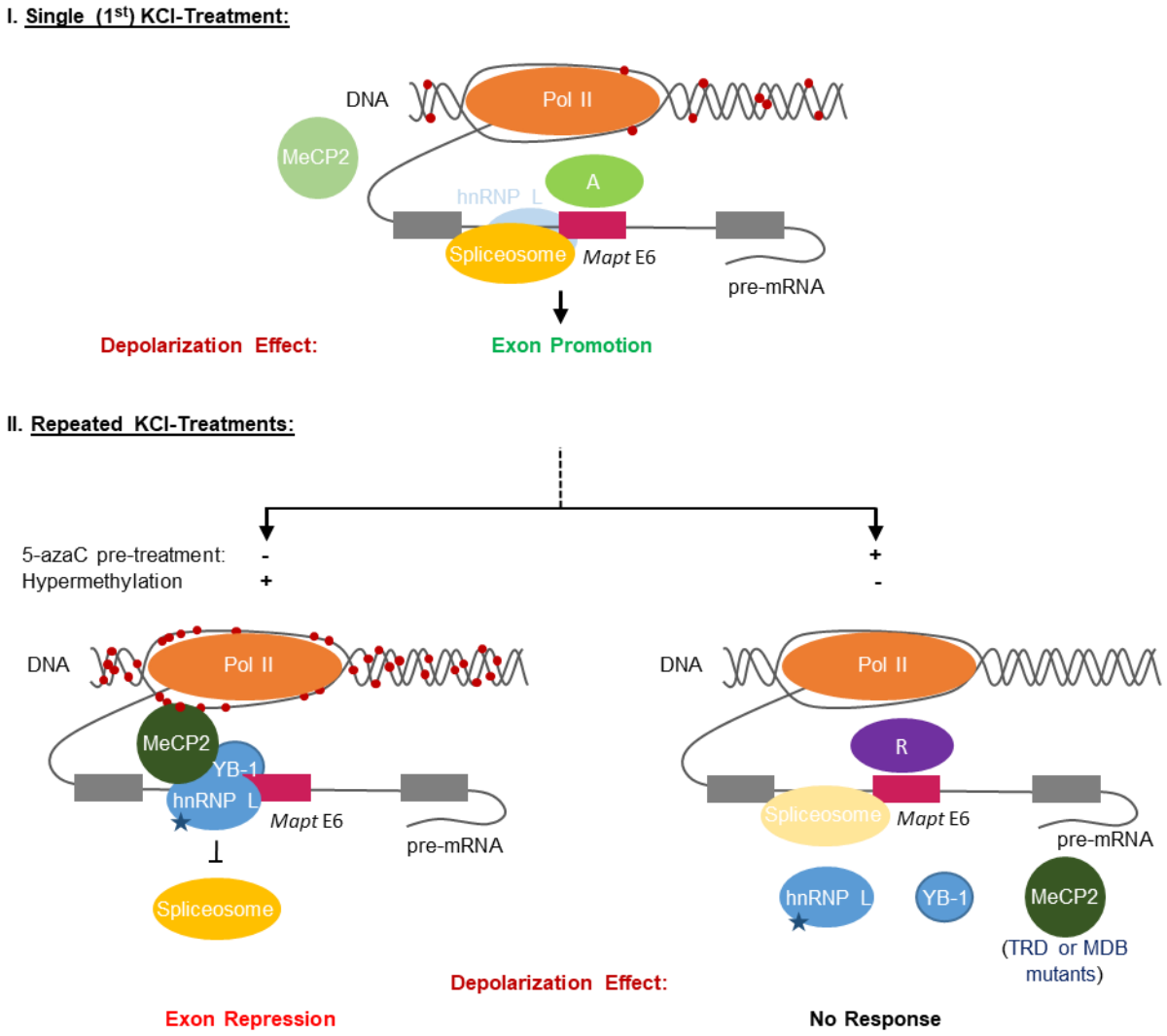

Figure 14. Summary of the methylation control of adaptive splicing.
(with the *Mapt* exon 6 as an example of the mostly exon-dependent, diverse changes of methylation/splicing). With a single round of KCl treatment (**I**), the DNA methylation is at a comparatively low level (54%); therefore, binding of MeCP2 and hnRNP L to the DNA and pre-mRNA is inefficient, and insufficient to overcome the effect of splicing activators (A) in cells. After repeated KCl-treatments (**II**), the DNA is hypermethylated (100%, Left) recruiting MeCP2 and associated hnRNP L/YB-1 leading to exon repression. With 5-azaC pre-treatment (Right), the methylation is greatly reduced (29%) and the splicing is inhibited by repressors (**R**) that are non-

responsive to depolarization. Similar decoupling of the methyl-DNA and associated splicing factors is likely most effective when the TRD and MDB domains of *MECP2* are mutated. The changes during the adaptive splicing in II and its disruption are also consistent with the *in vitro* methylation/mutagenesis data of the reporter exon in Fig. 14. Star: p-Ser^{513} of hnRNP L. Red dots on DNA: methyl-Cytosines. (kindly illustrated by Lei Lei)

Acknowledgments of the Results

We thank the University of Maryland Brain and Tissue Bank, a Brain and Tissue Repository of the NIH Biobank (at NIH NeuroBioBank Program: neurobiobank.nih.gov)., and the patient families who donated brain tissues for research, and Frederick Robidoux and Sylvie Laboissiere of the McGill University Genome Quebec Innovation Centre for their excellent service. We thank Etienne Leygue, Muhammad Sohail, Samuel Ogunsola and Sam Kung for their helpful comments on the manuscript. The work has been supported by a Manitoba Research Chair fund, a CIHR (Canadian Institutes of Health Research) operating grant, and in part by a NSERC (Natural Sciences & Engineering Research Council of Canada) discovery grant to J.X., and by University of Manitoba Rady Innovation Funds to M.R. and J.X, and NSERC-DG grant (2016-06035) to MR. L.L. has been supported by a UMGF scholarship.

Data and Code Availability

Raw data from Figures 8-14 and S_Figures 1, 2, 3, 5, 6 were deposited on Mendeley at http://dx.doi.org/10.17632/w4wy8g36gk.1 (The raw data will be public until Dec. 2021).

Supplementary Information For The Results

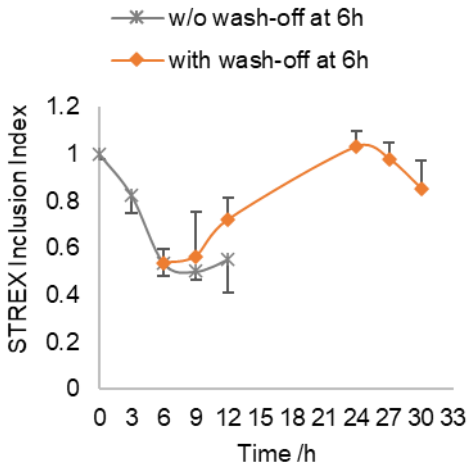

S_Figure 1. Time course of STREX splicing response to single KCl (50mM) treatment (gray dot and line) with or without KCl wash-off at 6h (orange dot and line). The inclusion of STREX was repressed at 3h and reach to the strongest repression at 6h after KCl addition and recovered completely 18h after washing off KCl. STREX inclusion index in the Y axis = STRX inclusion level (%) in the different time points / STREX inclusion level (%) before the KCl treatment (time 0 in the X axis). That is, the index of STREX inclusion level before the KCl treatment is normalized as 1.

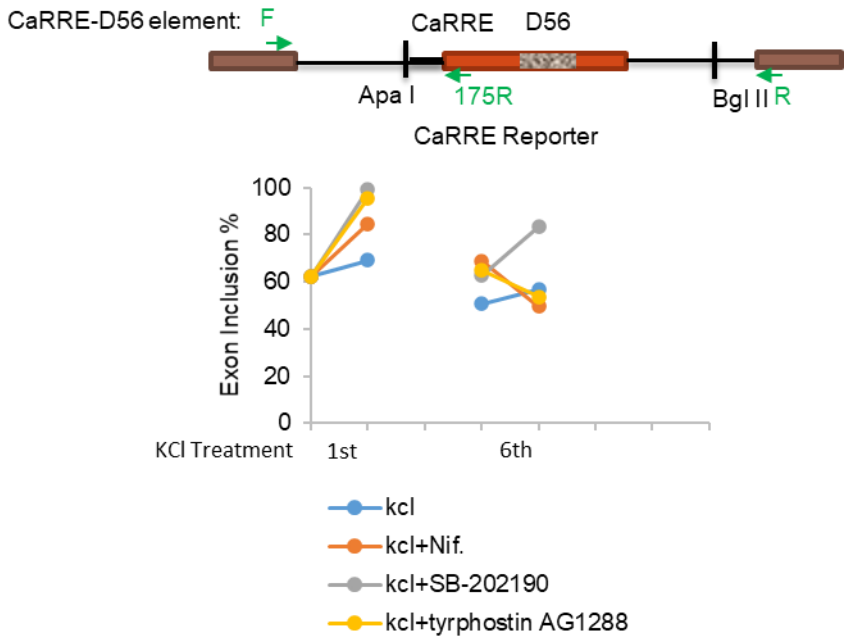

S_Figure 2. The adaptive splicing of a reporter exon is disrupted by specific signaling pathway inhibitors. Scatter plot showing that both tyrphostin AG 1288 and nifedipine but not SB202109 treatment switched the depolarization effect of the 6th KCl treatment on the reporter exon in the N1E cells. A group of signaling pathways were used to screen for the essential pathways controlling adaptive splicing. Based on previous studies, we tested SB-202190 (p38 MAPK pathway inhibitor [62]), Tyrphostin AG 1288 (Tyrosine kinases pathway inhibitor [205]) and nifedipine (Ca2+/CaMKIV pathway inhibitor [418]) by a splicing reporter minigene assay in N1E cells. 1 day after the transfection of the reporter plasmids DUP175-CaRRE-D56 (CaRRE: a CaMK IV-responsive RNA element [361], 53-nucleotide intron + 1-nucleotide STREX exon) in N1E cells, cells were treated with 50mM KCl and L-type Ca^{2+} channel inhibitor nifedipine, p38 MAPK pathway inhibitor SB-202190, or tyrosine kinases pathway inhibitor tyrphostin AG 1288 for 6h (10 μM for each inhibitor), then washed off drugs and added back fresh complete growth medium till the next treatment 18h later. The treatments were repeated up to 6 times. The inhibitor assays were carried out in duplicates. Green arrow: primers (F: forward primer, R: reverse primer, 175R: primer specifically binding to reporter exon.

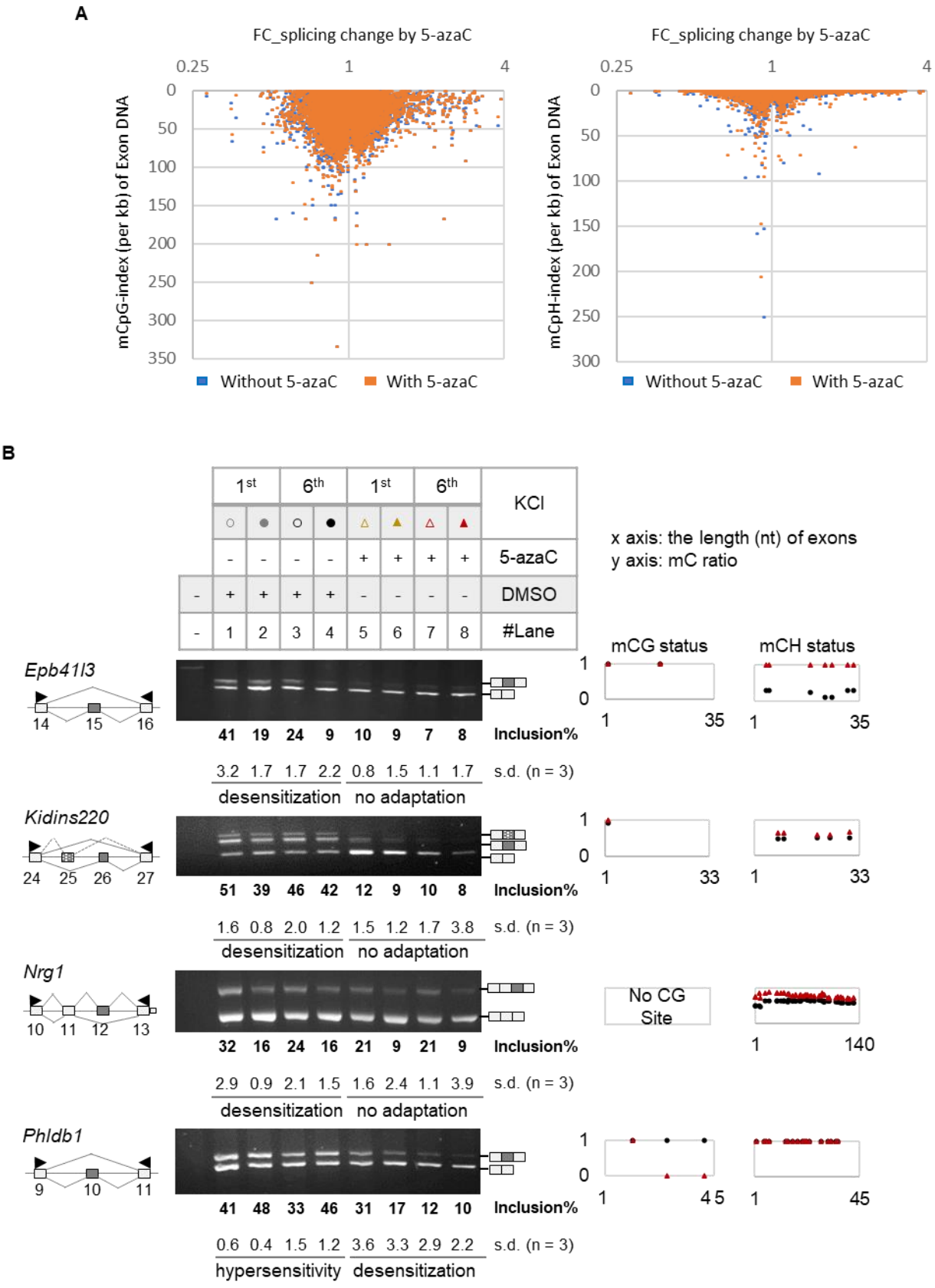
A
FC_splicing change by 5-azaC
0.25
1
4
mCpG-index (per kb) of Exon DNA
0
50
100
150
200
250
300
350
Without 5-azaC
With 5-azaC
FC_splicing change by 5-azaC
mCpH-index (per kb) of Exon DNA
Without 5-azaC
With 5-azaC
B
1st
6th
1st
6th
KCl
5-azaC
DMSO
#Lane
x axis: the length (nt) of exons
y axis: mC ratio
mCG status
mCH status
Epb41l3
14 15 16
41 19 24 9 10 9 7 8
Inclusion%
3.2 1.7 1.7 2.2 0.8 1.5 1.1 1.7
s.d. (n = 3)
desensitization
no adaptation
Kidins220
24 25 26 27
51 39 46 42 12 9 10 8
Inclusion%
1.6 0.8 2.0 1.2 1.5 1.2 1.7 3.8
s.d. (n = 3)
desensitization
no adaptation
Nrg1
10 11 12 13
No CG Site
32 16 24 16 21 9 21 9
Inclusion%
2.9 0.9 2.1 1.5 1.6 2.4 1.1 3.9
s.d. (n = 3)
desensitization
no adaptation
Phldb1
9 10 11
41 48 33 46 31 17 12 10
Inclusion%
0.6 0.4 1.5 1.2 3.6 3.3 2.9 2.2
s.d. (n = 3)
hypersensitivity
desensitization

S_Figure 3. Normalized methylation levels versus splicing changes (A) and additional examples of the adaptive splicing of synaptic exons disrupted by 5-azaC (B). **A**. Normalized exon methylation levels (per kilobases, without or with 5-azaC-treated) versus splicing changes by 5-azaC. **B**. Agarose gels **(the left panel)** of RT-PCR products, of examples of effects of 5-AzaC on exon inclusion level, splicing response to depolarization, adaptive splicing pattern to repeated depolarizations of a group of synapse-related genes in GH3 cells. Scatter plot **(the right panel)** of the individual DNA methylation status (mCG and/or mCH) of each exon upon the 6th KCl treatment with or w/o 5-AzaC treatment in GH3 cells. The flanking introns (+10nt) of exon always showed the same methylation level as the corresponding end of exon. Grey box: the tested alternative exons, white box: constitutive exons, black arrow: primers. The exon numbers were based on reference transcripts from the UCSC Genome Browser on Rat Jul. 2014 (RGSC 6.0/rn6) Assembly: *Epb41l3* exon 15, NM_053927.1; *Kidins220* exon 26, NM_053795.1; *Nrg1* exon 12, NM_001271128.1; *Phldb1* exon 10, X74226.

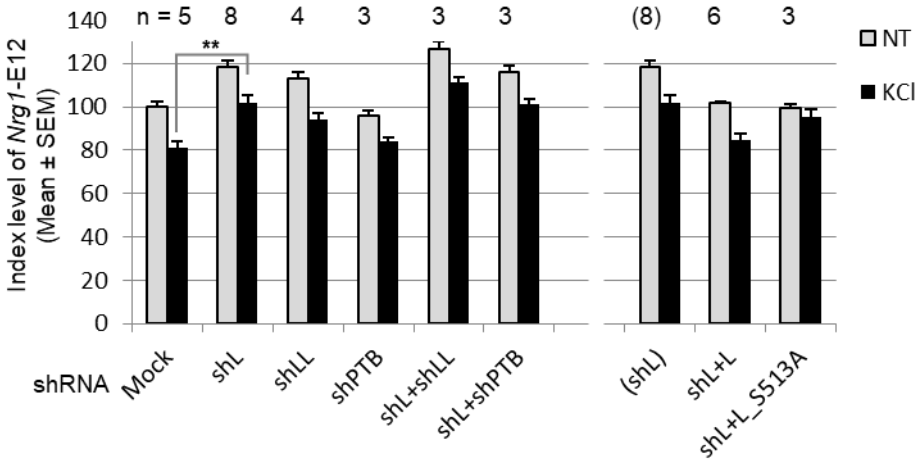

S_Figure 4. Examples of hnRNP L as a splicing regulator to regulate the adaptively spliced synapse-related *Nrg1* exon 12 disrupted by 5-azaC. Bar graphs of the exon inclusion levels of *Nrg1* exon12 in the non-treated (NT) or depolarized (KCl, 50mM, for 12 hs) cells that were without (mock) or with expression of shRNA against specific splicing factors hnRNP L (shL), LL (shLL) or PTB(shPTB). In GH3 cells, the Nrg1 exon 12 was reduced from 37% to 30% by depolarization (mock, p=0.001). To measure and compare potential consistent changes between different experiments for such an effect, we normalized all of the Nrg1 exon 12 levels to the mock control samples (without lentivirus or with vector only), which was taken as 100. In contrast to the reduction of the variant by depolarization, a significant increase was observed upon hnRNP L knock-down by shL (p = 0.004). A slight increase was observed in the shLL but not shPTB sample. Further increase was observed upon knocked-down of both hnRNP L and LL but not PTB. The depolarization-induced reduction of the variant was not abolished in any of these knockdown samples. *Nrg1* exon 12, based on NM_001271128.1 (RGSC 6.0/rn6).

Both hnRNP L and L-S513A restored the variant to its basal level, confirming that hnRNP L is indeed a repressor of the variant exon 12 and the Ser513 is not essential for this repression. However, the S513A mutant abolished the depolarization-induced reduction of the variant, suggesting that the mutant interferes with the function of another essential factor(s) for the depolarization effect.

[The data in this figure (S_Fig. 4) were collected by the previous lab member Jian-kun Yu.]

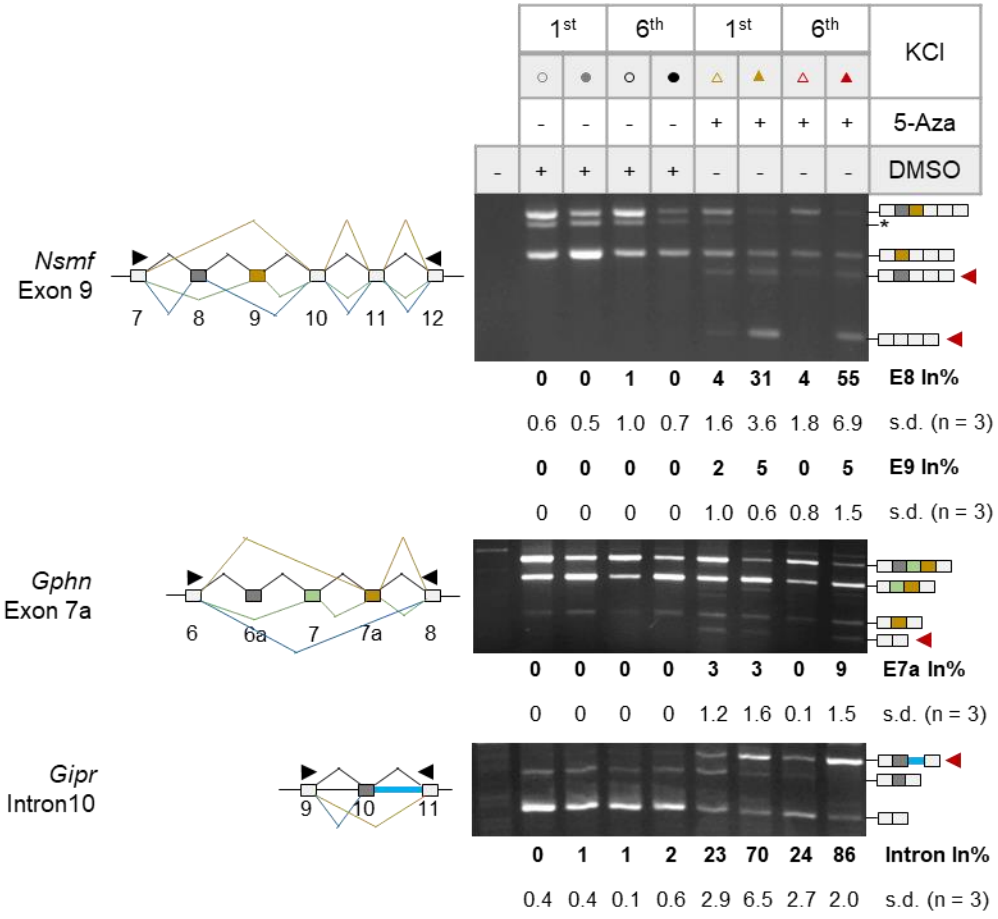

S_Figure 5. More examples of 5-azaC induced adaptively aberrant splicing of synaptic genes upon repeated depolarization. Agarose gels of RT-PCR of RNA from cells upon repeated KCl treatments with or without the pre-treatment of 5-azaC (50μM) in GH3 cells. white box: constitutive exon, grey box and light green box: alternative exon, orange box: aberrantly skipped exon, narrow blue box: aberrantly used intron; black arrow: primer, red arrow: PCR product with aberrant exon skipping or intron usage. n=3, triplicates. *: Unexpected products, which may be the heteroduplex created during the PCR reaction by the RNA-RNA base paring of the two single splice variants. The exon numbers are based on these reference transcripts: *Nsmf* exon 9, NM_057190.2; *Gphn* exon 7a, NM_022865.3, between exons 7 and 8; *Gipr* intron 10, NM_012714.1.

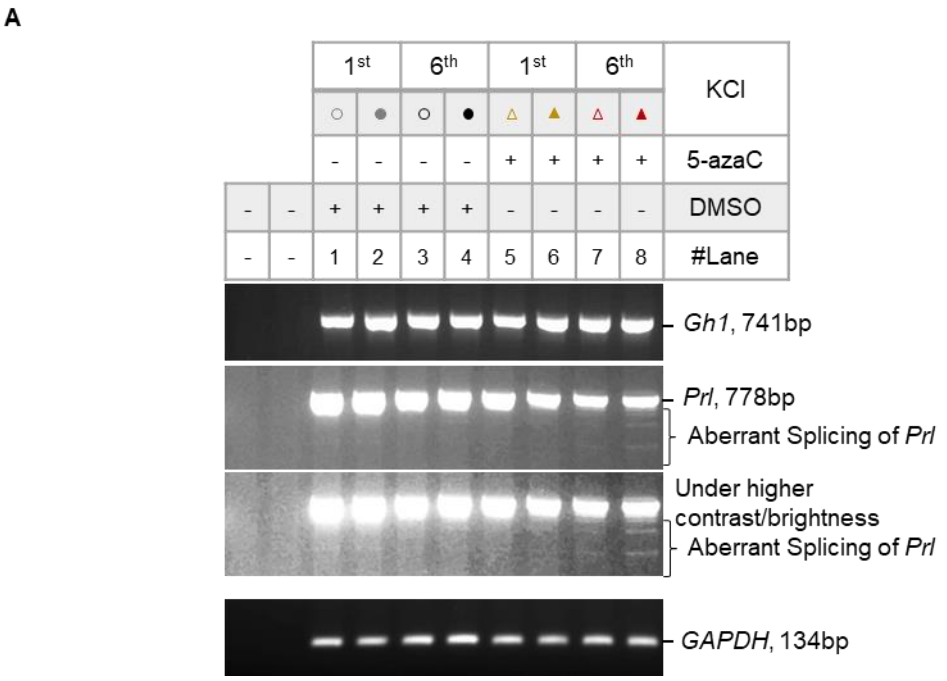
A
1st
6th
1st
6th
KCl
5-azaC
DMSO
#Lane
Gh1, 741bp
Prl, 778bp
Aberrant Splicing of Prl
Under higher contrast/brightness
Aberrant Splicing of Prl
GAPDH, 134bp

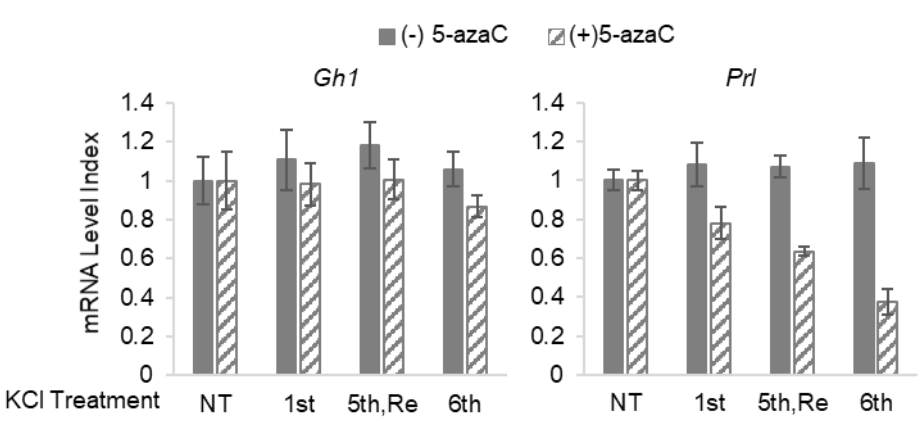
B
(-) 5-azaC
(+)5-azaC
Gh1
Prl
mRNA Level Index
KCl Treatment
NT
1st
5th,Re
6th

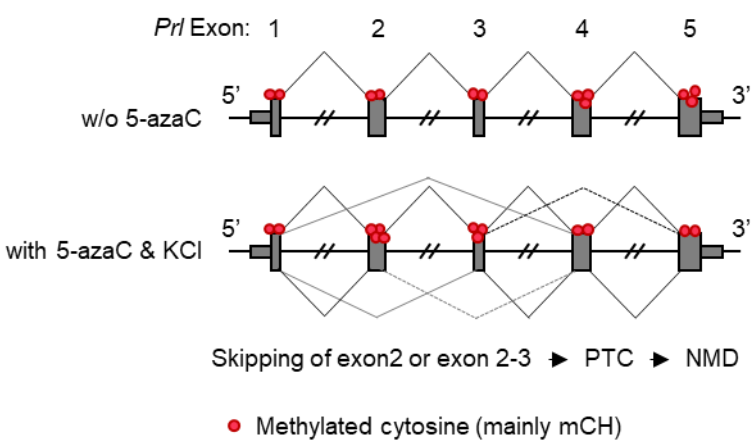
C
Prl Exon: 1 2 3 4 5
w/o 5-azaC
with 5-azaC & KCl
5'
3'
Skipping of exon2 or exon 2-3 ► PTC ► NMD
Methylated cytosine (mainly mCH)

S_Figure 6. Aberrant splicing of *prolactin* induced by 5-azaC upon repeated depolarizations in rat pituitary GH3 cells, accompanied with mRNA level change and exonic DNA methylation disruption. A. RT-PCR of RNA from cells upon repeated KCl treaments with or without 5-azaC. Without 5-azaC treatment, there are no significant change of splicing and the mRNA level of Gh1 and Prl upon either the 1st or the 6th KCl, suggesting that the cells have kept their major endocrine identities during the treatments. With 5-azaC treatment, the aberrant skipping of the Prolactin gene exons accompanied by reduced Prl transcript levels and exon methylation changes upon treatment with KCl and 5-azaC. The reduction was aggravated by repeated depolarization. GAPDH (Glyceraldehyde-3-Phosphate Dehydrogenase), RNA loading control. **B.** Bar graph of the normalized inclusion level of the *Prl* transcript. The inclusion level was normalized by the non-treated samples (without KCl and 5-azaC treatment), which was taken as the base level 1. **C.** Diagram of the *Prl* variants as well as the average DNA methylation level of each exon upon repeated KCl treaments with or without 5-azaC. Consistently, the methylation level of these skipped exons was disrupted by 5-azaC, with hypermethylation in exon 2 (from 50% to 87.5%) and 3 (from 53% to 72%) and hypomethylation in exon 4 and 5(from 77% to 45%).

The Prl promoters were hypermethylated (mCG and mCH, mainly mCH) from 42% to 83% by 5-azaC, suggesting that the transcriptional inhibition of PRL by 5-azaC were likely caused by DNA hypermethylation of Prl promoter as well. In comparison, consistent with the unchanged mRNA level and stable splicing upon 5-azaC treatment, the average methylation level of Gh1 promoter and exons weren't significantly changed by 5-azaC. Thus, exonic DNA methylation status likely plays a role in the homeostasis of full-length Prl, but not growth hormone 1, transcripts upon repeated depolarization in the rat pituitary cells. Grey box: exon, line: intron, red dot: methylated cytosine (mainly mCH).

Discussion

Most studies on gene expression particularly alternative splicing have examined the effect of single or sustained treatments on cells. However, cells often face repeated extracellular stimulations with recurrent gaps, like neurons, muscle cells or the hormone-producing pituitary cells during exercise training of an individual in a lifetime [7, 353]. Does alternative splicing in these cells respond to the same stimulus the same way or differently from a single/sustained treatment? This question prompted us to carry out the current study based on our past work on the STREX exon in the GH3 pituitary cells[75, 89, 110, 169, 407]. The observed adaptive splicing and its control by DNA methylation carry several implications in cell biology and diseases.

1. Adaptive splicing in response to repeated stimulations by extracellular factors

In a changing environment, adaptation allows cells to fit or survive, preferably with an optimal combination of novel products. Where gene regulation is involved, alternative splicing provides a molecular basis for a highly diverse proteome beyond the relatively small number of protein-coding genes[358, 359]. The hugely expanded repertoire of diverse variants with functional differences allows cells to selectively express a new assembly of variants to fine-tune their response to an external stimulus in activity-dependent splicing[169]. The expression of many alternative exons has been shown to fine-tune protein/cell properties or play critical roles in cellular adaptation. For instance, the STREX and other BK channel exons generate channel variants to form heterotetramers to fine-tune the electrical properties of the channels[419], or of the inner cochlear hair cells[420]. The selective use of the insulin receptor DAF-2c over the -2a variant is critical for associative learning in *C. elegans* [136]. Alternative splicing of the BK channel or AMPAR exons also play critical roles in the homeostasis of the electrical properties of neurons after chronic inactivities[133, 134].

Our adaptive splicing data here went further to demonstrate clearly that the cells adjusted their alternative splicing machinery after the 1st time stimulation to respond to the following stimulations with a novel combination of splice variants in an exon- and cell-dependent way (Fig. 8). The functions of the adaptively spliced variants in the synapse, vesicle secretion and other cellular processes suggest that such a change of variant combinations is perhaps part of the adaptation of these hormone-producing cells to stimulations such as exercise training, chronic stress or in the case of neurons, learning or long-term memory.

Another interesting exon in this study besides the STREX is the *MAPT* exon 10, whose increased usage due to genetic mutations at the downstream 5´ splice site causes dementia FTDP-17[408]. Its usage is reduced by *MECP2* mutations in the hippocampus of Rett syndrome patients (Fig. 13B-C), and by 5-azaC, KCl, or further by their combined treatment of GH3 cells (Figs. 9D-E), suggesting a potential role of the exon in the progression of Rett syndrome as well. The critical role of the activity-regulated exon in dementia and its aberrant splicing in Rett syndrome perhaps reflects the importance to maintain a fine balance of its usage (e.g., to avoid neurofilament aggregation in dementia); or else, either its dramatic increase or decrease could be detrimental. Moreover, two other *Mapt* exons 6 and 7a (equivalent to *hMAPT* exons 4a and 6, respectively) also changed adaptively in GH3 cells by repeated depolarization and/or 5-azaC treatments (Figs. 9D-E, & 11D), suggesting the synaptic *Mapt* gene as a prime target of activity-regulation of adaptive splicing.

Taken together, the adaptive splicing upon repeated stimulations distinctly from a single treatment allows cells to adjust their selection of splice variants, likely to adapt to the changing environment and may play a role in hormone production or the pathogenesis of neurological diseases.

2. DNA methylation on splicing, inducible splicing and adaptive splicing

Genome-wide evidence about the relationship between DNA methylation and splicing has been accumulating [297, 421, 422], though there are variable effects in splicing reporter assays [299, 302]. Here our data further show that DNA methylation is not only correlated but also essential for inducible splicing as well as adaptive splicing (Figs. 9-13). Moreover, the DNA methylation effect appears to be exon-dependent, which could help explain the different effects of different mini-gene splicing reporter assays in the previous reports[299, 302]. Furthermore, the DNA methylation effect could be augmented by repeated depolarization or CaMKIV (Figs. 9-12), similar to when *Mecp2* is mutated (Fig. 13A), supporting interactions between both epigenetic components and the splicing machinery in cell activities.

An important feature of DNA methylation is that it could be passed on to the next generation in the maintenance of cell types or in genomic imprinting[423]. The repeated treatment experiment with almost quadrupled total numbers of cells at day 5 (Fig. 8B) spanned about three generations. The altered splicing response in the third generation after repeated treatments is in

contrast to that treated for the 1st time (Figs. 1-2). These observations suggest that the 1st time-treatment effect on splicing was remembered and passed onto the daughter cells with modifications for a different response by a specific group of exons to repeated but not just a single treatment. This passage through generations of cells perhaps could be best explained by the methylation change/control of these splicing events (Fig. 9G).

The diverse effects of 5-azaC and *Mecp2* mutation on the inducible or adaptive splice variants also suggest that the involved splicing factors in the epigenetic control of splicing could be highly diverse (Figs. 2, 4 and 6A). In the case of the *Mapt* exon 6, the splicing factors (hnRNP L or YB-1) interact with the *cis*-acting element of the pre-mRNA/exon (Fig. 11). They also interact with the MeCP2[309, 313]. Therefore, for specific exons, their pre-mRNA elements and bound splicing factors likely provide the exon-specific signature for the regulation of adaptive splicing by the more general epigenetic factor. Indeed, for the MeCP2 and another epigenetic factor methyl-lysine binding protein HP1[424], diverse interacting splicing factors have been identified, for example, hnRNPs and arginine/serine-rich (SR) proteins[313, 317]. Thus, more splicing factors are likely to be identified in DNA methylation-controlled splicing in an exon-dependent way.

For the underlying molecular mechanisms, the aberrant splicing of the *EPB41L3* exon 15 and *MAPT* exon 10 in Rett syndrome patients is consistent with their reduction in the GH3 cells by increased and reduced mCpA methylation, respectively, upon 5-azaC treatment. The exon 15 change is consistent with the involvement of a splicing repressor such as hnRNP L or YB-1 (Fig. 11) in the presence of mCpA and MECP2; the latter with an unknown splicing enhancer. Further detailed experiments are needed to answer questions such as how the methylation changes upon depolarization in the course of the repeated treatments; what the dynamics of the methylation changes is in relation to the recruitment of the splicing factors; and how the hnRNP L at the 3´ splice site regulates splicing in response to the methylation changes within the site. In particular for the last question, our previous experiments have shown that the CA repeat elements at this location belong to a group of regulatory elements called CaRRE or in general REPA (regulatory element between the Py and 3´ AG)[110, 425, 426]. The CA repeats-recruited hnRNP L or G tracts-recruited hnRNP H/F compete off the U2AF65 in the early steps of splicing[75, 427]. However, recently a hairpin structure has been found between the branch point and 3´ AG in the cryoEM structure of post-catalysis spliceosomes after the 1st trans-esterification step[428, 429].

This suggests that the hairpin structure, which helps bring the 3´ exon in close proximity to the first exon to be poised for the 2nd transesterification step, could be a target of regulation by the REPA CA repeats or G-tracts. The REPAs are enriched in vertebrates[426, 430]. Whether they would open a window for widespread second or multi-step regulation of splicing of the same exons in vertebrates, and the role of DNA methylation, particularly of CA dinucleotides of neuronal genes (Figs. 2 & 4)[365, 366], is an interesting question worthy of further investigation.

3. Potential therapeutic targets of Rett syndrome

Besides aberrantly expressed genes, aberrant variants of critical neuronal functions could be another group of therapeutic targets. The aberrant splicing events likely have an important impact on neurological diseases. For example, increased inclusion of the *MAPT* exon 10 causes FTDP-17 dementia [408]. The dramatic increase of the brain-specific *EPB41L3* E15 results in a highly charged peptide in the spectrin actin binding (SAB) domain of the membrane protein[431, 432]. *KIDINS220* plays a critical role in intellectual ability [433]. *GPHN* encodes a synaptic organizer with a role in autism and GABAergic synaptic inhibition[434, 435]. Thus, manipulating their exon usage by small molecules or genetic manipulations is an appealing approach for therapy of disease phenotypes attributable to aberrant splice variants. For this purpose, selection of target exons could focus on the most strongly changed exons in the *Mecp2*-null mice of Rett syndrome with the least methylation of their exon DNA (Fig. 13A). For small molecules, 5-azaC or less toxic, DNA methylation-modulating agents such as the soy-derived genistein[436], perhaps could reverse the level of critical but aberrantly spliced exons in neurological diseases.

In summary, the control of the adaptive pre-mRNA splicing of synaptic exons by exonic DNA methylation and their aberrant splicing in Rett syndrome tissues implicate the epigenetic regulation of adaptive splicing in activity-dependent adaptive cell physiology and progressive neurological diseases. This also provides synaptic exons to study the interaction between DNA methylation and adaptive pre-mRNA processing as well as potential therapeutic targets.

4. Overall implications

The study provides a novel molecular dimension for activity-dependent cellular adaptation at the level of pre-messenger RNA splicing and further explores its underlying molecular mechanisms. This study provides clear evidence of the existence of adaptive splicing of synapse-related exons, and clarifies that it’s a process under the epigenetic regulation of DNA methylation

and the trans-acting regulation of splicing factor hnRNP L. It clearly demonstrated that the cells adjusted their alternative splicing events after the 1st time stimulation in order to fine-tune their response to the following stimulations with a novel combination of splice variants in an exon- and cell-dependent way, when the cells face spaced and repeated extracellular stimulations.

Also, this study indicates that some aberrant splicing events likely have an important impact on neurological diseases and the identified aberrant splicing of the synapse-related exon with critical neuronal functions could be the potential therapeutic targets of Rett syndrome.

CHAPTER V Conclusions

1. There are transcriptome-wide adaptive changes of a specific group of synapse-related exons upon repeated KCl treatments in rat pituitary GH3 cells, while the majority of exons kept their homeostatic levels.

2. STREX exon showed cell-dependent adaptive splicing upon repeated KCl-induced stimulations in endocrine and neuronal cell lines.

3. In rat pituitary GH3 cells, DNMT modulator 5-azaC globally:

- increased or decreased the inclusion level of alternative exons,
- altered the splicing response upon a single KCl treatment,
- disrupted adaptive splicing of a group of exons upon repeated KCl treatments,
- caused aberrant splicing of a group of synaptic genes, which were aggravated by repeated depolarization.

4. Using both whole-genome bisulfite DNA sequencing (WGBS) and RNA-Seq, it showed that

- The fold changes of exon inclusion induced by kainic acid are inversely correlated with the levels of DNA methylation of exons in the mouse hippocampus,
- The fold changes are generally augmented in the knockout mouse of the methyl-CpG binding protein MeCP2, a model of autism, with the biggest net changes in some of the least methylated exons.

5. A transient splicing assays using *in vitro* methylated reporter exons showed that exon DNA 5-mCG hypermethylation:

- increased the inclusion level of the target exon,
- augmented the splicing repression of reporter exon induced by co-expression of CaMKIV.

6. hnRNP L regulated some 5-azaC-disrupted synaptic exons, likely through a CA-rich consensus CAGCAG.

7. Aberrant splicing of the adaptive synaptic exons was observed in the hippocampus but not cerebellar tissue upon MECP2 mutations of the protein interaction or methyl-DNA binding domains in Rett syndrome patients.

CHAPTER VI Further Considerations and Future Directions

How does exonic DNA methylation level change upon repeated treatments by depolarization?

Is there transcriptome-wide adaptive DNA methylation corresponding to adaptive splicing?

Does the molecular basis for Rett syndrome also underlie the progress of other progressive or neurodegenerative diseases?

Like the dynamics of alternative splicing (discussed in detail in the section of '3.1 Activity-dependent alternative splicing and cellular adaptation'), DNA methylation is also a dynamic process [437]. (1) It is a reversible epigenetic modification. The methylation process could be established and maintained by different DNMTs, inhibited by DNMT inhibitors (discussed in detail in the section of '4.1.3 DNA methyltransferases (DNMTs) and DNMT inhibitors'), and demethylated by TET enzymes (TET1, TET2, and TET3) through the oxidation of 5mC and further hydroxylate 5hmC to generate 5-formylcytosine (5fC) and 5-carboxylcytosine (5caC) [438]. (3) It is also tissue- and cell-specific in different species, including humans [439], such as the confirmed differentially methylated regions (DMRs) in neural and non-neural tissue [440]. (2) It is under the precise spatiotemporal control, such as the spatiotemporal CG methylation dynamics at different developmental stages from embryogenesis to adulthood of mouse fetus [441] and motor neuron differentiation in humans [442]. (4) It is a flexible process under dynamic control in response to extracellular stimulation, according to my study. It showed that exonic cytosine sites displayed altered methylation changes in response to change of the exon inclusion level, a single KCl treatment. Moreover, there's a difference at DNA methylation level upon a single and repeated KCl treatment. These pieces of evidence suggested that DNA methylation likely dynamically changed upon repeated KCl treatments. However, little has been known about the change curve of DNA methylation upon repeated membrane depolarizations.

In my study, it showed that DNA methylation controls the decision of exon inclusion, splicing response to extracellular stimulation, and dynamic splicing response to repeated extracellular stimulations. Does the dynamic DNA methylation display the same trend of change as the patterns of adaptive splicing globally? The answer should be no. My study showed that the correlation between exonic DNA methylation and alternative splicing is not simply monotonic or linear. The 5-azaC-caused ratio changes of exon usage were inversely correlated with the total methylation levels of mCs for a group of exons, while the changes of the bulk of exons were in

various intermediate states. It indicates that the exonic DNA methylation change should be exon-dependent upon repeated extracellular stimulations. That is, for a specific group of exons that have a linear relationship between exonic DNA methylation and splicing response, exonic DNA methylation likely displays the same or opposite pattern of adaptive change just as that of alternative splicing in terms of the same exon upon repeated treatments. However, for other exons, the changing pattern of DNA methylation is hard to be predictive based on the existing pieces of evidence since adaptive splicing of these exons may be under a combined regulation of many factors or elements. Further investigation is needed to provide a more clear insight into the relationship of exonic DNA methylation and alternative splicing in the transcriptome, as well as of the regulation of DNA methylation in splicing response to extracellular change in the form of single or repeated treatments.

Previous studies showed that the dynamic feature of DNA methylation had been identified as the molecular basis of many physiological and pathophysiological events in the brain. For example, targeted bisulfite sequencing showed that genome-wide hemispheric differences of CpH methylation at enhancers and promoters from prefrontal cortex tissues mediated the hemispheric asymmetry in the brain [443]. In Parkinson's disease (PD) patients, there's a greater hemispheric asymmetry in DNA methylation between two independent sample cohorts [443]. As discussed in the section of '4.4 DNA methylation, pre-mRNA splicing and Rett syndrome', aberrant methylation changes are associated with many neurodegenerative diseases, such as Alzheimer's disease, Parkinson's disease, amyotrophic lateral sclerosis, Huntington's disease, hereditary ataxias, etc. Interestingly, a common aberrant DNA methylation pattern was observed in different neurodegenerative diseases, including Alzheimer's disease, dementia with Lewy bodies, Parkinson's disease and Alzheimer-like neurodegenerative profile associated with Down's syndrome through DNA methylation analysis of gray matter samples from the prefrontal cortex of control and neurodegenerative disease-associated cases [444]. It indicates that the molecular basis of Rett syndrome revealed in this thesis likely also underlies many other neurodegenerative diseases and further exploration is needed. It may provide some common biomarkers or therapies for the clinical application of neurodegenerative diseases.

Reference

1. Huether, S.E. and K.L. McCance, *Study Guide for Understanding Pathophysiology-E-Book*. 2016: Elsevier Health Sciences.
2. Coombs, C.H.J.J.o.E.P., *Adaptation of the galvanic response to auditory stimuli.* Journal of Experimental Psychology, 1938. **22**(3): p. 244.
3. Craik, K.J.W. and M.J.B.J.o.P. Vernon, *The nature of dark adaptation.* British Journal of Psychology, 1941. **32**(1): p. 62.
4. Vannotti, A., *The adaptation of the cell to effort, altitude and to pathological oxygen deficiency.* Schweizerische medizinische Wochenschrift, 1946. **76**: p. 899-903.
5. Johnson, S.M. and W.W. Fleming, *Mechanisms of cellular adaptive sensitivity changes: applications to opioid tolerance and dependence.* Pharmacol Rev, 1989. **41**(4): p. 435-88.
6. Fleming, W. and D. Westfall, *Adaptive supersensitivity*, in *Catecholamines I*. 1988, Springer. p. 509-559.
7. Wideman, L., et al., *Growth hormone release during acute and chronic aerobic and resistance exercise: recent findings.* Sports Med, 2002. **32**(15): p. 987-1004.
8. Kording, K.P., J.B. Tenenbaum, and R. Shadmehr, *The dynamics of memory as a consequence of optimal adaptation to a changing body.* Nat Neurosci, 2007. **10**(6): p. 779-86.
9. Anderson, M.C. and J.C. Hulbert, *Active Forgetting: Adaptation of Memory by Prefrontal Control.* Annu Rev Psychol, 2020.
10. Lau, C.M., et al., *Epigenetic control of innate and adaptive immune memory.* Nat Immunol, 2018. **19**(9): p. 963-972.
11. Lanting, C.P., et al., *Mechanisms of adaptation in human auditory cortex.* J Neurophysiol, 2013. **110**(4): p. 973-83.
12. Sanchez-Vives, M.V., L.G. Nowak, and D.A. McCormick, *Cellular mechanisms of long-lasting adaptation in visual cortical neurons in vitro.* J Neurosci, 2000. **20**(11): p. 4286-99.
13. Matthews, B.D., et al., *Cellular adaptation to mechanical stress: role of integrins, Rho, cytoskeletal tension and mechanosensitive ion channels.* J Cell Sci, 2006. **119**(Pt 3): p. 508-18.
14. Berget, S.M., C. Moore, and P.A. Sharp, *Spliced segments at the 5' terminus of adenovirus 2 late mRNA.* Proc Natl Acad Sci U S A, 1977. **74**(8): p. 3171-5.
15. Chow, L.T., et al., *An amazing sequence arrangement at the 5' ends of adenovirus 2 messenger RNA.* Cell, 1977. **12**(1): p. 1-8.
16. Darnell, J.E., Jr., *Implications of RNA-RNA splicing in evolution of eukaryotic cells.* Science, 1978. **202**(4374): p. 1257-60.
17. Knapp, G., et al., *Splicing of yeast tRNA precursors: structure of the reaction intermediates.* Cell, 1979. **18**(1): p. 37-45.
18. Konarska, M.M., et al., *Characterization of the branch site in lariat RNAs produced by splicing of mRNA precursors.* Nature, 1985. **313**(6003): p. 552-7.
19. Han, J., et al., *Pre-mRNA splicing: where and when in the nucleus.* Trends Cell Biol, 2011. **21**(6): p. 336-43.
20. Bringmann, P. and R. Luhrmann, *Purification of the individual snRNPs U1, U2, U5 and U4/U6 from HeLa cells and characterization of their protein constituents.* EMBO J, 1986. **5**(13): p. 3509-16.
21. Ding, F. and M.B. Elowitz, *Constitutive splicing and economies of scale in gene expression.* Nat Struct Mol Biol, 2019. **26**(6): p. 424-432.
22. Wang, Y., et al., *Mechanism of alternative splicing and its regulation.* Biomed Rep, 2015. **3**(2): p. 152-158.

23. Pan, Q., et al., *Deep surveying of alternative splicing complexity in the human transcriptome by high-throughput sequencing.* Nat Genet, 2008. **40**(12): p. 1413-5.
24. Wang, E.T., et al., *Alternative isoform regulation in human tissue transcriptomes.* Nature, 2008. **456**(7221): p. 470-6.
25. Blencowe, B.J., *The Relationship between Alternative Splicing and Proteomic Complexity.* Trends Biochem Sci, 2017. **42**(6): p. 407-408.
26. Clancy, S.J.N.E., *RNA splicing: introns, exons and spliceosome.* Nature Education, 2008. **1**(1): p. 31.
27. Shepard, P.J., et al., *Efficient internal exon recognition depends on near equal contributions from the 3' and 5' splice sites.* Nucleic Acids Res, 2011. **39**(20): p. 8928-37.
28. Lee, Y. and D.C. Rio, *Mechanisms and Regulation of Alternative Pre-mRNA Splicing.* Annu Rev Biochem, 2015. **84**: p. 291-323.
29. Long, J.C. and J.F. Caceres, *The SR protein family of splicing factors: master regulators of gene expression.* Biochem J, 2009. **417**(1): p. 15-27.
30. Manley, J.L. and A.R. Krainer, *A rational nomenclature for serine/arginine-rich protein splicing factors (SR proteins).* Genes Dev, 2010. **24**(11): p. 1073-4.
31. Zhou, Z. and X.D. Fu, *Regulation of splicing by SR proteins and SR protein-specific kinases.* Chromosoma, 2013. **122**(3): p. 191-207.
32. Martinez-Contreras, R., et al., *hnRNP proteins and splicing control.* Adv Exp Med Biol, 2007. **623**: p. 123-47.
33. Mayeda, A. and A.R. Krainer, *Regulation of alternative pre-mRNA splicing by hnRNP A1 and splicing factor SF2.* Cell, 1992. **68**(2): p. 365-75.
34. Konig, J., et al., *iCLIP reveals the function of hnRNP particles in splicing at individual nucleotide resolution.* Nat Struct Mol Biol, 2010. **17**(7): p. 909-15.
35. Darnell, R.B., *RNA protein interaction in neurons.* Annu Rev Neurosci, 2013. **36**: p. 243-70.
36. Jeong, S., *SR Proteins: Binders, Regulators, and Connectors of RNA.* Mol Cells, 2017. **40**(1): p. 1-9.
37. Shepard, P.J. and K.J. Hertel, *The SR protein family.* Genome Biol, 2009. **10**(10): p. 242.
38. Busch, A. and K.J. Hertel, *Evolution of SR protein and hnRNP splicing regulatory factors.* Wiley Interdiscip Rev RNA, 2012. **3**(1): p. 1-12.
39. Hanamura, A., et al., *Regulated tissue-specific expression of antagonistic pre-mRNA splicing factors.* RNA, 1998. **4**(4): p. 430-44.
40. ten Dam, G.B., et al., *Regulation of alternative splicing of CD45 by antagonistic effects of SR protein splicing factors.* J Immunol, 2000. **164**(10): p. 5287-95.
41. Erkelenz, S., et al., *Position-dependent splicing activation and repression by SR and hnRNP proteins rely on common mechanisms.* RNA, 2013. **19**(1): p. 96-102.
42. Kanopka, A., O. Muhlemann, and G. Akusjarvi, *Inhibition by SR proteins of splicing of a regulated adenovirus pre-mRNA.* Nature, 1996. **381**(6582): p. 535-8.
43. Bradley, T., M.E. Cook, and M. Blanchette, *SR proteins control a complex network of RNA-processing events.* RNA, 2015. **21**(1): p. 75-92.
44. Baralle, F.E., R.N. Singh, and S. Stamm, *RNA structure and splicing regulation.* Biochim Biophys Acta Gene Regul Mech, 2019. **1862**(11-12): p. 194448.
45. Bartys, N., R. Kierzek, and J. Lisowiec-Wachnicka, *The regulation properties of RNA secondary structure in alternative splicing.* Biochim Biophys Acta Gene Regul Mech, 2019. **1862**(11-12): p. 194401.
46. Graveley, B.R., *Mutually exclusive splicing of the insect Dscam pre-mRNA directed by competing intronic RNA secondary structures.* Cell, 2005. **123**(1): p. 65-73.

47. Singh, N.N., R.N. Singh, and E.J. Androphy, *Modulating role of RNA structure in alternative splicing of a critical exon in the spinal muscular atrophy genes.* Nucleic Acids Res, 2007. **35**(2): p. 371-89.
48. May, G.E., et al., *Competing RNA secondary structures are required for mutually exclusive splicing of the Dscam exon 6 cluster.* RNA, 2011. **17**(2): p. 222-9.
49. Cheah, M.T., et al., *Control of alternative RNA splicing and gene expression by eukaryotic riboswitches.* Nature, 2007. **447**(7143): p. 497-500.
50. Oberstrass, F.C., et al., *Structure of PTB bound to RNA: specific binding and implications for splicing regulation.* Science, 2005. **309**(5743): p. 2054-7.
51. Nasim, F.U., et al., *High-affinity hnRNP A1 binding sites and duplex-forming inverted repeats have similar effects on 5' splice site selection in support of a common looping out and repression mechanism.* RNA, 2002. **8**(8): p. 1078-89.
52. Shukla, S. and S. Oberdoerffer, *Co-transcriptional regulation of alternative pre-mRNA splicing.* Biochim Biophys Acta, 2012. **1819**(7): p. 673-83.
53. Fong, N., et al., *Pre-mRNA splicing is facilitated by an optimal RNA polymerase II elongation rate.* Genes Dev, 2014. **28**(23): p. 2663-76.
54. Dujardin, G., et al., *How slow RNA polymerase II elongation favors alternative exon skipping.* Mol Cell, 2014. **54**(4): p. 683-90.
55. Aslanzadeh, V., et al., *Transcription rate strongly affects splicing fidelity and cotranscriptionality in budding yeast.* Genome Res, 2018. **28**(2): p. 203-213.
56. Shukla, S., et al., *CTCF-promoted RNA polymerase II pausing links DNA methylation to splicing.* Nature, 2011. **479**(7371): p. 74-9.
57. Maunakea, A.K., et al., *Intragenic DNA methylation modulates alternative splicing by recruiting MeCP2 to promote exon recognition.* Cell Res, 2013. **23**(11): p. 1256-69.
58. Munoz, M.J., et al., *DNA damage regulates alternative splicing through inhibition of RNA polymerase II elongation.* Cell, 2009. **137**(4): p. 708-20.
59. de la Mata, M., et al., *A slow RNA polymerase II affects alternative splicing in vivo.* Mol Cell, 2003. **12**(2): p. 525-32.
60. de la Mata, M. and A.R. Kornblihtt, *RNA polymerase II C-terminal domain mediates regulation of alternative splicing by SRp20.* Nat Struct Mol Biol, 2006. **13**(11): p. 973-80.
61. Batsche, E., M. Yaniv, and C. Muchardt, *The human SWI/SNF subunit Brm is a regulator of alternative splicing.* Nat Struct Mol Biol, 2006. **13**(1): p. 22-9.
62. Allo, M., et al., *Chromatin and alternative splicing.* Cold Spring Harb Symp Quant Biol, 2010. **75**: p. 103-11.
63. Lin, S., et al., *The splicing factor SC35 has an active role in transcriptional elongation.* Nat Struct Mol Biol, 2008. **15**(8): p. 819-26.
64. Sterner, D.A., T. Carlo, and S.M. Berget, *Architectural limits on split genes.* Proc Natl Acad Sci U S A, 1996. **93**(26): p. 15081-5.
65. Bell, M.V., et al., *Influence of intron length on alternative splicing of CD44.* Mol Cell Biol, 1998. **18**(10): p. 5930-41.
66. Pai, A.A., et al., *Intron length and recursive sites are major determinants of splicing efficiency in flies.* bioRxiv, 2017: p. 107995.
67. Dewey, C.N., I.B. Rogozin, and E.V. Koonin, *Compensatory relationship between splice sites and exonic splicing signals depending on the length of vertebrate introns.* BMC Genomics, 2006. **7**: p. 311.
68. Wieringa, B., E. Hofer, and C. Weissmann, *A minimal intron length but no specific internal sequence is required for splicing the large rabbit beta-globin intron.* Cell, 1984. **37**(3): p. 915-25.

69. Zhu, L.Y., et al., *Epigenetic regulation of alternative splicing.* Am J Cancer Res, 2018. **8**(12): p. 2346-2358.
70. Zhang, W., et al., *Crystal structures and RNA-binding properties of the RNA recognition motifs of heterogeneous nuclear ribonucleoprotein L: insights into its roles in alternative splicing regulation.* J Biol Chem, 2013. **288**(31): p. 22636-49.
71. Huang, S., *Review: perinucleolar structures.* J Struct Biol, 2000. **129**(2-3): p. 233-40.
72. Rajan, P., et al., *Proteomic identification of heterogeneous nuclear ribonucleoprotein L as a novel component of SLM/Sam68 Nuclear Bodies.* BMC Cell Biol, 2009. **10**: p. 82.
73. Taguchi, F., et al., *hnRNP L enhances sensitivity of the cells to KW-2189.* Int J Cancer, 2004. **108**(5): p. 679-85.
74. Lee, S.Y.J.G. and Genomics, *Nuclear localization signal in human hnRNP L.* Genes & Genomics (구한국유전학회지), 2002. **24**(4): p. 377-381.
75. Liu, G., et al., *A conserved serine of heterogeneous nuclear ribonucleoprotein L (hnRNP L) mediates depolarization-regulated alternative splicing of potassium channels.* J Biol Chem, 2012. **287**(27): p. 22709-16.
76. Goehe, R.W., et al., *hnRNP L regulates the tumorigenic capacity of lung cancer xenografts in mice via caspase-9 pre-mRNA processing.* J Clin Invest, 2010. **120**(11): p. 3923-39.
77. Vu, N.T., et al., *hnRNP U enhances caspase-9 splicing and is modulated by AKT-dependent phosphorylation of hnRNP L.* J Biol Chem, 2013. **288**(12): p. 8575-84.
78. Hui, J., et al., *HnRNP L stimulates splicing of the eNOS gene by binding to variable-length CA repeats.* Nat Struct Biol, 2003. **10**(1): p. 33-7.
79. Motta-Mena, L.B., F. Heyd, and K.W. Lynch, *Context-dependent regulatory mechanism of the splicing factor hnRNP L.* Mol Cell, 2010. **37**(2): p. 223-34.
80. Hui, J., et al., *Intronic CA-repeat and CA-rich elements: a new class of regulators of mammalian alternative splicing.* EMBO J, 2005. **24**(11): p. 1988-98.
81. Rossbach, O., et al., *Crosslinking-immunoprecipitation (iCLIP) analysis reveals global regulatory roles of hnRNP L.* RNA Biol, 2014. **11**(2): p. 146-55.
82. Rossbach, O., et al., *Auto- and cross-regulation of the hnRNP L proteins by alternative splicing.* Mol Cell Biol, 2009. **29**(6): p. 1442-51.
83. Yu, J., et al., *The heterogeneous nuclear ribonucleoprotein L is an essential component in the Ca2+/calmodulin-dependent protein kinase IV-regulated alternative splicing through cytidine-adenosine repeats.* J Biol Chem, 2009. **284**(3): p. 1505-13.
84. Heiner, M., et al., *HnRNP L-mediated regulation of mammalian alternative splicing by interference with splice site recognition.* RNA Biol, 2010. **7**(1): p. 56-64.
85. Rothrock, C.R., A.E. House, and K.W. Lynch, *HnRNP L represses exon splicing via a regulated exonic splicing silencer.* EMBO J, 2005. **24**(15): p. 2792-802.
86. Loh, T.J., et al., *Suppression of 5' splice-sites through multiple exonic motifs by hnRNP L.* Biochim Biophys Acta Gene Regul Mech, 2017. **1860**(3): p. 363-373.
87. House, A.E. and K.W. Lynch, *An exonic splicing silencer represses spliceosome assembly after ATP-dependent exon recognition.* Nat Struct Mol Biol, 2006. **13**(10): p. 937-44.
88. Rahman, M.A., et al., *HnRNP L and hnRNP LL antagonistically modulate PTB-mediated splicing suppression of CHRNA1 pre-mRNA.* Sci Rep, 2013. **3**: p. 2931.
89. Lei, L., et al., *Multilevel Differential Control of Hormone Gene Expression Programs by hnRNP L and LL in Pituitary Cells.* Mol Cell Biol, 2018. **38**(12).
90. Chiou, N.T., G. Shankarling, and K.W. Lynch, *hnRNP L and hnRNP A1 induce extended U1 snRNA interactions with an exon to repress spliceosome assembly.* Mol Cell, 2013. **49**(5): p. 972-82.
91. Davenport, B., et al., *Signature Channels of Excitability no More: L-Type Channels in Immune Cells.* Front Immunol, 2015. **6**: p. 375.

92. Matikainen-Ankney, B.A., et al., *Parkinson's Disease-linked LRRK2-G2019S mutation alters synaptic plasticity and promotes resilience to chronic social stress in young adulthood.* J Neurosci., 2018. **38**(45): p. 9700-9711.
93. Pruunsild, P. and H. Bading, *Shaping the human brain: evolutionary cis-regulatory plasticity drives changes in synaptic activity-controlled adaptive gene expression.* Curr Opin Neurobiol, 2019. **59**: p. 34-40.
94. Wang, D.O., et al., *Synapse- and stimulus-specific local translation during long-term neuronal plasticity.* Science, 2009. **324**(5934): p. 1536-40.
95. Lee, H.K., et al., *Phosphorylation of the AMPA receptor GluR1 subunit is required for synaptic plasticity and retention of spatial memory.* Cell, 2003. **112**(5): p. 631-43.
96. Baker-Andresen, D., V.S. Ratnu, and T.W. Bredy, *Dynamic DNA methylation: a prime candidate for genomic metaplasticity and behavioral adaptation.* Trends Neurosci, 2013. **36**(1): p. 3-13.
97. Nestler, E.J. and C. Luscher, *The Molecular Basis of Drug Addiction: Linking Epigenetic to Synaptic and Circuit Mechanisms.* Neuron, 2019. **102**(1): p. 48-59.
98. Kim, S. and B.K. Kaang, *Epigenetic regulation and chromatin remodeling in learning and memory.* Exp Mol Med, 2017. **49**(1): p. e281.
99. Levenson, J.M., et al., *Evidence that DNA (cytosine-5) methyltransferase regulates synaptic plasticity in the hippocampus.* J Biol Chem, 2006. **281**(23): p. 15763-73.
100. Rudenko, A., et al., *Tet1 is critical for neuronal activity-regulated gene expression and memory extinction.* Neuron, 2013. **79**(6): p. 1109-1122.
101. Halder, R., et al., *DNA methylation changes in plasticity genes accompany the formation and maintenance of memory.* Nat Neurosci, 2016. **19**(1): p. 102-10.
102. Heyward, F.D. and J.D. Sweatt, *DNA Methylation in Memory Formation: Emerging Insights.* Neuroscientist, 2015. **21**(5): p. 475-89.
103. Eichler, J., *Modifying Post-Translational Modifications: A Strategy Used by Archaea for Adapting to Changing Environments?: Manipulating the Extent, Position, or Content of Post-Translational Modifications May Help Archaea Adapt to Environmental Change.* Bioessays, 2020. **42**(3): p. e1900207.
104. Rein, T., *Post-translational modifications and stress adaptation: the paradigm of FKBP51.* Biochem Soc Trans, 2020. **48**(2): p. 441-449.
105. Mizuno, M., et al., *CREB phosphorylation as a molecular marker of memory processing in the hippocampus for spatial learning.* Behav Brain Res, 2002. **133**(2): p. 135-41.
106. Guitart, X. and E.J. Nestler, *Second messenger and protein phosphorylation mechanisms underlying opiate addiction: studies in the rat locus coeruleus.* Neurochem Res, 1993. **18**(1): p. 5-13.
107. Xiao, W., *The hypoxia signaling pathway and hypoxic adaptation in fishes.* Sci China Life Sci, 2015. **58**(2): p. 148-55.
108. Jacko, D., et al., *Coordinated alpha-crystallin B phosphorylation and desmin expression indicate adaptation and deadaptation to resistance exercise-induced loading in human skeletal muscle.* Am J Physiol Cell Physiol, 2020. **319**(2): p. C300-C312.
109. Daoud, R., et al., *Activity-dependent regulation of alternative splicing patterns in the rat brain.* Eur J Neurosci, 1999. **11**(3): p. 788-802.
110. Xie, J. and D.L. Black, *A CaMK IV responsive RNA element mediates depolarization-induced alternative splicing of ion channels.* Nature, 2001. **410**(6831): p. 936-9.
111. Mu, Y., et al., *Activity-dependent mRNA splicing controls ER export and synaptic delivery of NMDA receptors.* Neuron, 2003. **40**(3): p. 581-94.
112. Hepp, R., et al., *NGF enhances depolarization effects on SNAP-25 expression: induction of SNAP-25b isoform.* Neuroreport, 2001. **12**(4): p. 673-7.

113. Schor, I.E., et al., *Neuronal cell depolarization induces intragenic chromatin modifications affecting NCAM alternative splicing.* Proc Natl Acad Sci U S A, 2009. **106**(11): p. 4325-30.
114. Rozic-Kotliroff, G. and N. Zisapel, *Ca2+ -dependent splicing of neurexin IIalpha.* Biochem Biophys Res Commun, 2007. **352**(1): p. 226-30.
115. Iijima, T., et al., *SAM68 regulates neuronal activity-dependent alternative splicing of neurexin-1.* Cell, 2011. **147**(7): p. 1601-14.
116. Nelson, A.B., A.H. Gittis, and S. du Lac, *Decreases in CaMKII activity trigger persistent potentiation of intrinsic excitability in spontaneously firing vestibular nucleus neurons.* Neuron, 2005. **46**(4): p. 623-31.
117. Bettinger, J.C. and A.G. Davies, *The role of the BK channel in ethanol response behaviors: evidence from model organism and human studies.* Front Physiol, 2014. **5**: p. 346.
118. Oh, K.H. and H. Kim, *BK channel clustering is required for normal behavioral alcohol sensitivity in C. elegans.* Sci Rep, 2019. **9**(1): p. 10224.
119. Kreifeldt, M., et al., *BK Channel beta1 Subunit Contributes to Behavioral Adaptations Elicited by Chronic Intermittent Ethanol Exposure.* Alcohol Clin Exp Res, 2015. **39**(12): p. 2394-402.
120. Choi, T.Y., et al., *Cereblon Maintains Synaptic and Cognitive Function by Regulating BK Channel.* J Neurosci, 2018. **38**(14): p. 3571-3583.
121. Typlt, M., et al., *Mice with deficient BK channel function show impaired prepulse inhibition and spatial learning, but normal working and spatial reference memory.* PLoS One, 2013. **8**(11): p. e81270.
122. Griguoli, M., M. Sgritta, and E. Cherubini, *Presynaptic BK channels control transmitter release: physiological relevance and potential therapeutic implications.* J Physiol, 2016. **594**(13): p. 3489-500.
123. Vattino, L.G., et al., *Functional Postnatal Maturation of the Medial Olivocochlear Efferent-Outer Hair Cell Synapse.* J Neurosci, 2020. **40**(25): p. 4842-4857.
124. Xie, J., *Control of alternative pre-mRNA splicing by Ca(++) signals.* Biochim Biophys Acta, 2008. **1779**(8): p. 438-52.
125. Xie, J. and D.P. McCobb, *Control of alternative splicing of potassium channels by stress hormones.* Science, 1998. **280**(5362): p. 443-6.
126. Hanaoka, K., et al., *A 59 amino acid insertion increases Ca(2+) sensitivity of rbslo1, a Ca2+ -activated K(+) channel in renal epithelia.* J Membr Biol, 1999. **172**(3): p. 193-201.
127. MacDonald, S.H., et al., *Increased large conductance calcium-activated potassium (BK) channel expression accompanied by STREX variant downregulation in the developing mouse CNS.* BMC Dev Biol, 2006. **6**: p. 37.
128. Wamsley, B., et al., *Rbfox1 Mediates Cell-type-Specific Splicing in Cortical Interneurons.* Neuron, 2018. **100**(4): p. 846-859 e7.
129. Furlanis, E. and P. Scheiffele, *Regulation of Neuronal Differentiation, Function, and Plasticity by Alternative Splicing.* Annu Rev Cell Dev Biol, 2018. **34**: p. 451-469.
130. Gantz, S.C., et al., *Distinct regulation of dopamine D2S and D2L autoreceptor signaling by calcium.* Elife, 2015. **4**.
131. Siegfried, Z. and R. Karni, *The role of alternative splicing in cancer drug resistance.* Curr Opin Genet Dev, 2018. **48**: p. 16-21.
132. Chang, S., et al., *Epigenetic regulation of osteopontin splicing isoform c defines its role as a microenvironmental factor to promote the survival of colon cancer cells from 5-FU treatment.* Cancer Cell Int, 2020. **20**: p. 452.
133. Li, B., et al., *Neuronal Inactivity Co-opts LTP Machinery to Drive Potassium Channel Splicing and Homeostatic Spike Widening.* Cell, 2020. **181**(7): p. 1547-1565 e15.

134. Penn, A.C., et al., *Activity-mediated AMPA receptor remodeling, driven by alternative splicing in the ligand-binding domain.* Neuron, 2012. **76**(3): p. 503-10.
135. Nakajo, H., et al., *Hunger Potentiates the Habenular Winner Pathway for Social Conflict by Orexin-Promoted Biased Alternative Splicing of the AMPA Receptor Gene.* Cell Rep, 2020. **31**(12): p. 107790.
136. Ohno, H., et al., *Role of synaptic phosphatidylinositol 3-kinase in a behavioral learning response in C. elegans.* Science, 2014. **345**(6194): p. 313-7.
137. Huang, B., et al., *Genome-Wide Analysis of Alternative Splicing Provides Insights into Stress Adaptation of the Pacific Oyster.* Mar Biotechnol (NY), 2016. **18**(5): p. 598-609.
138. Zhang, X., et al., *Genome-Wide Analysis of Alternative Splicing Provides Insights Into Stress Response of the Pacific White Shrimp Litopenaeus vanname.* Front Genet, 2019. **10**: p. 845.
139. Feng, J., et al., *Chronic cocaine-regulated epigenomic changes in mouse nucleus accumbens.* Genome Biol, 2014. **15**(4): p. R65.
140. Robinson, B.G., et al., *Cocaine-induced adaptation of dopamine D2S, but not D2L autoreceptors.* Elife, 2017. **6**.
141. Dragicevic, E., et al., *Cav1.3 channels control D2-autoreceptor responses via NCS-1 in substantia nigra dopamine neurons.* Brain, 2014. **137**(Pt 8): p. 2287-302.
142. Perra, S., et al., *In vivo ethanol experience increases D(2) autoinhibition in the ventral tegmental area.* Neuropsychopharmacology, 2011. **36**(5): p. 993-1002.
143. Antunes-Martins, A., et al., *Sex-dependent up-regulation of two splicing factors, Psf and Srp20, during hippocampal memory formation.* Learn Mem, 2007. **14**(10): p. 693-702.
144. Barnett, M.W. and P.M. Larkman, *The action potential.* Pract Neurol, 2007. **7**(3): p. 192-7.
145. Myers, J.B., et al., *Phorbol ester-stimulated human neutrophil membrane depolarization is dependent on Ca2(+)-regulated Cl- efflux.* Am J Physiol, 1990. **259**(4 Pt 1): p. C531-40.
146. Rosen, L.B., et al., *Membrane depolarization and calcium influx stimulate MEK and MAP kinase via activation of Ras.* Neuron, 1994. **12**(6): p. 1207-21.
147. Kilb, W., et al., *Depolarizing glycine responses in Cajal-Retzius cells of neonatal rat cerebral cortex.* Neuroscience, 2002. **112**(2): p. 299-307.
148. Reichling, D.B., et al., *Mechanisms of GABA and glycine depolarization-induced calcium transients in rat dorsal horn neurons.* J Physiol, 1994. **476**(3): p. 411-21.
149. Blanke, M.L. and A.M.J. VanDongen, *Activation Mechanisms of the NMDA Receptor*, in *Biology of the NMDA Receptor*, A.M. Van Dongen, Editor. 2009: Boca Raton (FL).
150. Robinson, J.H. and S.A. Deadwyler, *Kainic acid produces depolarization of CA3 pyramidal cells in the vitro hippocampal slice.* Brain Res, 1981. **221**(1): p. 117-27.
151. Werz, M.A. and R.L. Macdonald, *Phorbol esters: voltage-dependent effects on calcium-dependent action potentials of mouse central and peripheral neurons in cell culture.* J Neurosci, 1987. **7**(6): p. 1639-47.
152. Cameron, M.A., et al., *Differential effect of brief electrical stimulation on voltage-gated potassium channels.* J Neurophysiol, 2017. **117**(5): p. 2014-2024.
153. Catterall, W.A., *Voltage-gated calcium channels.* Cold Spring Harb Perspect Biol, 2011. **3**(8): p. a003947.
154. Helton, T.D., W. Xu, and D. Lipscombe, *Neuronal L-type calcium channels open quickly and are inhibited slowly.* J Neurosci, 2005. **25**(44): p. 10247-51.
155. Mondadori, C., et al., *NMDA receptor antagonists can enhance or impair learning performance in animals.* Exp Brain Res, 1989. **75**(3): p. 449-56.
156. Gulenay, M. and J.K. Mathai, *Depolarizing Neuromuscular Blocking Drugs*, in *StatPearls*. 2020: Treasure Island (FL).

157. Hodgkin, A.L. and A.F.J.N. Huxley, *Action potentials recorded from inside a nerve fibre.* Nature, 1939. **144**(3651): p. 710-711.
158. Heyd, F. and K.W. Lynch, *Degrade, move, regroup: signaling control of splicing proteins.* Trends Biochem Sci, 2011. **36**(8): p. 397-404.
159. Chen, Y., et al., *Mutually exclusive acetylation and ubiquitylation of the splicing factor SRSF5 control tumor growth.* Nat Commun, 2018. **9**(1): p. 2464.
160. Roberts, K., et al., *Molecular biology of the cell.* New York: Garland Science;, 2002.
161. Soderling, T.R. and J.T. Stull, *Structure and regulation of calcium/calmodulin-dependent protein kinases.* Chem Rev, 2001. **101**(8): p. 2341-52.
162. Xiao, R.P., et al., *Dual regulation of Ca2+/calmodulin-dependent kinase II activity by membrane voltage and by calcium influx.* Proc Natl Acad Sci U S A, 1994. **91**(20): p. 9659-63.
163. Waltereit, R. and M. Weller, *Signaling from cAMP/PKA to MAPK and synaptic plasticity.* Mol Neurobiol, 2003. **27**(1): p. 99-106.
164. Takai, Y., et al., *Calcium-dependent activation of a multifunctional protein kinase by membrane phospholipids.* J Biol Chem, 1979. **254**(10): p. 3692-5.
165. Xia, Z., et al., *Calcium influx via the NMDA receptor induces immediate early gene transcription by a MAP kinase/ERK-dependent mechanism.* J Neurosci, 1996. **16**(17): p. 5425-36.
166. Swulius, M.T. and M.N. Waxham, *Ca(2+)/calmodulin-dependent protein kinases.* Cell Mol Life Sci, 2008. **65**(17): p. 2637-57.
167. Selbert, M.A., et al., *Phosphorylation and activation of Ca(2+)-calmodulin-dependent protein kinase IV by Ca(2+)-calmodulin-dependent protein kinase Ia kinase. Phosphorylation of threonine 196 is essential for activation.* J Biol Chem, 1995. **270**(29): p. 17616-21.
168. Chatila, T., et al., *A unique phosphorylation-dependent mechanism for the activation of Ca2+/calmodulin-dependent protein kinase type IV/GR.* J Biol Chem, 1996. **271**(35): p. 21542-8.
169. Razanau, A. and J. Xie, *Emerging mechanisms and consequences of calcium regulation of alternative splicing in neurons and endocrine cells.* Cell Mol Life Sci, 2013. **70**(23): p. 4527-36.
170. Colwill, K., et al., *The Clk/Sty protein kinase phosphorylates SR splicing factors and regulates their intranuclear distribution.* EMBO J, 1996. **15**(2): p. 265-75.
171. Aksaas, A.K., et al., *Protein kinase a-dependent phosphorylation of serine 119 in the proto-oncogenic serine/arginine-rich splicing factor 1 modulates its activity as a splicing enhancer protein.* Genes Cancer, 2011. **2**(8): p. 841-51.
172. Shi, J., et al., *Cyclic AMP-dependent protein kinase regulates the alternative splicing of tau exon 10: a mechanism involved in tau pathology of Alzheimer disease.* J Biol Chem, 2011. **286**(16): p. 14639-48.
173. Gu, J., et al., *Cyclic AMP-dependent protein kinase regulates 9G8-mediated alternative splicing of tau exon 10.* FEBS Lett, 2012. **586**(16): p. 2239-44.
174. Chen, C., et al., *Cyclic AMP-dependent protein kinase enhances SC35-promoted Tau exon 10 inclusion.* Mol Neurobiol, 2014. **49**(1): p. 615-24.
175. Xie, J., et al., *Protein kinase A phosphorylation modulates transport of the polypyrimidine tract-binding protein.* Proc Natl Acad Sci U S A, 2003. **100**(15): p. 8776-81.
176. Tormanen Persson, H., et al., *Two cellular protein kinases, DNA-PK and PKA, phosphorylate the adenoviral L4-33K protein and have opposite effects on L1 alternative RNA splicing.* PLoS One, 2012. **7**(2): p. e31871.
177. Jarnaess, E., et al., *Splicing factor arginine/serine-rich 17A (SFRS17A) is an A-kinase anchoring protein that targets protein kinase A to splicing factor compartments.* J Biol Chem, 2009. **284**(50): p. 35154-64.
178. Black, A.R. and J.D. Black, *Protein kinase C signaling and cell cycle regulation.* Front Immunol, 2012. **3**: p. 423.

179. Newton, A.C., *Protein kinase C: perfectly balanced.* Crit Rev Biochem Mol Biol, 2018. **53**(2): p. 208-230.
180. Callender, J.A. and A.C. Newton, *Conventional protein kinase C in the brain: 40 years later.* Neuronal Signal, 2017. **1**(2): p. NS20160005.
181. Jiang, X., R. Sando, and T.C. Sudhof, *Multiple signaling pathways are essential for synapse formation induced by synaptic adhesion molecules.* Proc Natl Acad Sci U S A, 2021. **118**(3).
182. Wu-Zhang, A.X. and A.C. Newton, *Protein kinase C pharmacology: refining the toolbox.* Biochem J, 2013. **452**(2): p. 195-209.
183. Revil, T., et al., *Protein kinase C-dependent control of Bcl-x alternative splicing.* Mol Cell Biol, 2007. **27**(24): p. 8431-41.
184. Rozic, G., et al., *Dynamic changes in neurexins' alternative splicing: role of Rho-associated protein kinases and relevance to memory formation.* PLoS One, 2011. **6**(4): p. e18579.
185. Verma, S.K., et al., *Reactivation of fetal splicing programs in diabetic hearts is mediated by protein kinase C signaling.* J Biol Chem, 2013. **288**(49): p. 35372-86.
186. Morrison, D.K., *MAP kinase pathways.* Cold Spring Harb Perspect Biol, 2012. **4**(11).
187. Maharana, C., K.P. Sharma, and S.K. Sharma, *Feedback mechanism in depolarization-induced sustained activation of extracellular signal-regulated kinase in the hippocampus.* Sci Rep, 2013. **3**: p. 1103.
188. Park, J.H., et al., *Protein kinase A activity is required for depolarization-induced proline-rich tyrosine kinase 2 and mitogen-activated protein kinase activation in PC12 cells.* Neurosci Lett, 2000. **290**(1): p. 25-8.
189. Machado, H.B., L.J. Vician, and H.R. Herschman, *The MAPK pathway is required for depolarization-induced "promiscuous" immediate-early gene expression but not for depolarization-restricted immediate-early gene expression in neurons.* J Neurosci Res, 2008. **86**(3): p. 593-602.
190. Liang, H.L., S.S. Dhar, and M.T. Wong-Riley, *p38 mitogen-activated protein kinase and calcium channels mediate signaling in depolarization-induced activation of peroxisome proliferator-activated receptor gamma coactivator-1alpha in neurons.* J Neurosci Res, 2010. **88**(3): p. 640-9.
191. Mihail, S.M., et al., *MNK-eIF4E signalling is a highly conserved mechanism for sensory neuron axonal plasticity: evidence from Aplysia californica.* Philos Trans R Soc Lond B Biol Sci, 2019. **374**(1785): p. 20190289.
192. Wu, G.Y., K. Deisseroth, and R.W. Tsien, *Spaced stimuli stabilize MAPK pathway activation and its effects on dendritic morphology.* Nat Neurosci, 2001. **4**(2): p. 151-8.
193. Bailey, C.H., D. Bartsch, and E.R. Kandel, *Toward a molecular definition of long-term memory storage.* Proc Natl Acad Sci U S A, 1996. **93**(24): p. 13445-52.
194. Kogan, J.H., et al., *Spaced training induces normal long-term memory in CREB mutant mice.* Curr Biol, 1997. **7**(1): p. 1-11.
195. Michael, D., et al., *Repeated pulses of serotonin required for long-term facilitation activate mitogen-activated protein kinase in sensory neurons of Aplysia.* Proc Natl Acad Sci U S A, 1998. **95**(4): p. 1864-9.
196. Mortensen, O.V., *MKP3 eliminates depolarization-dependent neurotransmitter release through downregulation of L-type calcium channel Cav1.2 expression.* Cell Calcium, 2013. **53**(3): p. 224-30.
197. Bluthgen, N., et al., *Profiling the MAPK/ERK dependent and independent activity regulated transcriptional programs in the murine hippocampus in vivo.* Sci Rep, 2017. **7**: p. 45101.
198. van der Houven van Oordt, W., et al., *The MKK(3/6)-p38-signaling cascade alters the subcellular distribution of hnRNP A1 and modulates alternative splicing regulation.* J Cell Biol, 2000. **149**(2): p. 307-16.

199. Dumont, A.A., et al., *p38alpha MAPK proximity assay reveals a regulatory mechanism of alternative splicing in cardiomyocytes.* Biochim Biophys Acta Mol Cell Res, 2019. **1866**(12): p. 118557.
200. Cai, H., et al., *Angiotensin II Influences Pre-mRNA Splicing Regulation by Enhancing RBM20 Transcription Through Activation of the MAPK/ELK1 Signaling Pathway.* Int J Mol Sci, 2019. **20**(20).
201. Buxade, M., et al., *The Mnks are novel components in the control of TNF alpha biosynthesis and phosphorylate and regulate hnRNP A1.* Immunity, 2005. **23**(2): p. 177-89.
202. Buxade, M., et al., *The PSF.p54nrb complex is a novel Mnk substrate that binds the mRNA for tumor necrosis factor alpha.* J Biol Chem, 2008. **283**(1): p. 57-65.
203. Cargnello, M. and P.P. Roux, *Activation and function of the MAPKs and their substrates, the MAPK-activated protein kinases.* Microbiol Mol Biol Rev, 2011. **75**(1): p. 50-83.
204. Robinson, D.R., Y.M. Wu, and S.F. Lin, *The protein tyrosine kinase family of the human genome.* Oncogene, 2000. **19**(49): p. 5548-57.
205. Purcell, A.L. and T.J. Carew, *Tyrosine kinases, synaptic plasticity and memory: insights from vertebrates and invertebrates.* Trends Neurosci, 2003. **26**(11): p. 625-30.
206. Yang, Y., et al., *Computational discovery and experimental verification of tyrosine kinase inhibitor pazopanib for the reversal of memory and cognitive deficits in rat model neurodegeneration.* Chem Sci, 2015. **6**(5): p. 2812-2821.
207. Zwick, E., et al., *Critical role of calcium- dependent epidermal growth factor receptor transactivation in PC12 cell membrane depolarization and bradykinin signaling.* J Biol Chem, 1997. **272**(40): p. 24767-70.
208. Du, J., et al., *Regulation of TrkB receptor tyrosine kinase and its internalization by neuronal activity and Ca2+ influx.* J Cell Biol, 2003. **163**(2): p. 385-95.
209. Kingsbury, T.J., et al., *Ca(2+)-dependent regulation of TrkB expression in neurons.* J Biol Chem, 2003. **278**(42): p. 40744-8.
210. Mills, R.D., M. Mita, and M.P. Walsh, *A role for the Ca(2+)-dependent tyrosine kinase Pyk2 in tonic depolarization-induced vascular smooth muscle contraction.* J Muscle Res Cell Motil, 2015. **36**(6): p. 479-89.
211. Faure, C., et al., *Calcineurin is essential for depolarization-induced nuclear translocation and tyrosine phosphorylation of PYK2 in neurons.* J Cell Sci, 2007. **120**(Pt 17): p. 3034-44.
212. Lev, S., et al., *Protein tyrosine kinase PYK2 involved in Ca(2+)-induced regulation of ion channel and MAP kinase functions.* Nature, 1995. **376**(6543): p. 737-45.
213. Soler, R.M., et al., *Calmodulin is involved in membrane depolarization-mediated survival of motoneurons by phosphatidylinositol-3 kinase- and MAPK-independent pathways.* J Neurosci, 1998. **18**(4): p. 1230-9.
214. Radha, V., S. Nambirajan, and G. Swarup, *Association of Lyn tyrosine kinase with the nuclear matrix and cell-cycle-dependent changes in matrix-associated tyrosine kinase activity.* Eur J Biochem, 1996. **236**(2): p. 352-9.
215. Su, B. and M. Karin, *Mitogen-activated protein kinase cascades and regulation of gene expression.* Curr Opin Immunol, 1996. **8**(3): p. 402-11.
216. Teutschbein, J., et al., *Gene expression analysis after receptor tyrosine kinase activation reveals new potential melanoma proteins.* BMC Cancer, 2010. **10**: p. 386.
217. Li, W., et al., *Heat Shock-induced Phosphorylation of TAR DNA-binding Protein 43 (TDP-43) by MAPK/ERK Kinase Regulates TDP-43 Function.* J Biol Chem, 2017. **292**(12): p. 5089-5100.
218. Polymenidou, M., et al., *Long pre-mRNA depletion and RNA missplicing contribute to neuronal vulnerability from loss of TDP-43.* Nat Neurosci, 2011. **14**(4): p. 459-68.

219. Tollervey, J.R., et al., *Characterizing the RNA targets and position-dependent splicing regulation by TDP-43.* Nat Neurosci, 2011. **14**(4): p. 452-8.
220. Buratti, E. and F.E. Baralle, *The multiple roles of TDP-43 in pre-mRNA processing and gene expression regulation.* RNA Biol, 2010. **7**(4): p. 420-9.
221. Kim, M., M. Baek, and D.J. Kim, *Protein Tyrosine Signaling and its Potential Therapeutic Implications in Carcinogenesis.* Curr Pharm Des, 2017. **23**(29): p. 4226-4246.
222. Yaish, P., et al., *Blocking of EGF-dependent cell proliferation by EGF receptor kinase inhibitors.* Science, 1988. **242**(4880): p. 933-5.
223. Jiao, Q., et al., *Advances in studies of tyrosine kinase inhibitors and their acquired resistance.* Mol Cancer, 2018. **17**(1): p. 36.
224. Luco, R.F., et al., *Epigenetics in alternative pre-mRNA splicing.* Cell, 2011. **144**(1): p. 16-26.
225. Portela, A. and M. Esteller, *Epigenetic modifications and human disease.* Nat Biotechnol, 2010. **28**(10): p. 1057-68.
226. Gillette, T.G. and J.A. Hill, *Readers, writers, and erasers: chromatin as the whiteboard of heart disease.* Circ Res, 2015. **116**(7): p. 1245-53.
227. Zhou, H.L., et al., *Regulation of alternative splicing by local histone modifications: potential roles for RNA-guided mechanisms.* Nucleic Acids Res, 2014. **42**(2): p. 701-13.
228. Saha, R.N. and K. Pahan, *HATs and HDACs in neurodegeneration: a tale of disconcerted acetylation homeostasis.* Cell Death Differ, 2006. **13**(4): p. 539-50.
229. Greer, E.L. and Y. Shi, *Histone methylation: a dynamic mark in health, disease and inheritance.* Nat Rev Genet, 2012. **13**(5): p. 343-57.
230. Sharma, A., et al., *Calcium-mediated histone modifications regulate alternative splicing in cardiomyocytes.* Proc Natl Acad Sci U S A, 2014. **111**(46): p. E4920-8.
231. Ding, X., et al., *Activity-induced histone modifications govern Neurexin-1 mRNA splicing and memory preservation.* Nat Neurosci, 2017. **20**(5): p. 690-699.
232. Schor, I.E., et al., *Intragenic epigenetic changes modulate NCAM alternative splicing in neuronal differentiation.* EMBO J, 2013. **32**(16): p. 2264-74.
233. Xue, Y., et al., *NURD, a novel complex with both ATP-dependent chromatin-remodeling and histone deacetylase activities.* Mol Cell, 1998. **2**(6): p. 851-61.
234. Brackertz, M., et al., *p66alpha and p66beta of the Mi-2/NuRD complex mediate MBD2 and histone interaction.* Nucleic Acids Res, 2006. **34**(2): p. 397-406.
235. LeMasson, G., E. Marder, and L. Abbott, *Activity-dependent regulation of conductances in model neurons.* Science, 1993. **259**(5103): p. 1915-1917.
236. Siegel, M., E. Marder, and L.F. Abbott, *Activity-dependent current distributions in model neurons.* Proc Natl Acad Sci U S A, 1994. **91**(24): p. 11308-12.
237. Marder, E., et al., *Memory from the dynamics of intrinsic membrane currents.* Proc Natl Acad Sci U S A, 1996. **93**(24): p. 13481-6.
238. Nanou, E. and W.A. Catterall, *Calcium Channels, Synaptic Plasticity, and Neuropsychiatric Disease.* Neuron, 2018. **98**(3): p. 466-481.
239. Zhang, W.H., et al., *Chronic Stress Causes Projection-Specific Adaptation of Amygdala Neurons via Small-Conductance Calcium-Activated Potassium Channel Downregulation.* Biol Psychiatry, 2019. **85**(10): p. 812-828.
240. Dubrovina, A.S., et al., *The calcium-dependent protein kinase gene VaCPK29 is involved in grapevine responses to heat and osmotic stresses.* Plant Growth Regul, 2017. **82**(1): p. 79-89.
241. Bambico, F.R., et al., *A Key Role for Prefrontocortical Small Conductance Calcium-Activated Potassium Channels in Stress Adaptation and Rapid Antidepressant Response.* Cereb Cortex, 2020. **30**(3): p. 1559-1572.

242. Kapoor, M., et al., *Analysis of whole genome-transcriptomic organization in brain to identify genes associated with alcoholism.* Transl Psychiatry, 2019. **9**(1): p. 89.
243. Lister, R., et al., *Human DNA methylomes at base resolution show widespread epigenomic differences.* Nature, 2009. **462**(7271): p. 315-22.
244. Burger, L., et al., *Identification of active regulatory regions from DNA methylation data.* Nucleic Acids Res, 2013. **41**(16): p. e155.
245. Law, J.A. and S.E. Jacobsen, *Establishing, maintaining and modifying DNA methylation patterns in plants and animals.* Nat Rev Genet, 2010. **11**(3): p. 204-20.
246. Siegfried, Z. and I. Simon, *DNA methylation and gene expression.* Wiley Interdiscip Rev Syst Biol Med, 2010. **2**(3): p. 362-71.
247. Jones, P.A., *Functions of DNA methylation: islands, start sites, gene bodies and beyond.* Nat Rev Genet, 2012. **13**(7): p. 484-92.
248. Chatterjee, R. and C. Vinson, *CpG methylation recruits sequence specific transcription factors essential for tissue specific gene expression.* Biochim Biophys Acta, 2012. **1819**(7): p. 763-70.
249. Hellman, A. and A. Chess, *Gene body-specific methylation on the active X chromosome.* Science, 2007. **315**(5815): p. 1141-3.
250. Feng, S., et al., *Conservation and divergence of methylation patterning in plants and animals.* Proc Natl Acad Sci U S A, 2010. **107**(19): p. 8689-94.
251. Lou, S., et al., *Whole-genome bisulfite sequencing of multiple individuals reveals complementary roles of promoter and gene body methylation in transcriptional regulation.* Genome Biol, 2014. **15**(7): p. 408.
252. Jjingo, D., et al., *On the presence and role of human gene-body DNA methylation.* Oncotarget, 2012. **3**(4): p. 462-74.
253. Schroeder, D.I., et al., *Early Developmental and Evolutionary Origins of Gene Body DNA Methylation Patterns in Mammalian Placentas.* PLoS Genet, 2015. **11**(8): p. e1005442.
254. Weber, M., et al., *Distribution, silencing potential and evolutionary impact of promoter DNA methylation in the human genome.* Nat Genet, 2007. **39**(4): p. 457-66.
255. Jones, P.A. and D. Takai, *The role of DNA methylation in mammalian epigenetics.* Science, 2001. **293**(5532): p. 1068-70.
256. Greenberg, M.V.C. and D. Bourc'his, *The diverse roles of DNA methylation in mammalian development and disease.* Nat Rev Mol Cell Biol, 2019. **20**(10): p. 590-607.
257. Teissandier, A. and D. Bourc'his, *Gene body DNA methylation conspires with H3K36me3 to preclude aberrant transcription.* EMBO J, 2017. **36**(11): p. 1471-1473.
258. Yoder, J.A., C.P. Walsh, and T.H. Bestor, *Cytosine methylation and the ecology of intragenomic parasites.* Trends Genet, 1997. **13**(8): p. 335-40.
259. Matsuda, Y., et al., *Hypomethylation of Alu repetitive elements in esophageal mucosa, and its potential contribution to the epigenetic field for cancerization.* Cancer Causes Control, 2012. **23**(6): p. 865-73.
260. Baba, Y., et al., *Epigenomic diversity of colorectal cancer indicated by LINE-1 methylation in a database of 869 tumors.* Mol Cancer, 2010. **9**: p. 125.
261. Ponomaryova, A.A., et al., *Aberrant Methylation of LINE-1 Transposable Elements: A Search for Cancer Biomarkers.* Cells, 2020. **9**(9).
262. Bollati, V., et al., *DNA methylation in repetitive elements and Alzheimer disease.* Brain Behav Immun, 2011. **25**(6): p. 1078-83.
263. Neri, F., et al., *Intragenic DNA methylation prevents spurious transcription initiation.* Nature, 2017. **543**(7643): p. 72-77.
264. Kulis, M., et al., *Intragenic DNA methylation in transcriptional regulation, normal differentiation and cancer.* Biochim Biophys Acta, 2013. **1829**(11): p. 1161-74.

265. Zhou, W., et al., *DNA methylation enables transposable element-driven genome expansion.* Proc Natl Acad Sci U S A, 2020. **117**(32): p. 19359-19366.
266. Robertson, K.D., et al., *The human DNA methyltransferases (DNMTs) 1, 3a and 3b: coordinate mRNA expression in normal tissues and overexpression in tumors.* Nucleic Acids Res, 1999. **27**(11): p. 2291-8.
267. Subramaniam, D., et al., *DNA methyltransferases: a novel target for prevention and therapy.* Front Oncol, 2014. **4**: p. 80.
268. Azzi, A., et al., *Circadian behavior is light-reprogrammed by plastic DNA methylation.* Nat Neurosci, 2014. **17**(3): p. 377-82.
269. Kim, A.Y., et al., *Obesity-induced DNA hypermethylation of the adiponectin gene mediates insulin resistance.* Nat Commun, 2015. **6**: p. 7585.
270. Metivier, R., et al., *Cyclical DNA methylation of a transcriptionally active promoter.* Nature, 2008. **452**(7183): p. 45-50.
271. Stresemann, C. and F. Lyko, *Modes of action of the DNA methyltransferase inhibitors azacytidine and decitabine.* Int J Cancer, 2008. **123**(1): p. 8-13.
272. Zhou, L., et al., *Zebularine: a novel DNA methylation inhibitor that forms a covalent complex with DNA methyltransferases.* J Mol Biol, 2002. **321**(4): p. 591-9.
273. Schneider-Stock, R., et al., *5-Aza-cytidine is a potent inhibitor of DNA methyltransferase 3a and induces apoptosis in HCT-116 colon cancer cells via Gadd45- and p53-dependent mechanisms.* J Pharmacol Exp Ther, 2005. **312**(2): p. 525-36.
274. Brueckner, B., et al., *Epigenetic reactivation of tumor suppressor genes by a novel small-molecule inhibitor of human DNA methyltransferases.* Cancer Res, 2005. **65**(14): p. 6305-11.
275. Schermelleh, L., et al., *Trapped in action: direct visualization of DNA methyltransferase activity in living cells.* Nat Methods, 2005. **2**(10): p. 751-6.
276. Brueckner, B., et al., *Delivery of 5-azacytidine to human cancer cells by elaidic acid esterification increases therapeutic drug efficacy.* Mol Cancer Ther, 2010. **9**(5): p. 1256-64.
277. Ghoshal, K., et al., *5-Aza-deoxycytidine induces selective degradation of DNA methyltransferase 1 by a proteasomal pathway that requires the KEN box, bromo-adjacent homology domain, and nuclear localization signal.* Mol Cell Biol, 2005. **25**(11): p. 4727-41.
278. Palii, S.S., et al., *DNA methylation inhibitor 5-Aza-2'-deoxycytidine induces reversible genome-wide DNA damage that is distinctly influenced by DNA methyltransferases 1 and 3B.* Mol Cell Biol, 2008. **28**(2): p. 752-71.
279. Cheng, J.C., et al., *Continuous zebularine treatment effectively sustains demethylation in human bladder cancer cells.* Mol Cell Biol, 2004. **24**(3): p. 1270-8.
280. Nyce, J., *Drug-induced DNA hypermethylation and drug resistance in human tumors.* Cancer Res, 1989. **49**(21): p. 5829-36.
281. Melka, M.G., et al., *Olanzapine induced DNA methylation changes support the dopamine hypothesis of psychosis.* J Mol Psychiatry, 2013. **1**(1): p. 19.
282. Kawasaki, H. and K. Taira, *Induction of DNA methylation and gene silencing by short interfering RNAs in human cells.* Nature, 2004. **431**(7005): p. 211-7.
283. Itou, D., et al., *Induction of DNA methylation by artificial piRNA production in male germ cells.* Curr Biol, 2015. **25**(7): p. 901-6.
284. Hannon, E., et al., *A role for CaV1 and calcineurin signaling in depolarization-induced changes in neuronal DNA methylation.* Neuroepigenetics, 2015. **3**: p. 1-6.
285. Bird, A., *DNA methylation patterns and epigenetic memory.* Genes Dev, 2002. **16**(1): p. 6-21.
286. Weng, N.P., Y. Araki, and K. Subedi, *The molecular basis of the memory T cell response: differential gene expression and its epigenetic regulation.* Nat Rev Immunol, 2012. **12**(4): p. 306-15.

287. Jaenisch, R. and A. Bird, *Epigenetic regulation of gene expression: how the genome integrates intrinsic and environmental signals.* Nat Genet, 2003. **33 Suppl**: p. 245-54.
288. Wischnewski, F., K. Pantel, and H. Schwarzenbach, *Promoter demethylation and histone acetylation mediate gene expression of MAGE-A1, -A2, -A3, and -A12 in human cancer cells.* Mol Cancer Res, 2006. **4**(5): p. 339-49.
289. Wagner, J.R., et al., *The relationship between DNA methylation, genetic and expression inter-individual variation in untransformed human fibroblasts.* Genome Biol, 2014. **15**(2): p. R37.
290. Hashimoto, S., et al., *Coordinated changes in DNA methylation in antigen-specific memory CD4 T cells.* J Immunol, 2013. **190**(8): p. 4076-91.
291. Udali, S., et al., *Global DNA methylation and hydroxymethylation differ in hepatocellular carcinoma and cholangiocarcinoma and relate to survival rate.* Hepatology, 2015. **62**(2): p. 496-504.
292. Deaton, A.M. and A. Bird, *CpG islands and the regulation of transcription.* Genes Dev, 2011. **25**(10): p. 1010-22.
293. de Almeida, S.F., et al., *Splicing enhances recruitment of methyltransferase HYPB/Setd2 and methylation of histone H3 Lys36.* Nat Struct Mol Biol, 2011. **18**(9): p. 977-83.
294. Sun, Z., et al., *H3K36me3, message from chromatin to DNA damage repair.* Cell Biosci, 2020. **10**: p. 9.
295. Jones, P.L., et al., *Methylated DNA and MeCP2 recruit histone deacetylase to repress transcription.* Nat Genet, 1998. **19**(2): p. 187-91.
296. Goldstrohm, A.C., A.L. Greenleaf, and M.A. Garcia-Blanco, *Co-transcriptional splicing of pre-messenger RNAs: considerations for the mechanism of alternative splicing.* Gene, 2001. **277**(1-2): p. 31-47.
297. Flores, K., et al., *Genome-wide association between DNA methylation and alternative splicing in an invertebrate.* BMC Genomics, 2012. **13**: p. 480.
298. Gao, D., et al., *DNA methylation/hydroxymethylation regulate gene expression and alternative splicing during terminal granulopoiesis.* Epigenomics, 2018.
299. Shayevitch, R., et al., *The importance of DNA methylation of exons on alternative splicing.* RNA, 2018. **24**(10): p. 1351-1362.
300. de la Mata, M., C. Lafaille, and A.R. Kornblihtt, *First come, first served revisited: factors affecting the same alternative splicing event have different effects on the relative rates of intron removal.* RNA, 2010. **16**(5): p. 904-12.
301. Fededa, J.P., et al., *A polar mechanism coordinates different regions of alternative splicing within a single gene.* Mol Cell, 2005. **19**(3): p. 393-404.
302. Nanan, K.K., et al., *Independence between pre-mRNA splicing and DNA methylation in an isogenic minigene resource.* Nucleic Acids Res, 2017. **45**(22): p. 12780-12797.
303. Ip, J.Y., et al., *Global impact of RNA polymerase II elongation inhibition on alternative splicing regulation.* Genome Res, 2011. **21**(3): p. 390-401.
304. Kornblihtt, A.R., *CTCF: from insulators to alternative splicing regulation.* Cell Res, 2012. **22**(3): p. 450-2.
305. Marina, R.J., et al., *TET-catalyzed oxidation of intragenic 5-methylcytosine regulates CTCF-dependent alternative splicing.* EMBO J, 2016. **35**(3): p. 335-55.
306. Marina, R.J. and S. Oberdoerffer, *Epigenomics meets splicing through the TETs and CTCF.* Cell Cycle, 2016. **15**(11): p. 1397-9.
307. Lopez Soto, E.J. and D. Lipscombe, *Cell-specific exon methylation and CTCF binding in neurons regulate calcium ion channel splicing and function.* Elife, 2020. **9**.
308. Nanavaty, V., et al., *DNA Methylation Regulates Alternative Polyadenylation via CTCF and the Cohesin Complex.* Mol Cell, 2020. **78**(4): p. 752-764 e6.

309. Young, J.I., et al., *Regulation of RNA splicing by the methylation-dependent transcriptional repressor methyl-CpG binding protein 2.* Proc Natl Acad Sci U S A, 2005. **102**(49): p. 17551-8.
310. Li, R., et al., *Misregulation of Alternative Splicing in a Mouse Model of Rett Syndrome.* PLoS Genet, 2016. **12**(6): p. e1006129.
311. Wong, J.J., et al., *Intron retention is regulated by altered MeCP2-mediated splicing factor recruitment.* Nat Commun, 2017. **8**: p. 15134.
312. Zheng, Z., G. Ambigapathy, and J. Keifer, *MeCP2 regulates Tet1-catalyzed demethylation, CTCF binding, and learning-dependent alternative splicing of the BDNF gene in Turtle.* Elife, 2017. **6**.
313. Cheng, T.L., et al., *Regulation of mRNA splicing by MeCP2 via epigenetic modifications in the brain.* Sci Rep, 2017. **7**: p. 42790.
314. Chhatbar, K., et al., *Quantitative analysis questions the role of MeCP2 in alternative splicing.* PLoS Genet., 2020.
315. Osenberg, S., et al., *Activity-dependent aberrations in gene expression and alternative splicing in a mouse model of Rett syndrome.* Proc Natl Acad Sci U S A, 2018. **115**(23): p. E5363-E5372.
316. Brito, D.V., K.G. Karaca, and A.M.J.b. Oliveira, *MeCP2 gates spatial learning-induced alternative splicing events in the mouse hippocampus.* Mol Brain., 2020.
317. Yearim, A., et al., *HP1 is involved in regulating the global impact of DNA methylation on alternative splicing.* Cell Rep, 2015. **10**(7): p. 1122-34.
318. Calle-Fabregat, C., O. Morante-Palacios, and E. Ballestar, *Understanding the Relevance of DNA Methylation Changes in Immune Differentiation and Disease.* Genes (Basel), 2020. **11**(1).
319. Liu, Y., et al., *Epigenome-wide association data implicate DNA methylation as an intermediary of genetic risk in rheumatoid arthritis.* Nat Biotechnol., 2013. **31**(2): p. 142.
320. Barres, R. and J.R.J.T.A.j.o.c.n. Zierath, *DNA methylation in metabolic disorders.* Am J Clin Nutr., 2011. **93**(4): p. 897S-900S.
321. Ahmed, S.A.H., et al., *The role of DNA methylation in the pathogenesis of type 2 diabetes mellitus.* Clin Epigenetics, 2020. **12**(1): p. 1-23.
322. Stenvinkel, P., et al., *Impact of inflammation on epigenetic DNA methylation–a novel risk factor for cardiovascular disease?* J Intern Med., 2007. **261**(5): p. 488-499.
323. Haas, J., et al., *Alterations in cardiac DNA methylation in human dilated cardiomyopathy.* EMBO Mol Med., 2013. **5**(3): p. 413-429.
324. Smyth, L.J., et al., *DNA hypermethylation and DNA hypomethylation is present at different loci in chronic kidney disease.* Epigenetics., 2014. **9**(3): p. 366-376.
325. Lu, H., et al., *DNA methylation, a hand behind neurodegenerative diseases.* Front Aging Neurosci., 2013. **5**: p. 85.
326. Mastroeni, D., et al., *Epigenetic changes in Alzheimer's disease: decrements in DNA methylation.* Neurobiol Aging., 2010. **31**(12): p. 2025-2037.
327. Bienvenu, T. and J.J.N.R.G. Chelly, *Molecular genetics of Rett syndrome: when DNA methylation goes unrecognized.* Nat Rev Genet., 2006. **7**(6): p. 415-426.
328. Ng, C.W., et al., *Extensive changes in DNA methylation are associated with expression of mutant huntingtin.* Proc Natl Acad Sci U S A., 2013. **110**(6): p. 2354-2359.
329. Velasco, G. and C.J.C.g. Francastel, *Genetics meets DNA methylation in rare diseases.* Clin Genet., 2019. **95**(2): p. 210-220.
330. Klein, C.J., et al., *Mutations in DNMT1 cause hereditary sensory neuropathy with dementia and hearing loss.* Nat Genet. , 2011. **43**(6): p. 595-600.
331. Esteller, M., J.G.J.T.J.o.P.A.J.o.t.P.S.o.G.B. Herman, and Ireland, *Cancer as an epigenetic disease: DNA methylation and chromatin alterations in human tumours.* J Pathol., 2002. **196**(1): p. 1-7.
332. Yang, X., L. Yan, and N.E.J.E.-r.c. Davidson, *DNA methylation in breast cancer.* Endocrine Related Cancer, 2001. **8**(2): p. 115-127.

333. Yoon, H.K., et al., *Intron-derived aberrant splicing of A20 transcript in rheumatoid arthritis.* Rheumatology (Oxford). 2013. **52**(3): p. 427-437.
334. Gahete, M.D., et al., *Changes in splicing machinery components influence, precede, and early predict the development of type 2 diabetes: from the cordioprev study.* EBioMedicine., 2018. **37**: p. 356-365.
335. Biesiadecki, B.J., et al., *Cardiac troponin T variants produced by aberrant splicing of multiple exons in animals with high instances of dilated cardiomyopathy.* J Biol Chem., 2002. **277**(52): p. 50275-50285.
336. Tan, Y.C., et al., *Aberrant PKD2 splicing due to a presumed novel missense mutation in autosomal‐dominant polycystic kidney disease.* Clin Genet., 2011. **80**(3): p. 287-292.
337. De Jonghe, C., et al., *Aberrant splicing in the presenilin-1 intron 4 mutation causes presenile Alzheimer's disease by increased Aβ42 secretion.* Human Molecular Genetics, 1999. **8**(8): p. 1529-1540.
338. Osenberg, S., et al., *Activity-dependent aberrations in gene expression and alternative splicing in a mouse model of Rett syndrome.* Proc Natl Acad Sci U S A, 2018. **115**(23): p. E5363-E5372.
339. Sathasivam, K., et al., *Aberrant splicing of HTT generates the pathogenic exon 1 protein in Huntington disease.* Proc Natl Acad Sci U S A., 2013. **110**(6): p. 2366-2370.
340. Gao, H.-M. and J.-S.J.T.i.i. Hong, *Why neurodegenerative diseases are progressive: uncontrolled inflammation drives disease progression.* Trends Immunol., 2008. **29**(8): p. 357-365.
341. Wullner, U., et al., *DNA methylation in Parkinson's disease.* J Neurochem, 2016. **139 Suppl 1**: p. 108-120.
342. Fedotova, E.Y. and S.N. Illarioshkin, *DNA Methylation in Neurodegenerative Diseases.* Russian Journal of Genetics, 2019. **55**(3): p. 271-277.
343. McKinney, B., et al., *DNA methylation as a putative mechanism for reduced dendritic spine density in the superior temporal gyrus of subjects with schizophrenia.* Transl Psychiatry, 2017. **7**(2): p. e1032.
344. Gold, W.A., et al., *Rett Syndrome: A Genetic Update and Clinical Review Focusing on Comorbidities.* ACS Chem Neurosci, 2018. **9**(2): p. 167-176.
345. Amir, R.E., et al., *Rett syndrome is caused by mutations in X-linked MECP2, encoding methyl-CpG-binding protein 2.* Nat Genet, 1999. **23**(2): p. 185-8.
346. Percy, A.K., et al., *Rett syndrome: North American database.* J Child Neurol, 2007. **22**(12): p. 1338-41.
347. Watson, P., et al., *Angelman syndrome phenotype associated with mutations in MECP2, a gene encoding a methyl CpG binding protein.* J Med Genet, 2001. **38**(4): p. 224-8.
348. Couvert, P., et al., *MECP2 is highly mutated in X-linked mental retardation.* Hum Mol Genet, 2001. **10**(9): p. 941-6.
349. Neul, J.L., et al., *Specific mutations in methyl-CpG-binding protein 2 confer different severity in Rett syndrome.* Neurology, 2008. **70**(16): p. 1313-21.
350. Cuddapah, V.A., et al., *Methyl-CpG-binding protein 2 (MECP2) mutation type is associated with disease severity in Rett syndrome.* J Med Genet, 2014. **51**(3): p. 152-8.
351. Lamonica, J.M., et al., *Elevating expression of MeCP2 T158M rescues DNA binding and Rett syndrome-like phenotypes.* J Clin Invest, 2017. **127**(5): p. 1889-1904.
352. Booth, F.W. and D.B. Thomason, *Molecular and cellular adaptation of muscle in response to exercise: perspectives of various models.* Physiol Rev, 1991. **71**(2): p. 541-85.
353. Egan, B. and J.R. Zierath, *Exercise metabolism and the molecular regulation of skeletal muscle adaptation.* Cell Metab, 2013. **17**(2): p. 162-84.
354. Ling, C. and T. Ronn, *Epigenetic adaptation to regular exercise in humans.* Drug Discov Today, 2014. **19**(7): p. 1015-8.

355. Lee, P., N.S. Chandel, and M.C. Simon, *Cellular adaptation to hypoxia through hypoxia inducible factors and beyond.* Nat Rev Mol Cell Biol, 2020. **21**(5): p. 268-283.
356. Yap, E.L. and M.E. Greenberg, *Activity-Regulated Transcription: Bridging the Gap between Neural Activity and Behavior.* Neuron, 2018. **100**(2): p. 330-348.
357. Browne, C.J., et al., *Epigenetic Mechanisms of Opioid Addiction.* Biol Psychiatry, 2020. **87**(1): p. 22-33.
358. Maniatis, T. and B. Tasic, *Alternative pre-mRNA splicing and proteome expansion in metazoans.* Nature, 2002. **418**(6894): p. 236-43.
359. Blencowe, B.J., *Alternative splicing: new insights from global analyses.* Cell, 2006. **126**(1): p. 37-47.
360. Lee, J.A., et al., *Depolarization and CaM kinase IV modulate NMDA receptor splicing through two essential RNA elements.* PLoS Biol, 2007. **5**(2): p. e40.
361. Xie, J., et al., *A consensus CaMK IV-responsive RNA sequence mediates regulation of alternative exons in neurons.* RNA, 2005. **11**(12): p. 1825-34.
362. Sharma, A. and H. Lou, *Depolarization-mediated regulation of alternative splicing.* Front Neurosci, 2011. **5**: p. 141.
363. Dos Santos, C.O., et al., *An epigenetic memory of pregnancy in the mouse mammary gland.* Cell Rep, 2015. **11**(7): p. 1102-9.
364. Gelfman, S., et al., *DNA-methylation effect on cotranscriptional splicing is dependent on GC architecture of the exon-intron structure.* Genome Res, 2013. **23**(5): p. 789-99.
365. Lagger, S., et al., *MeCP2 recognizes cytosine methylated tri-nucleotide and di-nucleotide sequences to tune transcription in the mammalian brain.* PLoS Genet, 2017. **13**(5): p. e1006793.
366. Kinde, B., et al., *DNA methylation in the gene body influences MeCP2-mediated gene repression.* Proc Natl Acad Sci U S A, 2016. **113**(52): p. 15114-15119.
367. Boxer, L.D., et al., *MeCP2 Represses the Rate of Transcriptional Initiation of Highly Methylated Long Genes.* Mol Cell, 2020. **77**(2): p. 294-309 e9.
368. Nan, X., et al., *Transcriptional repression by the methyl-CpG-binding protein MeCP2 involves a histone deacetylase complex.* Nature, 1998. **393**(6683): p. 386-9.
369. Bienvenu, T. and J. Chelly, *Molecular genetics of Rett syndrome: when DNA methylation goes unrecognized.* Nat Rev Genet, 2006. **7**(6): p. 415-26.
370. Al-Mateen, M., M. Philippart, and W.D.J.A.J.o.D.o.C. Shields, *Rett syndrome: a commonly overlooked progressive encephalopathy in girls.* Am J Dis Child., 1986. **140**(8): p. 761-765.
371. Operto, F.F., et al., *Epilepsy and genetic in Rett syndrome: A review.* Brain Behav, 2019. **9**(5): p. e01250.
372. Krajnc, N., *Management of epilepsy in patients with Rett syndrome: perspectives and considerations.* Ther Clin Risk Manag, 2015. **11**: p. 925-32.
373. Gabel, H.W., et al., *Disruption of DNA-methylation-dependent long gene repression in Rett syndrome.* Nature, 2015. **522**(7554): p. 89-93.
374. Juang, Y.T., et al., *Systemic lupus erythematosus serum IgG increases CREM binding to the IL-2 promoter and suppresses IL-2 production through CaMKIV.* J Clin Invest, 2005. **115**(4): p. 996-1005.
375. Hedrich, C.M., T. Rauen, and G.C. Tsokos, *cAMP-responsive element modulator (CREM)alpha protein signaling mediates epigenetic remodeling of the human interleukin-2 gene: implications in systemic lupus erythematosus.* J Biol Chem, 2011. **286**(50): p. 43429-36.
376. Hedrich, C.M., et al., *cAMP response element modulator alpha controls IL2 and IL17A expression during CD4 lineage commitment and subset distribution in lupus.* Proc Natl Acad Sci U S A, 2012. **109**(41): p. 16606-11.

377. Buchthal, B., et al., *Nuclear calcium signaling controls methyl-CpG-binding protein 2 (MeCP2) phosphorylation on serine 421 following synaptic activity.* J Biol Chem, 2012. **287**(37): p. 30967-74.
378. Long, S.W., et al., *A brain-derived MeCP2 complex supports a role for MeCP2 in RNA processing.* Biosci Rep, 2011. **31**(5): p. 333-43.
379. Chhatbar, K., et al., *Quantitative analysis questions the role of MeCP2 as a global regulator of alternative splicing.* PLoS Genet, 2020. **16**(10): p. e1009087.
380. Strober, W., *Trypan Blue Exclusion Test of Cell Viability.* Curr Protoc Immunol, 2015. **111**: p. A3 B 1-A3 B 3.
381. Anders, S., A. Reyes, and W. Huber, *Detecting differential usage of exons from RNA-seq data.* Genome Res, 2012. **22**(10): p. 2008-17.
382. Shen, S., et al., *MATS: a Bayesian framework for flexible detection of differential alternative splicing from RNA-Seq data.* Nucleic Acids Res, 2012. **40**(8): p. e61.
383. Andrews, S., *FastQC: a quality control tool for high throughput sequence data*. 2010, Babraham Bioinformatics, Babraham Institute, Cambridge, United Kingdom.
384. Xi, Y. and W.J.B.b. Li, *BSMAP: whole genome bisulfite sequence MAPping program.* BMC Bioinformatics., 2009. **10**(1): p. 232.
385. Thorvaldsdottir, H., J.T. Robinson, and J.P. Mesirov, *Integrative Genomics Viewer (IGV): high-performance genomics data visualization and exploration.* Brief Bioinform, 2013. **14**(2): p. 178-92.
386. Dennis, G., Jr., et al., *DAVID: Database for Annotation, Visualization, and Integrated Discovery.* Genome Biol, 2003. **4**(5): p. P3.
387. Schneider, C.A., W.S. Rasband, and K.W. Eliceiri, *NIH Image to ImageJ: 25 years of image analysis.* Nat Methods, 2012. **9**(7): p. 671-5.
388. Guo, J.U., et al., *Distribution, recognition and regulation of non-CpG methylation in the adult mammalian brain.* Nat Neurosci, 2014. **17**(2): p. 215-22.
389. Olson, C.O., et al., *MECP2 Mutation Interrupts Nucleolin-mTOR-P70S6K Signaling in Rett Syndrome Patients.* Front Genet, 2018. **9**: p. 635.
390. Pejhan, S., et al., *Differential brain region-specific expression of MeCP2 and BDNF in Rett Syndrome patients: a distinct grey-white matter variation.* Neuropathol Appl Neurobiol, 2020.
391. Pejhan, S., M.R. Del Bigio, and M. Rastegar, *The MeCP2E1/E2-BDNF-miR132 Homeostasis Regulatory Network Is Region-Dependent in the Human Brain and Is Impaired in Rett Syndrome Patients.* Front Cell Dev Biol, 2020. **8**: p. 763.
392. Renbaum, P., et al., *Cloning, characterization, and expression in Escherichia coli of the gene coding for the CpG DNA methylase from Spiroplasma sp. strain MQ1(M.SssI).* Nucleic Acids Res, 1990. **18**(5): p. 1145-52.
393. Nur, I., et al., *Procaryotic and eucaryotic traits of DNA methylation in spiroplasmas (mycoplasmas).* J Bacteriol, 1985. **164**(1): p. 19-24.
394. Lu, Q. and B. Richardson, *Methods for Analyzing the Role of DNA Methylation and Chromatin Structure in Regulating T Lymphocyte Gene Expression.* Biol Proced Online, 2004. **6**: p. 189-203.
395. Doerfler, W., *DNA methylation and gene activity.* Annu Rev Biochem, 1983. **52**: p. 93-124.
396. Fierro, J., Jr., D.R. Haynes, and P. Washbourne, *4.1Ba is necessary for glutamatergic synapse formation in the sensorimotor circuit of developing zebrafish.* PLoS One, 2018. **13**(10): p. e0205255.
397. Biundo, F., et al., *A role for tau in learning, memory and synaptic plasticity.* Sci Rep, 2018. **8**(1): p. 3184.
398. Shamir, A., et al., *The importance of the NRG-1/ErbB4 pathway for synaptic plasticity and behaviors associated with psychiatric disorders.* J Neurosci, 2012. **32**(9): p. 2988-97.

399. Wu, S.H., et al., *The ankyrin repeat-rich membrane spanning (ARMS)/Kidins220 scaffold protein is regulated by activity-dependent calpain proteolysis and modulates synaptic plasticity.* J Biol Chem, 2010. **285**(52): p. 40472-8.
400. Zhao, W., Y. Shen, and S. Ren, *Endogenous expression of Neuregulin-1 (Nrg1) as a potential modulator of prolactin (PRL) secretion in GH3 cells.* Cell Tissue Res, 2011. **344**(2): p. 313-20.
401. Christman, J.K., *5-Azacytidine and 5-aza-2'-deoxycytidine as inhibitors of DNA methylation: mechanistic studies and their implications for cancer therapy.* Oncogene, 2002. **21**(35): p. 5483-95.
402. Christman, J.K., et al., *Effect of 5-azacytidine on differentiation and DNA methylation in human promyelocytic leukemia cells (HL-60).* Cancer Res, 1983. **43**(2): p. 763-9.
403. Hansen, K.D., B. Langmead, and R.A. Irizarry, *BSmooth: from whole genome bisulfite sequencing reads to differentially methylated regions.* Genome Biol, 2012. **13**(10): p. R83.
404. Li, L.H., et al., *Cytotoxicity and mode of action of 5-azacytidine on L1210 leukemia.* Cancer Res, 1970. **30**(11): p. 2760-9.
405. Khoddami, V. and B.R. Cairns, *Identification of direct targets and modified bases of RNA cytosine methyltransferases.* Nat Biotechnol, 2013. **31**(5): p. 458-64.
406. Toma, C., et al., *Association study of six candidate genes asymmetrically expressed in the two cerebral hemispheres suggests the involvement of BAIAP2 in autism.* J Psychiatr Res, 2011. **45**(2): p. 280-2.
407. Liu, G., et al., *Refinement of the spectra of exon usage by combined effects of extracellular stimulus and intracellular factors.* Biochim Biophys Acta, 2014. **1839**(7): p. 537-45.
408. Hutton, M., et al., *Association of missense and 5'-splice-site mutations in tau with the inherited dementia FTDP-17.* Nature, 1998. **393**(6686): p. 702-5.
409. Fischer, I. and P.W. Baas, *Resurrecting the Mysteries of Big Tau.* Trends Neurosci, 2020. **43**(7): p. 493-504.
410. Stickeler, E., et al., *The RNA binding protein YB-1 binds A/C-rich exon enhancers and stimulates splicing of the CD44 alternative exon v4.* EMBO J, 2001. **20**(14): p. 3821-30.
411. Soler, J., et al., *Genetic variability in scaffolding proteins and risk for schizophrenia and autism-spectrum disorders: a systematic review.* J Psychiatry Neurosci, 2018. **43**(4): p. 223-244.
412. West, A.E. and M.E. Greenberg, *Neuronal activity-regulated gene transcription in synapse development and cognitive function.* Cold Spring Harb Perspect Biol, 2011. **3**(6).
413. Guerrini, R. and E. Parrini, *Epilepsy in Rett syndrome, and CDKL5- and FOXG1-gene-related encephalopathies.* Epilepsia, 2012. **53**(12): p. 2067-78.
414. Moretti, P., et al., *Learning and memory and synaptic plasticity are impaired in a mouse model of Rett syndrome.* J Neurosci, 2006. **26**(1): p. 319-27.
415. Ghosh, R.P., et al., *Rett syndrome-causing mutations in human MeCP2 result in diverse structural changes that impact folding and DNA interactions.* J Biol Chem, 2008. **283**(29): p. 20523-34.
416. Free, A., et al., *DNA recognition by the methyl-CpG binding domain of MeCP2.* J Biol Chem, 2001. **276**(5): p. 3353-60.
417. Kammoun, F., et al., *Screening of MECP2 coding sequence in patients with phenotypes of decreasing likelihood for Rett syndrome: a cohort of 171 cases.* J Med Genet, 2004. **41**(6): p. e85.
418. Reid, K., et al., *Nifedipine, an L-type calcium channel blocker, restores the hypnotic response in rats made tolerant to the alpha-2 adrenergic agonist dexmedetomidine.* J Pharmacol Exp Ther, 1997. **283**(3): p. 993-9.
419. Tian, L., et al., *Distinct stoichiometry of BKCa channel tetramer phosphorylation specifies channel activation and inhibition by cAMP-dependent protein kinase.* Proc Natl Acad Sci U S A, 2004. **101**(32): p. 11897-902.

420. Ramanathan, K., et al., *A molecular mechanism for electrical tuning of cochlear hair cells.* Science, 1999. **283**(5399): p. 215-7.
421. Linker, S.M., et al., *Combined single-cell profiling of expression and DNA methylation reveals splicing regulation and heterogeneity.* Genome Biol, 2019. **20**(1): p. 30.
422. Gao, D., et al., *DNA methylation/hydroxymethylation regulate gene expression and alternative splicing during terminal granulopoiesis.* Epigenomics, 2019. **11**(1): p. 95-109.
423. Tucci, V., et al., *Genomic Imprinting and Physiological Processes in Mammals.* Cell, 2019. **176**(5): p. 952-965.
424. Bannister, A.J., et al., *Selective recognition of methylated lysine 9 on histone H3 by the HP1 chromo domain.* Nature, 2001. **410**(6824): p. 120-4.
425. Sohail, M., et al., *Evolutionarily emerged G tracts between the polypyrimidine tract and 3' AG are splicing silencers enriched in genes involved in cancer.* BMC Genomics, 2014. **15**: p. 1143.
426. Nguyen, H. and J. Xie, *Widespread Separation of the Polypyrimidine Tract From 3′ AG by G Tracts in Association With Alternative Exons in Metazoa and Plants.* Frontiers in genetics, 2018. **9**.
427. Sohail, M. and J. Xie, *Evolutionary emergence of a novel splice variant of opposite effect on cell cycle.* Molecular and cellular biology, 2015: p. MCB. 00190-15.
428. Wilkinson, M.E., et al., *Postcatalytic spliceosome structure reveals mechanism of 3'-splice site selection.* Science, 2017. **358**(6368): p. 1283-1288.
429. Liu, S., et al., *Structure of the yeast spliceosomal postcatalytic P complex.* Science, 2017. **358**(6368): p. 1278-1283.
430. Xie, J., *Differential evolution of signal-responsive RNA elements and upstream factors that control alternative splicing.* Cell Mol Life Sci, 2014. **71**(22): p. 4347-60.
431. Kittiniyom, K., et al., *Allele-specific loss of heterozygosity at the DAL-1/4.1B (EPB41L3) tumor-suppressor gene locus in the absence of mutation.* Genes Chromosomes Cancer, 2004. **40**(3): p. 190-203.
432. Rangel, L., et al., *Alternative polyadenylation in a family of paralogous EPB41 genes generates protein 4.1 diversity.* RNA Biol, 2017. **14**(2): p. 236-244.
433. Josifova, D.J., et al., *Heterozygous KIDINS220/ARMS nonsense variants cause spastic paraplegia, intellectual disability, nystagmus, and obesity.* Hum Mol Genet, 2016. **25**(11): p. 2158-2167.
434. Dejanovic, B., et al., *Exonic microdeletions of the gephyrin gene impair GABAergic synaptic inhibition in patients with idiopathic generalized epilepsy.* Neurobiol Dis, 2014. **67**: p. 88-96.
435. Lionel, A.C., et al., *Rare exonic deletions implicate the synaptic organizer Gephyrin (GPHN) in risk for autism, schizophrenia and seizures.* Hum Mol Genet, 2013. **22**(10): p. 2055-66.
436. Day, J.K., et al., *Genistein alters methylation patterns in mice.* J Nutr, 2002. **132**(8 Suppl): p. 2419S-2423S.
437. Luo, C., P. Hajkova, and J.R. Ecker, *Dynamic DNA methylation: In the right place at the right time.* Science, 2018. **361**(6409): p. 1336-1340.
438. Wu, X. and Y. Zhang, *TET-mediated active DNA demethylation: mechanism, function and beyond.* Nat Rev Genet, 2017. **18**(9): p. 517-534.
439. Zhou, J., et al., *Tissue-specific DNA methylation is conserved across human, mouse, and rat, and driven by primary sequence conservation.* BMC Genomics, 2017. **18**(1): p. 724.
440. Ghosh, S., et al., *Tissue specific DNA methylation of CpG islands in normal human adult somatic tissues distinguishes neural from non-neural tissues.* Epigenetics, 2010. **5**(6): p. 527-38.
441. He, Y., et al., *Spatiotemporal DNA methylome dynamics of the developing mouse fetus.* Nature, 2020. **583**(7818): p. 752-759.

442. Ziller, M.J., et al., *Dissecting the Functional Consequences of De Novo DNA Methylation Dynamics in Human Motor Neuron Differentiation and Physiology.* Cell Stem Cell, 2018. **22**(4): p. 559-574 e9.
443. Li, P., et al., *Hemispheric asymmetry in the human brain and in Parkinson's disease is linked to divergent epigenetic patterns in neurons.* Genome Biol, 2020. **21**(1): p. 61.
444. Sanchez-Mut, J.V., et al., *Human DNA methylomes of neurodegenerative diseases show common epigenomic patterns.* Transl Psychiatry, 2016. **6**: p. e718.